THE WORLD BANK
IBRD • IDA | WORLD BANK GROUP

ESMAP
Energy Sector Management Assistance Program

SOLAR RESOURCE MEASUREMENT CAMPAIGN - NEPAL

24- MONTH SITE MEASUREMENT REPORT

December 2020

This report was prepared by **CSP Services GmbH,** under contract to the World Bank.

It is one of several outputs of the activity "Renewable Energy Resource Mapping and Resource Mapping and Geospatial Planning Nepal [Project ID: P150328]. This activity is funded and supported by the Energy Sector Management Assistance Program (ESMAP), a multi-donor trust fund administered by the World Bank, under a global initiative on Renewable Energy Resource Mapping. Further details on the initiative can be obtained from the ESMAP website.

The content of this document is the sole responsibility of the consultant authors. Any improved or validated solar resource data will be incorporated into the Global Solar Atlas.

Attribution

Please cite the work as follows: World Bank. 2018. Solar Resource Measurement Campaign in Nepal, Installation Reports. Washington, DC: World Bank.

CSP Services GmbH, Köln, Germany

Client: The World Bank
Washington D.C., USA

Selection #: 1230234

- Solar Resource Measurement Campaign Nepal –

24-Month Site Measurement Report
ESMAP Solar Measurements in Nepal

Birk Kraas
Roman Affolter

CSP Services GmbH
Friedrich-Ebert-Ufer 30
51143 Köln/Cologne, Germany
Email: b.kraas@cspservices.de
Version 04 December 2020

CSP Services
CONCENTRATING SOLAR POWER SERVICES

Introduction

Within the ESMAP Solar Measurement Campaign, five Tier1 weather stations were installed at different locations throughout Nepal. The main objective was to collect two years of continuous high-quality ground measurement data of solar irradiance and other meteorological parameters to validate satellite-based and numerical weather models for the generation of solar resource maps within the Global Solar Atlas[1]. All measurement data is published on the energy data info portal of World Bank[2]

The selected sites are shown in Table 1 and Figure 1. The site selection procedure is summarized in the project implementation plan.

Table 1: Ground measurement sites ESMAP Solar Measurement Campaign Nepal

Site	Short name	Type	Coordinates	Elevation	Installed
IOE Purwanchal Campus, Dharan	NP-Dha	Tier 1	26.79291°N 87.29263°E	310 m	2018-06-18
Hotel Kanjirowa, Jumla	NP-Jum	Tier 1	29.27237°N 82.19351°E	2368 m	2018-07-28
IOE Pulchowk Campus, Kathmandu	NP-Kat	Tier 1	27.68155°N 85.31877°E	1315 m	2018-06-15
DHM Agromet station, Lumle	NP-Lum	Tier 1	28.29666°N 83.81800°E	1750 m	2018-06-22
NARC Regional Center, Nepalgunj	NP-Npg	Tier 1	28.11290°N 81.58900°E	150 m	2018-06-28

This report summarizes the results of the two years of measurement at the five sites. Each site is reported on individually.

[1] http://globalsolaratlas.info/

[2] https://energydata.info/dataset/nepal-solar-radiation-measurement-data

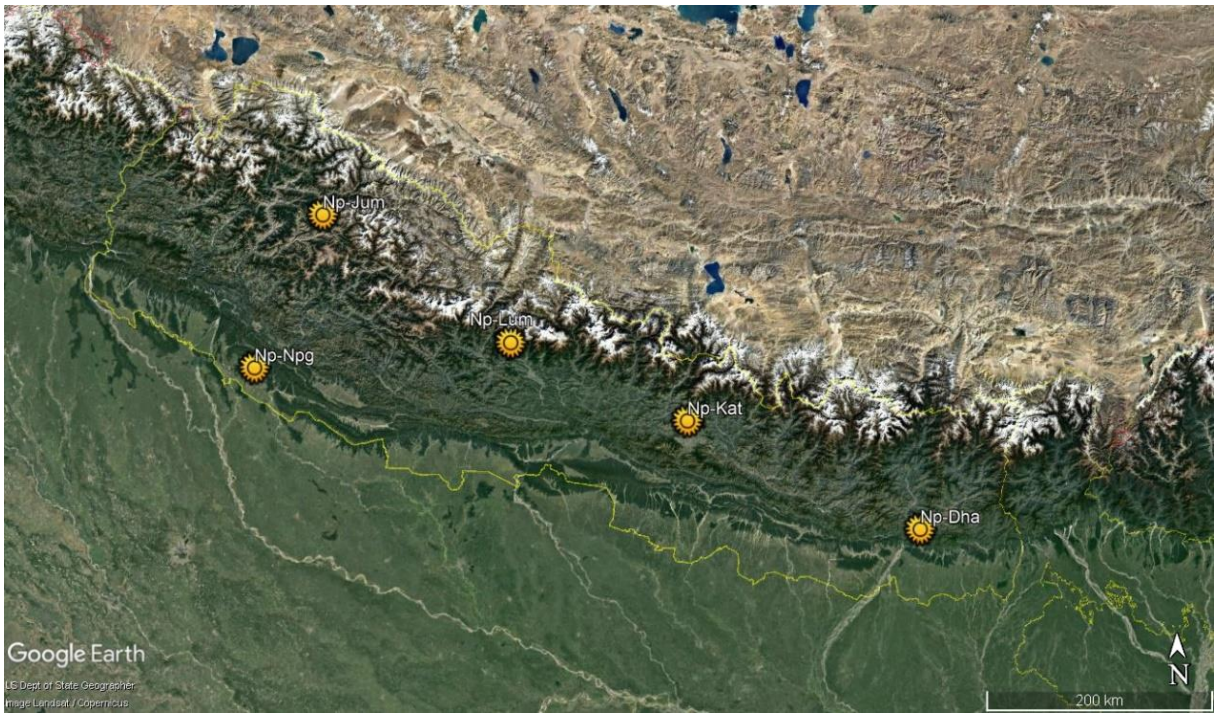

Figure 1: Overview of sites in Nepal

ESMAP Tier1 stations are equipped with a sun tracker, pyrheliometer and two ventilated pyranometers – one shaded for diffuse, one for global irradiance measurement. Further sensors are installed for temperature and humidity, barometric pressure, wind speed and direction on 10 m, and a tipping bucket rain gauge.

The stations were installed by CSPS, PITCO and PACE staff between 12 June and 29 July 2018. Data retrieval and quality review was done by CSPS; station maintenance was (and is) performed by local staff (OMT, On-Site Maintenance Team) appointed by the station host. Upon installation, the local personnel was briefed on the maintenance tasks. Their main task was to visually inspect the station and to clean the irradiance sensors on a work-daily basis – regular cleaning is important to maintain the high measurement accuracy of the equipment.

Regular inspection and maintenance visits were originally planned to be conducted in roughly six-month intervals.

The first inspection visit was done earlier than planned (between June and November 2018, different for each individual station) to rectify some operation ramp-up issues such as tracker misalignments, and to check on the equipment at the end of the first monsoon season.

After the end of the first year of measurement, a field verification of the irradiance sensor calibrations was carried out by co-locating traveling standard sensors for the duration of several hours. This field calibration verification was carried out in October 2019 during the regular maintenance visits. The result of this calibration verification was summarized in the 12 month site measurement report for each station. The traveling standard sensors are a pyrheliometer and pyranometer of identical model (Kipp&Zonen CHP1 and CMP21), calibrated directly against the World Radiometric Reference (WRR) in Davos by the World

Radiation Centre (WRC) at Physikalisch-Meteorologisches Observatorium Davos (PMOD) in June 2018.

Scheduled maintenance visits in 2020 could not be carried out as planned due to the COVID-19 pandemic. This also affected the repeated field calibration verification that was planned for the last scheduled maintenance visit. In late September and October 2020, some of the maintenance visits could be carried out (to three of five locations) and the planned field calibration verification of the irradiance sensors against the same traveling standard sensors was performed for those sites. The results are reported below for each of these stations individually.

The pandemic also prevented the planned handover of the weather stations to Nepalese institutions immediately after the 24 months ground measurement campaign, and the operation and maintenance of the stations by the Consultant was extended, although on a low-effort level only to ensure that functional weather stations will be handed over at the end of the project.

CSP Services GmbH, Köln, Germany

CSPS Technical Documentation

Client: The World Bank

Selection #: 1230234

- Solar Resource Measurement Campaign Nepal –

24-Month Site Measurement Report Dharan, Nepal

Birk Kraas
Anne Forstinger

CSP Services GmbH
Friedrich-Ebert-Ufer 30
51143 Köln/Cologne, Germany
Email: b.kraas@cspservices.de

Version 04 December 2020

CSP Services
CONCENTRATING SOLAR POWER SERVICES

Table 1: Site and installation information

Site and Installation Information	
Site:	General Classroom Building Rooftop Institute of Engineering, Purwanchal Campus, Dharan
Coordinates, Elevation:	26.79291°N, 87.29263°E (WGS84), 310 m
Station Type:	ESMAP Tier1 automatic weather station
Date of installation:	2018-06-19
Date of maintenance visits:	2018-10-25, 2019-10-15 & -16, 2020-10-08 to -10

1 Contents

2 Executive summary

25 months of meteorological measurement data was collected at the measurement site in Dharan between July 2018 and July 2020. This report summarizes the station operation during the reported measurement period.

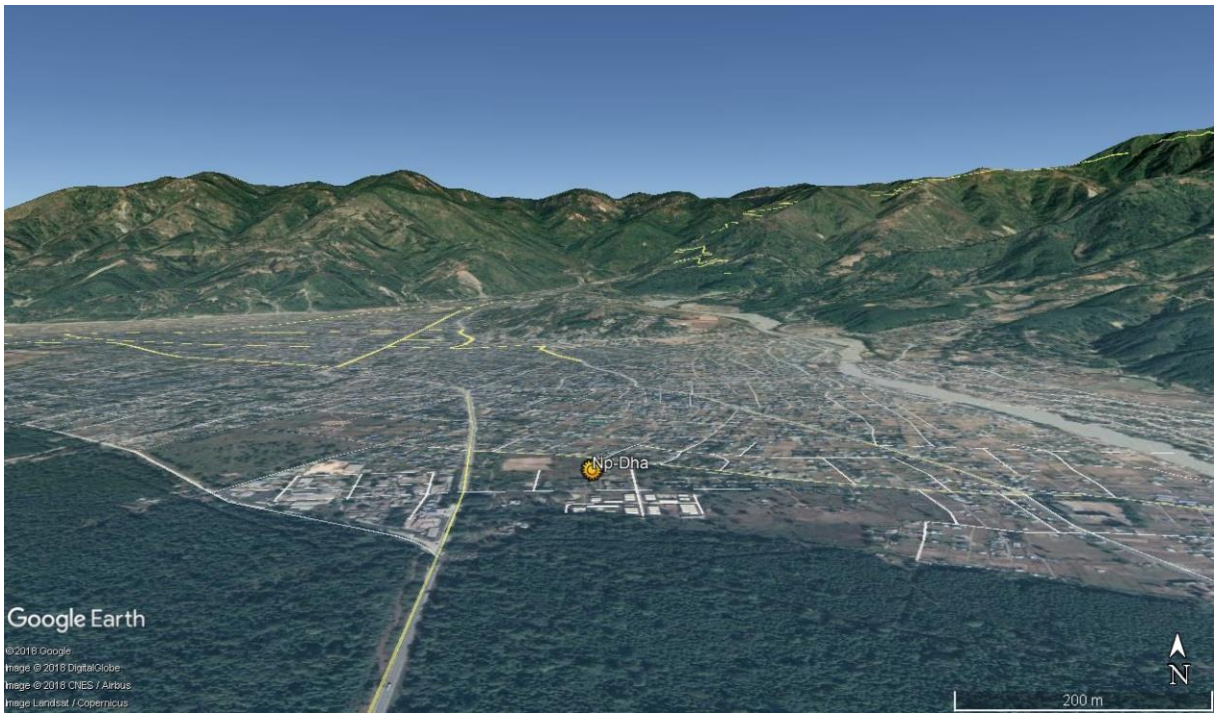

Figure 1: Site location south of Dharan (Image: Google Earth)

The Tier1 meteorological measurement station was installed at the site in Dharan on 19 June 2018 and visited for regular maintenance visit on 25 October 2018 and 16 October 2019.

Further scheduled maintenance visits in spring 2020 could not be conducted due to the lockdown and travel restrictions imposed resulting from the COVID-19 pandemic. One final maintenance visit with solar irradiance sensor comparison to reference sensors was conducted in October 2020, after the 24-month measurement period. Sensor comparison results are also reported in this document.

After an initial phase with sun tracker misalignment, the station was operating correctly, the data availability was 100% (no data gaps) and the local maintenance (work-daily sensor cleaning and visual check) was done mostly on schedule and according to the defined procedures.

The measurement data collected after the reporting period is not subject of this report.

3 Equipment description and functionality, sensor calibration

3.1 Measurement equipment

The Tier1 automatic weather station is equipped with a datalogger and a GSM modem, a sun tracker equipped with an ISO9060 First Class pyrheliometer for DNI measurement and ISO9060 Secondary Standard pyranometers for measurement of GHI and DHI. As additional meteorological sensors, an anemometer and a wind vane for wind speed and direction measurement on 10 m height, a barometric pressure sensor, a tipping bucket rain gauge and a temperature and humidity sensor are installed. The exact types of sensor/equipment and serial numbers are listed in the tables below.

Table 2: Equipment and serial numbers

Equipment and serial numbers		
Automatic Weather Station	CSP Services MHP Automatic Weather Station	CSPS.MT.18.203
Main Control Box	CSP Services	CSPS.CA.18.202.0002
Datalogger	Campbell CR1000	E12051
Datalogger peripherals	CFM100 CF Module	14203
Sun Tracker	K&Z Solys2	180408
Sun Sensor	K&Z Sun Sensor Kit	170321
GSM Modem	Sierra Wireless Xtend	
GPS Module	Garmin 16x HVS	1A4250265
Power Supply	4x100 W PV modules, 4x150 Ah solar battery	Connected as 200 W, 300 Ah @24VDC

Table 3: Measured Parameters and Sensors

Measured parameter	Unit	Sensor type	Serial number
GHI	W/m²	K&Z CMP21, w. CVF4 ventilation unit	170862
DHI	W/m²	K&Z CMP21, w. CVF4 ventilation unit	170863
DNI	W/m²	K&Z CHP1	180581
Temperature	°C	Campbell CS215	E20178
Humidity	%	Campbell CS215	E20178
Pressure	hPa	Setra 278	7225860
Precipitation	mm	Young 52203	TB 14378
Wind Speed	m/s	NRG #40C anemometer	1795-00303667
Wind direction	°N	NRG #200P wind vane	1799-00019689

3.2 Equipment functionality

After an initial alignment problem of the sun tracker in July 2018, the functionality of the equipment was good, the station was operating without significant problems.

The barometric pressure data had to be replaced with elevation-adapted data from a different measurement station (Np-Npg in Nepalgunj) for extended periods. The measurement error was due to insects nesting in the tube connecting the barometric pressure sensor with the exterior of the control box (pressure exchange tube). On some occasions, the sun tracker was not well aligned. This may have been due to changes of alignment resulting from loosening bolts or similar. Where possible, data was corrected by modeling/interpolating DHI and calculating DNI from the modeled DHI.

On several occasions, dew or droplets on the pyrheliometer was noticed. This presumably happened at fog events or in the morning. Impact on the data was negligible since the dew evaporated quickly. Further, the DHI pyranometer ventilation unit failed at several occasions and was replaced in October 2019 and October 2020.

Notable events at the station are listed in Table 4.

Table 4: Notable events during operation

Date	Event
2018-07-01 to -22	Sun tracker misaligned, no DNI and DHI measurement data available in this period. Due to this misalignment, one month was added to total measurement duration
2018-07-22	Station maintenance (improvement of sun tracker alignment)
2018-10-25	Station maintenance (regular maintenance visit)
2018-10-28 to 10-31	BP data replaced
2019-05-21	BP data replaced
2019-06-07 to 06-14	BP data replaced
2019-06-16 to 09-18	BP data replaced
2019-06-18	Dew on pyrheliometer front window
2019-09-11, -15, -16, -21	Dew on pyrheliometer front window
2019-10-07, -08, -11, -12, -13, -15	Sun tracker misaligned in the morning; DHI modeled, DNI calculated from GHI and modeled DHI
2019-10-15, -16	Station maintenance (regular maintenance visit)
2019-10-26	Ventilation unit failure, DHI offset corrected
2019-12-28	Ventilation unit failure, DHI offset corrected
2020-01-05	Dew on pyrheliometer front window
2020-01-11	Ventilation unit failure, DHI offset corrected
2020-01-31	Ventilation unit failure, DHI offset corrected

3.3 Sensor calibrations

Factory calibrations

All sensors were calibrated before deployment in the field. The thermopile pyranometers and pyrheliometers were calibrated in the factory by the manufacturer according to applicable ISO standards. Other meteorological sensors (wind speed sensor, barometric pressure sensors) were also calibrated by the respective manufacturer. Calibration certificates were handed over with the installation report.

Pyrheliometer and pyranometer field calibration verification

Upon the second and third maintenance visits, an irradiance sensor comparison against traveling standard sensors was performed. The travelling standard sensors were calibrated against the World Radiometric Reference (WRR) at Davos (Switzerland) prior to their delivery to Nepal. The following equipment was installed for the comparison measurement:

- An additional pyrheliometer mounting clamp for a travelling standard reference pyrheliometer on the sun tracker
- An instrument table with mounting place for a reference pyranometer (to have the reference pyranometer installed on the same height as the other pyranometers on the ventilation units)
- Reference sensors at the described additional mounting places:
    - CHP1 Pyrheliometer SN 180580, Sensitivity: 8.096 µV/Wm²
    - CMP21 Pyranometer SN 170858, Sensitivity: 8.84 µV/Wm²

  Calibration certificates from PMOD WRC are attached to this report.

Figure 2: Tracker with regular (1) and reference pyrheliometer (2), reference pyranometer (3)

Figure 3: Tracker with DHI pyranometer (4) GHI pyranometer (5), reference pyranometer (3)

All sensors were measured with 1 Hz resolution, and the measurements were stored on the datalogger in 1 min averages.

3.4 Comparison method - pyrheliometer

The comparison measurement for pyrheliometers was set up following the measurement set-up procedures and recommendations described in ISO 9059 as closely as possible. *Please note: This cross-comparison is not a full ISO-compatible calibration, as this was not the scope of the cross-comparison. The ISO standard was only followed as far as possible to obtain comparable results while adhering to best practices procedures.*

If both pyrheliometers are calibrated correctly, the observed deviation between the compared instruments should be within the combined calibration uncertainty. For the installed CHP1 sensor, Kipp&Zonen specifies a calibration uncertainty of ±1.1%. For the reference sensor, a calibration uncertainty of ±0.32 % is specified by PMOD (both at 95% coverage probability, stated in the calibration certificates). The combined calibration uncertainty is therefore ±1.15%. No other additional uncertainty contributions are added, since both devices are of identical model and installed on the same sun tracker, using the same datalogger. The final combined uncertainty is therefore ±1.15%, which can be interpreted as a strict limit since instrument-specific uncertainty contributions such as instrument temperature or individual alignment are neglected.

The measurement data from both sensors (reference and sensor to be compared) was filtered as follows:

- Only data where no soiling correction was applied (perfectly clean sensor windows)
- Only values with DNI >700 W/m² were used (acc. to ISO 9059) where this was possible.
- Outliers filtered and discarded (e.g., temporary shading of a single instrument due to maintenance staff passing the station or similar)
- Stable irradiance conditions (ideally, clear-sky conditions), if possible

Enough data was available to apply these filter criteria and still have a sufficient amount of comparison data for all individual sensors.

The graph in the result section shows the perfect fit (exact identical measurement of reference and tested sensor) as the angle bisector in red. Above and below the bisecting line is the corridor defined by adding/subtracting the combined calibration uncertainty. If the used calibration constant of the tested sensor is correct, the vast majority of all measurement values (shown as blue triangle markers and named as "DNI") must be within this corridor.

3.5 Comparison results - pyrheliometer

The results shown in this report refer only to the comparison on 9 October 2020. The previous comparison in 2019 was reported on in the 12 Month Site Measurement Report.

113 values (1-minute averages) remain after applying the filters. This is a sufficient amount of data for a comparison.

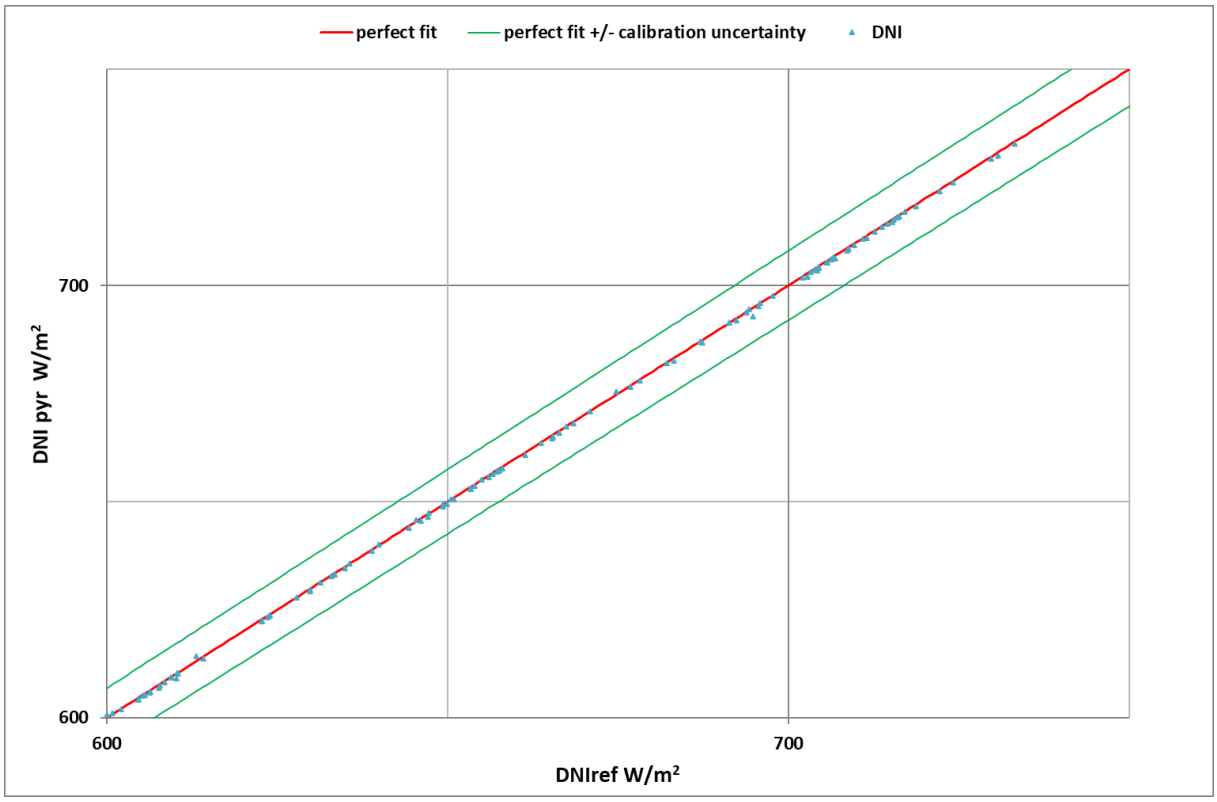

Figure 4: Comparison of pyrheliometer CHP1 SN180581 (vertical axis) to traveling standard pyrheliometer CHP1 SN180580 (horizontal axis)

All measurement values lie inside of the specified combined measurement uncertainty of ±1.15 %. The outliers may be due to interactions of the staff working at the station during the maintenance visit.

The sensitivity calibration of this sensor is accepted as correct and valid.

3.6 Comparison method - pyranometers

The comparison measurement for pyranometers was set up following the measurement set-up procedures and recommendations described in ISO 9847 as closely as possible. *Please note: This cross-comparison is not a full ISO-compatible calibration, as this was not the scope of the cross-comparison. The ISO standard was only followed as far as possible to obtain comparable results while adhering to best practices procedures.*

If both instruments are calibrated correctly, the observed deviation between the compared instruments should be within the combined calibration uncertainty. For the installed CMP21 pyranometers, Kipp&Zonen specifies a calibration uncertainty of ±1.35%. For the reference sensor, a calibration uncertainty of ±1.24 % is specified by PMOD (both at 95% coverage probability, stated in the calibration certificates). The combined calibration uncertainty is therefore ±1.83%. No other additional uncertainty contributions are added, since all devices are of identical model and installed on the same sun tracker, using the same datalogger. The final combined uncertainty is therefore ±1.83%, which can be interpreted as a strict limit since instrument-specific uncertainty contributions such as instrument temperature or individual alignment are neglected.

These values were determined at high incidence angles and with high global irradiance values. The uncertainty for lower sun elevations and lower GHI values may be significantly higher [1]. Therefore, only high sun elevation and high GHI values were utilized for the comparison.

The measurement data from all three sensors (reference and sensors to be compared) was filtered as follows:

- Only values with sun elevation > 20° were used (acc. to ISO 9847)
- Only values with GHI > 300 W/m² were used to exclude bad weather conditions
- Only series of minimum numbers of consecutive values were used for the comparison (following ISO 9847)
    - In periods with cloudless skies: min. 10 consecutive values
    - In periods with some clouds: min. 1-5 consecutive values
    - In cloudy sky (overcast): not used
- Outliers not considered (e.g., temporary shading of a single instrument due to maintenance staff cleaning the sensor or similar)

Enough data was available to apply these filter criteria and still have a sufficient amount of comparison data.

The graphs in the result section show the perfect fit (exact identical measurement of reference and tested sensor) as the angle bisector in red. Above and below is the corridor defined by adding/subtracting the combined calibration uncertainty. If the calibration factor or the tested sensor is corrected, the vast majority of all measurement values (shown as blue triangle markers named as "GHI Pyranometer" or "DHI Pyranometer", the naming refers to the mounting place on the tracker and for which measurement these pyranometers are usually used) must be within this corridor.

3.7 Comparison results - pyranometers

The results shown in this report refer only to the comparison on 9 October 2020. The previous comparison in 2019 was reported on in the 12 Month Site Measurement Report.

292 values (1-minute averages) on 9 October 2020 fulfilled the selection criteria. This is a sufficient amount of data for this comparison.

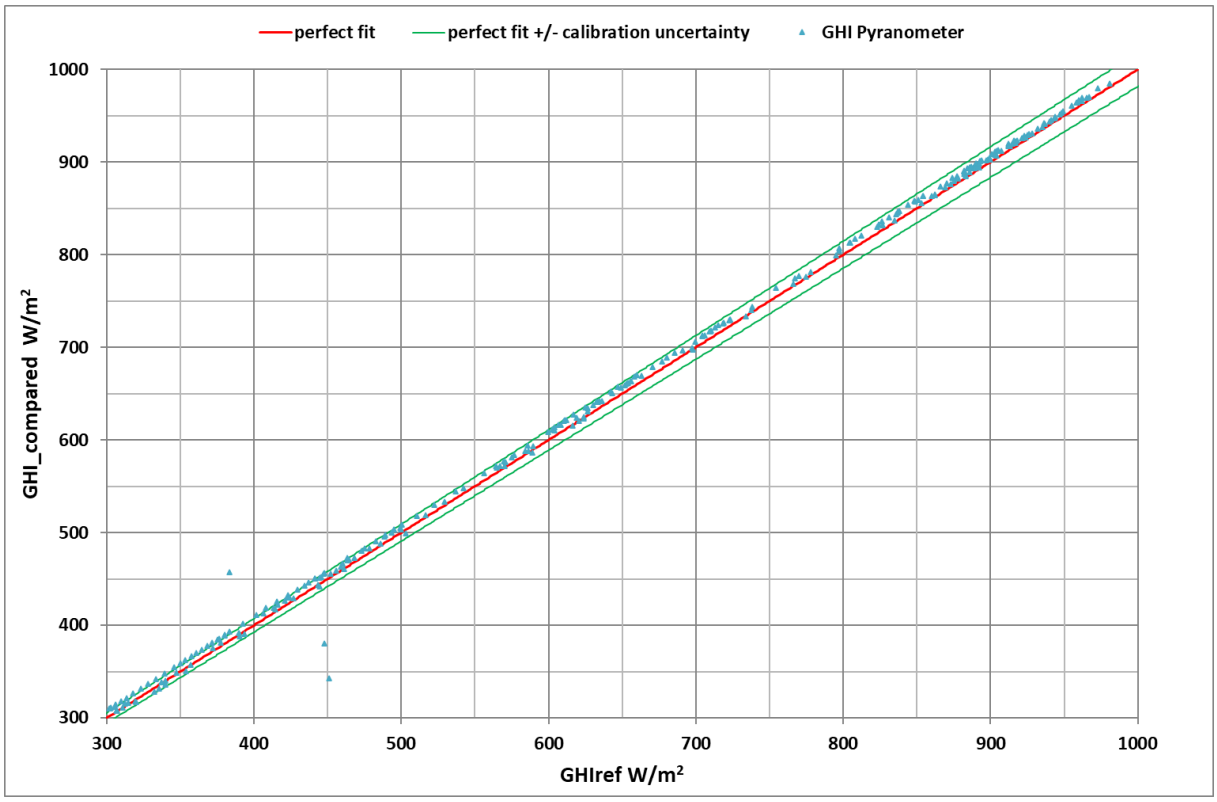

Figure 5: Comparison of GHI pyranometer CMP21 SN170862 (vertical axis) to traveling standard pyranometer CMP21 SN170585 (horizontal axis)

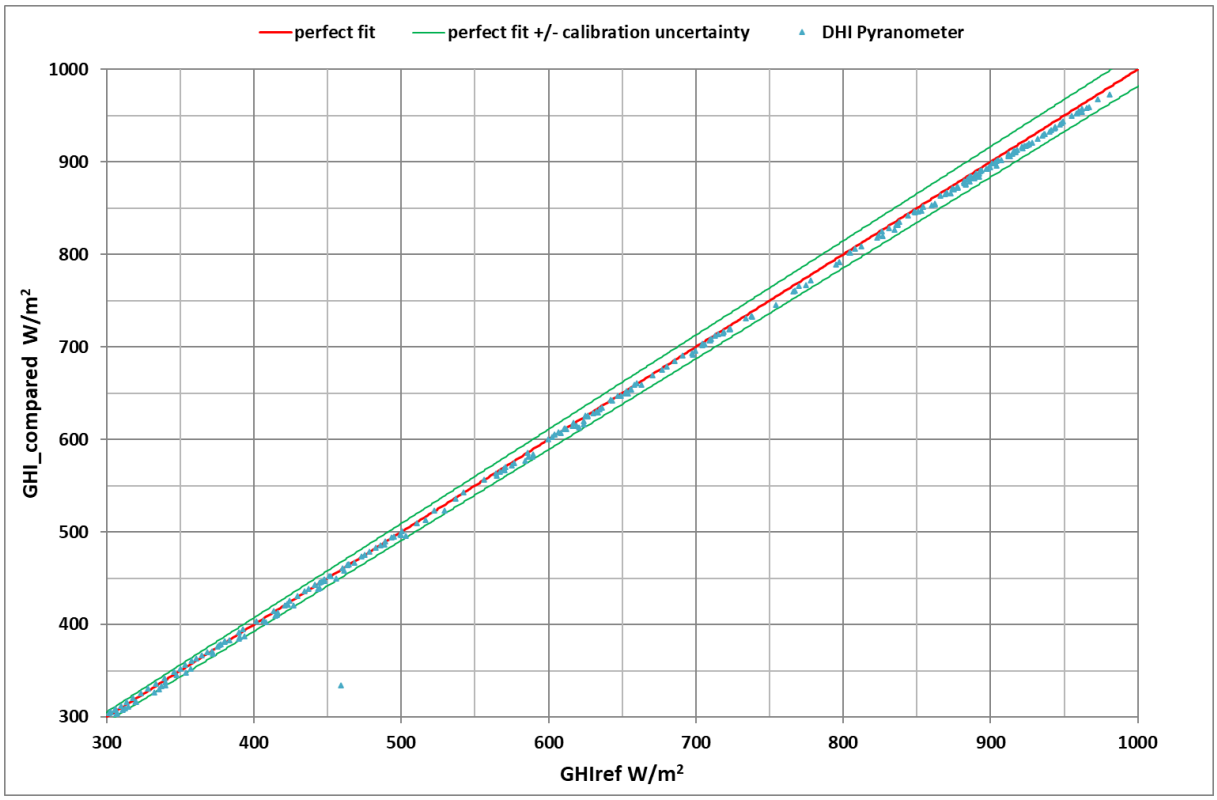

Figure 6: Comparison of DHI pyranometer CMP21 SN170863 (vertical axis) to traveling standard pyranometer CMP21 SN170585 (horizontal axis)

Except for a few outliers due to work on the station or external influence, all measurement values from the dataset lie inside of the specified combined measurement uncertainty of ±1.83 %. The sensitivity calibration of both sensors is accepted as correct and valid.

4 Measurement results

Table 5 shows the monthly summary values of all measurement variables at this weather station. Each parameter is discussed in more detail in the following sections.

***Table 5: Monthly irradiation sums and average meteorological data** (*incomplete month/year)*

Month	Irradiance sums [kWh/m²]			Avg. Temp. [°C]	Avg. RH [%]	Avg. WS [m/s]	Avg. Press [hPa]	Sum Rain [mm]	Usable data
	GHI	DNI	DHI						
Jul 2018*	157	-*	-*	28.5	83	1.7	964	377	-
Aug 2018	149	69	94	28.3	84	1.1	965	140	100 %
Sep 2018	136	80	78	27.6	84	0.9	971	252	100 %
Oct 2018	149	120	71	25.0	73	1.2	976	33	100 %
Nov 2018	122	126	50	22.0	66	1.2	978	0	100 %
Dec 2018	108	135	38	18.9	61	1.1	979	0	100 %
Jan 2019	109	116	47	18.2	57	1.3	980	0	100 %
Feb 2019	103	76	55	19.4	67	1.4	978	76	100 %
Mar 2019	156	115	74	23.2	55	1.6	975	38	100 %
Apr 2019	171	106	87	26.2	66	1.9	972	100	100 %
May 2019	173	86	101	27.7	75	1.7	969	70	100 %
Jun 2019	161	77	96	28.9	78	1.5	966	156	100 %
Jul 2019	130	60	84	27.5	87	1.6	964	710	100 %
Year 1	**1667**	**1166**	**875**	**24.4**	**71**	**1.4**	**973**	**1575**	**100 %**
Aug 2019	161	97	89	28.9	82	1.4	966	49	100 %
Sep 2019	134	83	72	26.9	86	1.2	973	0	100 %
Oct 2019	133	100	69	25.0	81	0.9	976	1	100 %
Nov 2019	118	112	54	23.4	72	1.1	977	0	100 %
Dec 2019	105	115	45	17.2	71	1.2	980	2	100 %
Jan 2020	95	73	54	15.9	77	1.1	979	14	100 %
Feb 2020	117	82	65	19.1	65	1.5	979	36	100 %
Mar 2020	156	123	69	22.8	66	1.4	975	52	100 %
Apr 2020	160	103	82	25.6	61	1.7	974	61	100 %
May 2020	159	85	90	26.3	78	1.5	970	150	100 %
Jun 2020	131	57	87	27.5	86	1.3	967	418	100 %
Jul 2020	120	38	89	27.3	90	1.0	967	562	100 %
Year 2	**1589**	**1068**	**865**	**23.8**	**76**	**1.3**	**974**	**1345**	**100 %**

July 2018 is not used for annual total or average values due to tracker misalignment in that period. DNI and DHI values were not measured correctly. Therefore, the measurement period was extended by one month in order to obtain complete 24 months including DNI and DHI values.

4.1 Solar irradiance

Figure 7 shows the measured monthly irradiance sums in a bar chart. A seasonal dependency of the irradiance sums is visible. Monthly global irradiance sums are generally higher in the summer season whereas the monthly direct irradiance sums are generally higher in winter, with diffuse irradiance behaving the opposite way to direct irradiance. This can be explained with the monsoon season that reduced DNI during the monsoon months with strong cloud cover. GHI is still high in these months because of the longer daylight duration per day and high sun elevation. In winter (dry season), the sky is more often showing clear-sky conditions leading to higher DNI values.

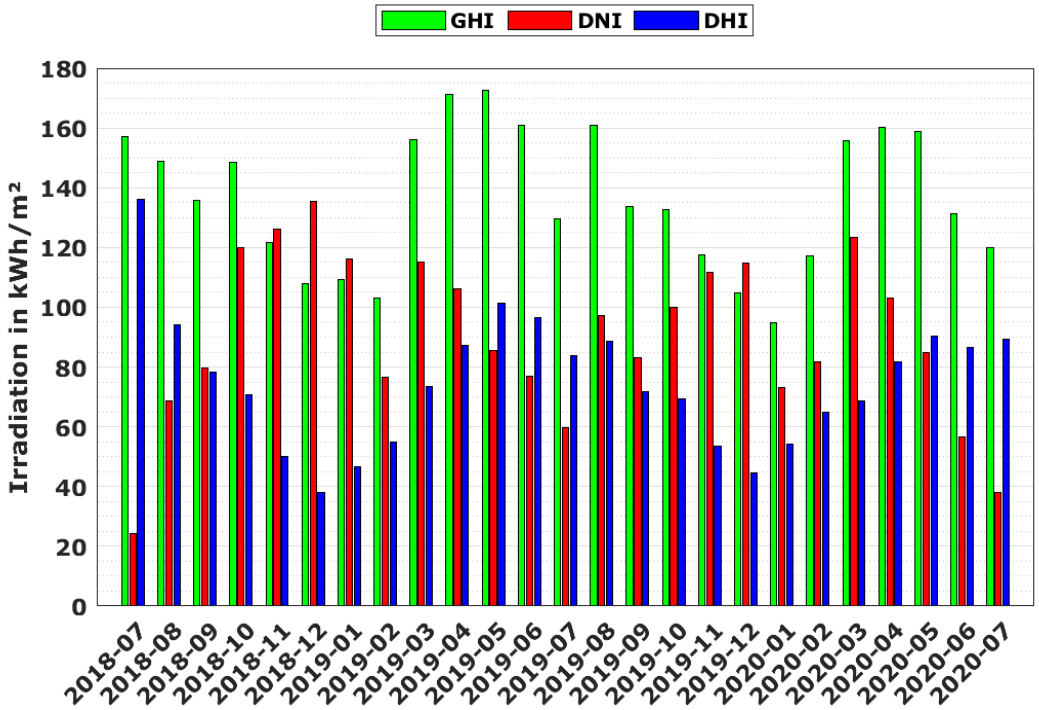

Figure 7: Monthly irradiation sums 2018-07 to 2020-07

As mentioned before, the sun tracker was misaligned until 22 July 2018. No DNI or DHI data is available for the period before. Therefore, in July 2018 DNI sum is small and DHI sum appears overly large because during most of the time, DHI was measured identical to GHI. The DNI and DHI bars in Figure 7 can therefore be ignored for July 2018.

The frequency distribution of hourly irradiance values (Figure 8) shows occurrence peaks for DNI (scale on the left axis) and DHI (scale on the right axis). The frequency distribution of GHI values (scale on left axis) is broad with no expressed occurrence peak. The broad peak for DNI values is just above 600 W/m² and generally, DNI values above 300 W/m² are frequent, but high values of more than 900 W/m² almost do not occur. The diffuse hourly irradiance frequency peaks at around 150 W/m².

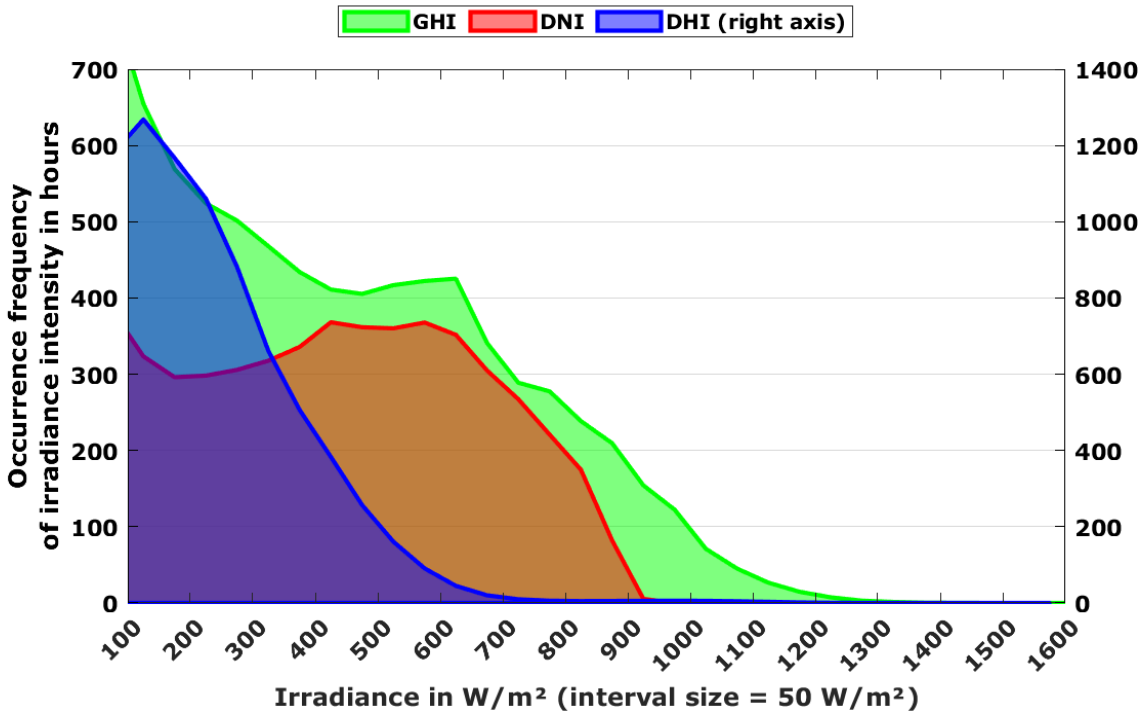

Figure 8: Frequency distribution of hourly irradiance averages 2018-07 to 2020-07

Figure 9 and Figure 10 show the irradiance intensity for GHI and DNI over the 25 months measurement period. The irradiation intensity and the length of the days vary with the seasons.

GHI is strongest during the summer period (Figure 9), corresponding to the high solar elevation periods. Cloudy periods with low GHI values occur mostly in the monsoon period.

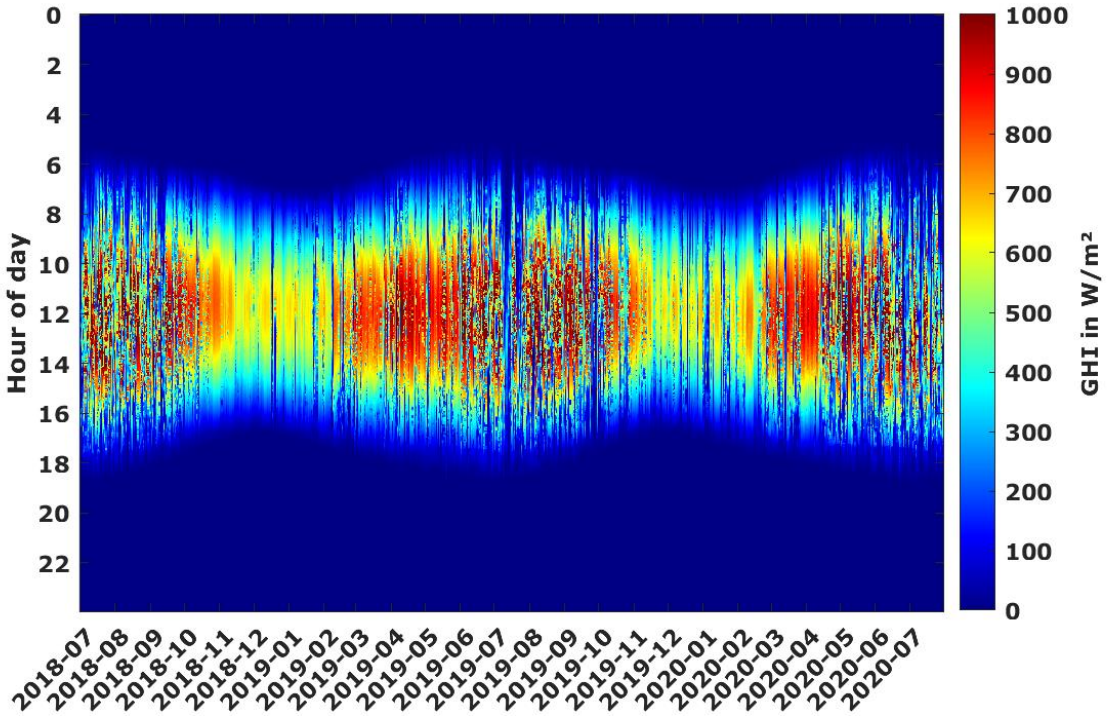

Figure 9: GHI irradiance intensity 2018-07 to 2020-07

The DNI values (Figure 10) show high irradiance intensities of above 700 W/m² and more during brief periods in the winter months and after the end of the monsoon. Periods with low or no DNI (cloud cover or aerosol load) occur mainly in monsoon season. Due to the higher sensitivity of DNI to reductions by cloud cover or aerosols, low DNI periods occur more often than for GHI, hence the more fragmented appearance of the DNI plot.

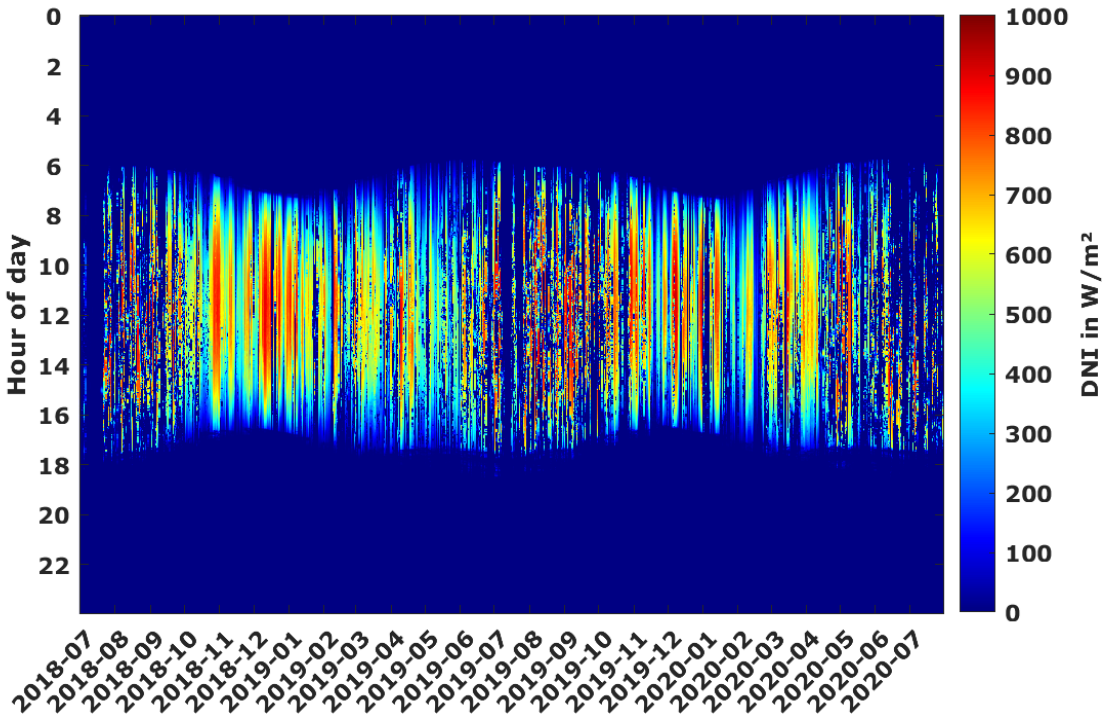

Figure 10: DNI irradiance intensity 2018-07 to 2020-07

4.2 Temperature and humidity

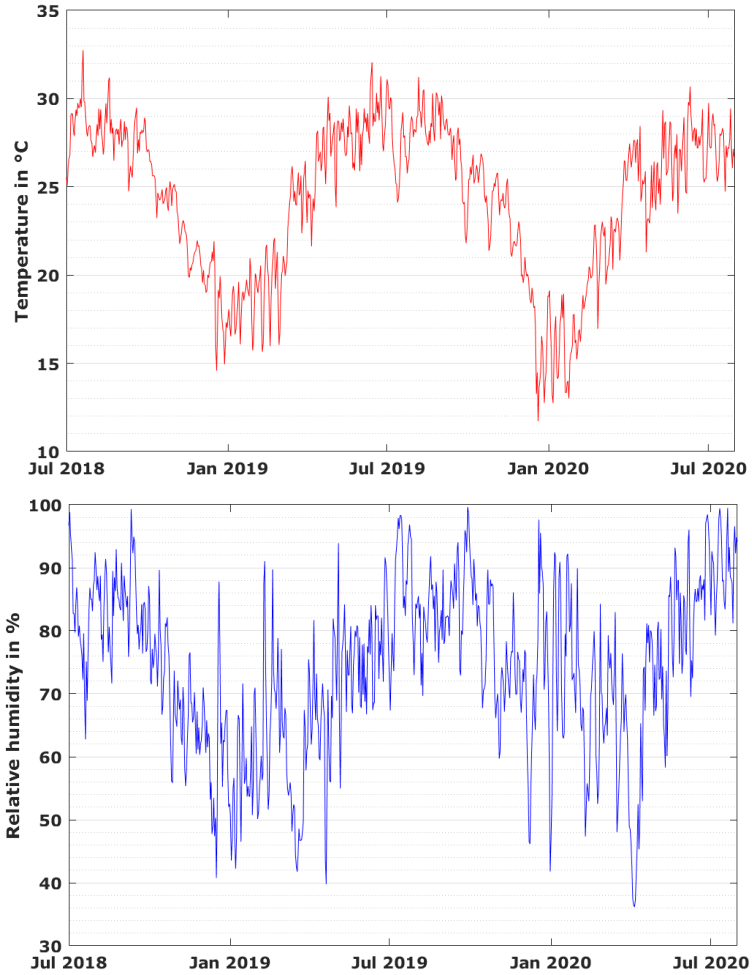

Figure 11: Daily temperature and relative humidity averages

Figure 11 shows daily averages of temperate and relative humidity. A seasonal dependency is visible. Temperature is lowest in the northern hemisphere winter months (November to February) and high in the summer months. The month with the highest average temperature is June, the coldest monthly average temperature was in January. The most frequent temperature is 27°C (Figure 12). Daily relative humidity averages were highly variable, with tendentially lower humidity in the winter months (which were also the months with highest DNI sums) and high humidity during the monsoon season.

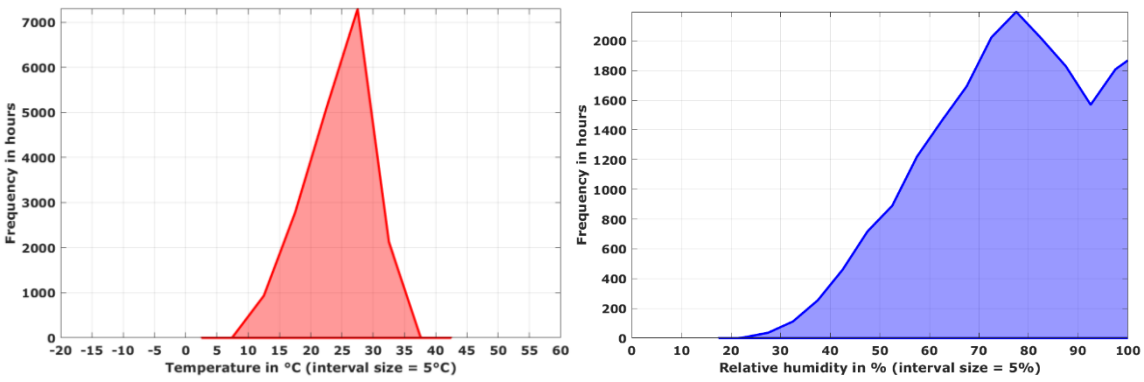

Figure 12: Frequency distribution of temperature and relative humidity (1-minute resolution)

4.3 Barometric pressure

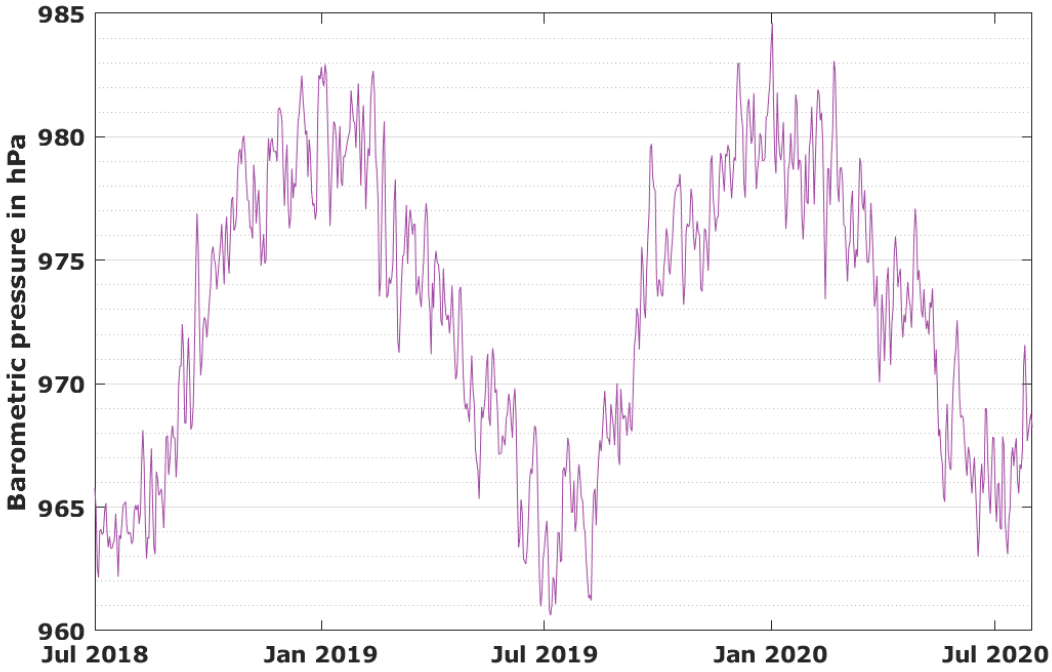

Figure 13: Daily averages of barometric pressure

Figure 13 shows daily averages of barometric pressure. Again, a clear seasonal dependence is visible: Higher pressure in the winter months and lower pressure in the summer months. Figure 14 shows the frequency distribution of recorded 1-minute resolution barometric pressure values.

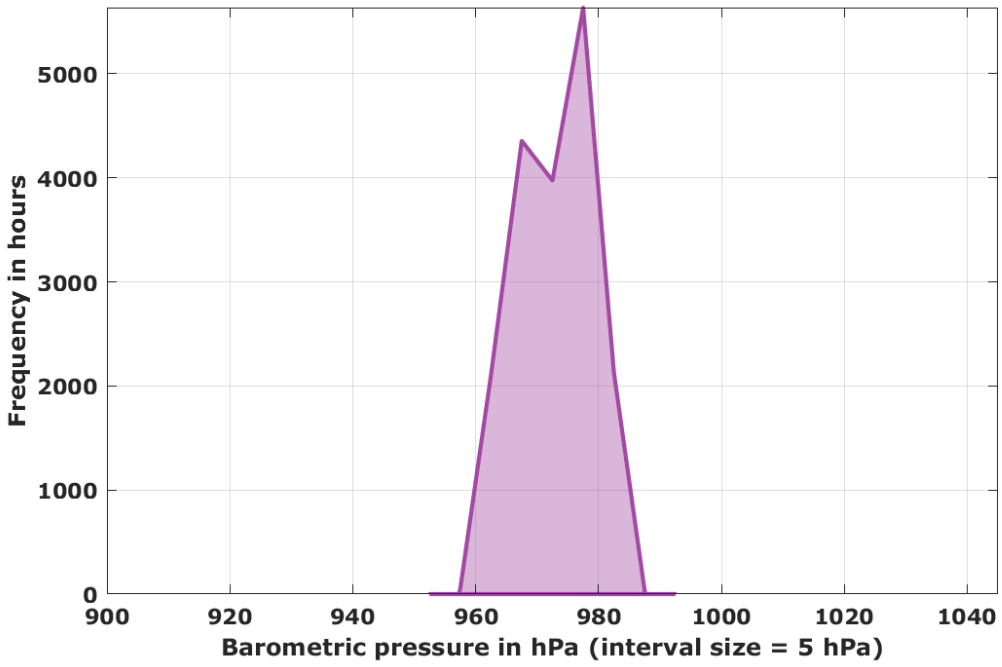

Figure 14: Frequency distribution of barometric pressure (1-minute resolution)

4.4 Precipitation

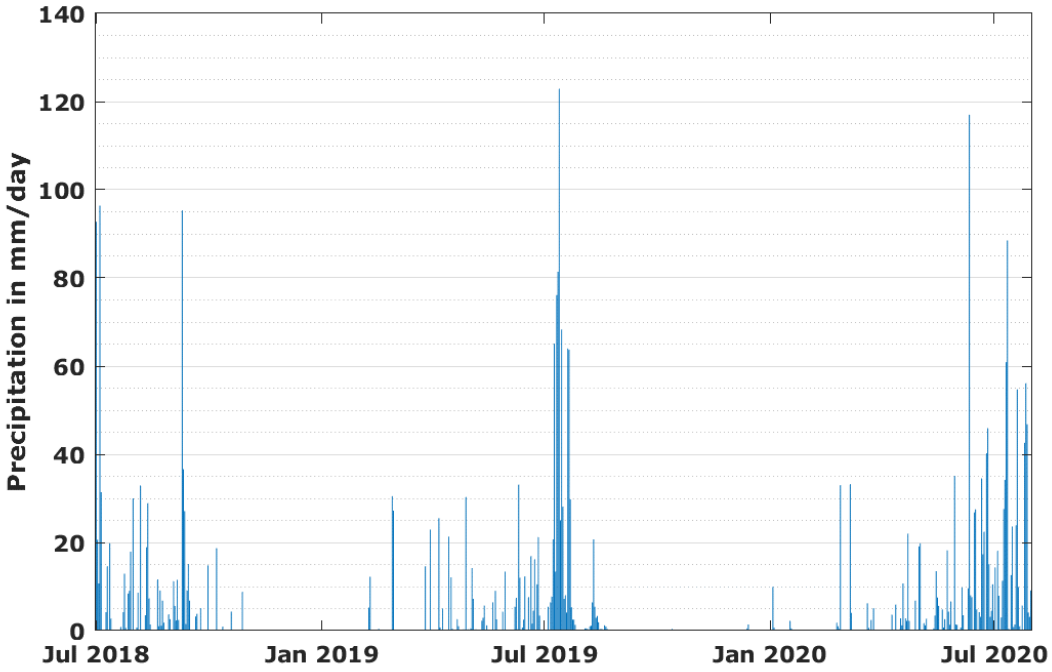

Figure 15: Daily sums of precipitation

Figure 15 shows the daily sums of precipitation. Again, a clear seasonal variability was observed with a dry period with no precipitation from November to January and an expressed rainy season in the months of June to September. The periods differed slightly in both years of the measurement campaign, e.g. in the second year, no rainfall was recorded in September while in the first year, it was a month with high rainfall.

4.5 Wind speed and direction

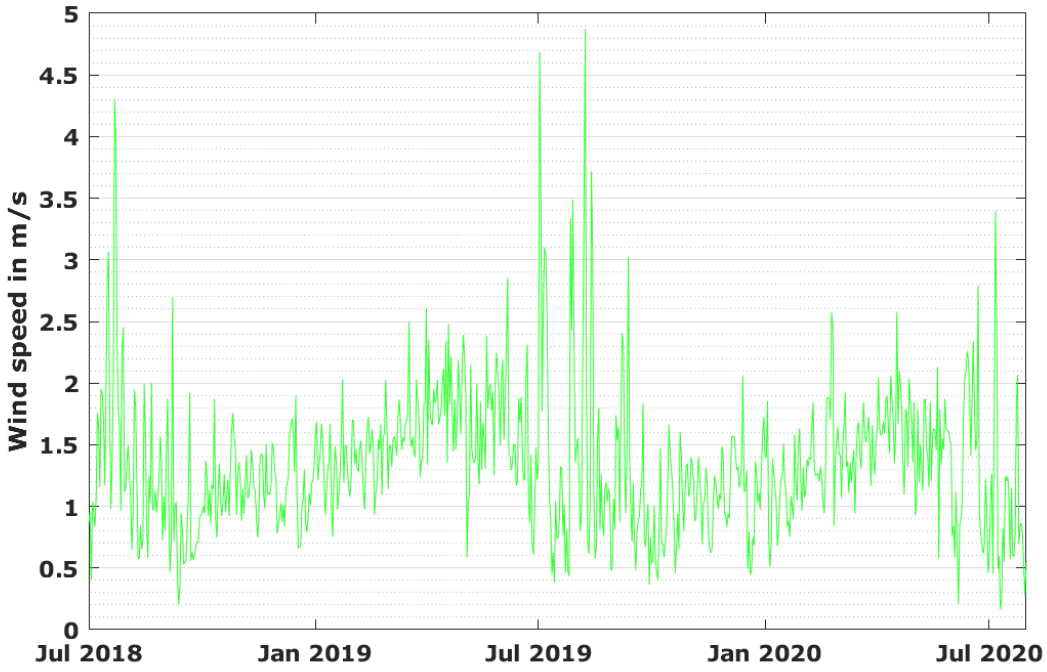

Figure 16: Daily averages of wind speed

Figure 16 shows the daily averages of wind speed. They are continuously low and almost no seasonal dependency was observed. The frequency distribution, shown in Figure 17, emphasizes that wind speeds of <4 m/s are common and wind gusts of up to only 8 m/s were observed with any meaningful quantity.

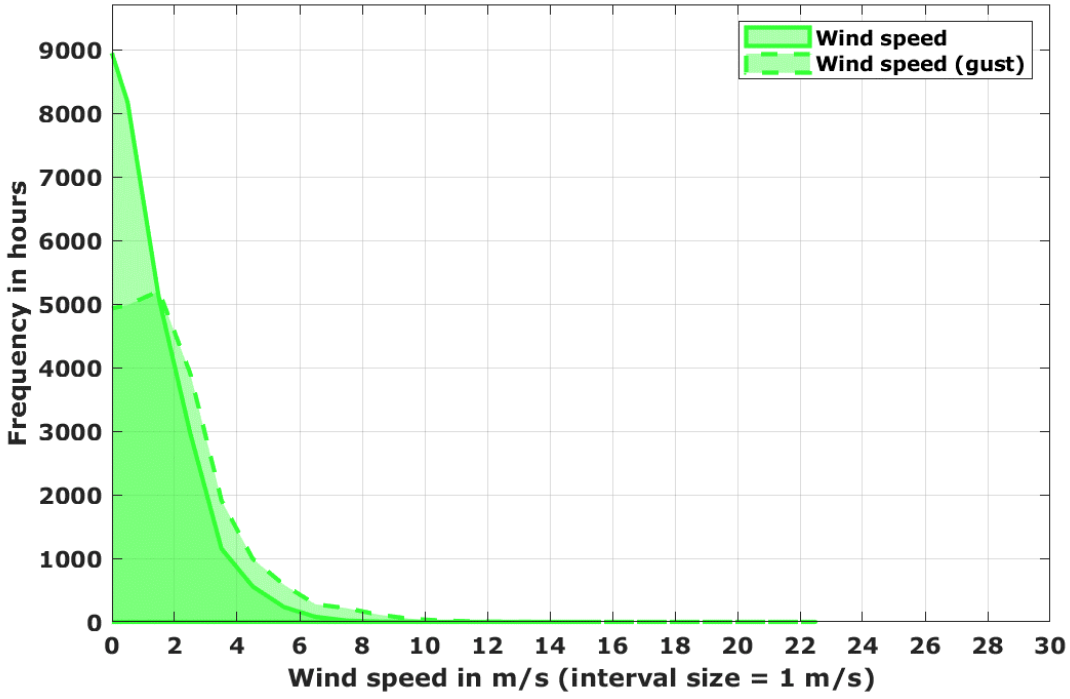

Figure 17: Frequency distribution of wind speeds (1-minute values)

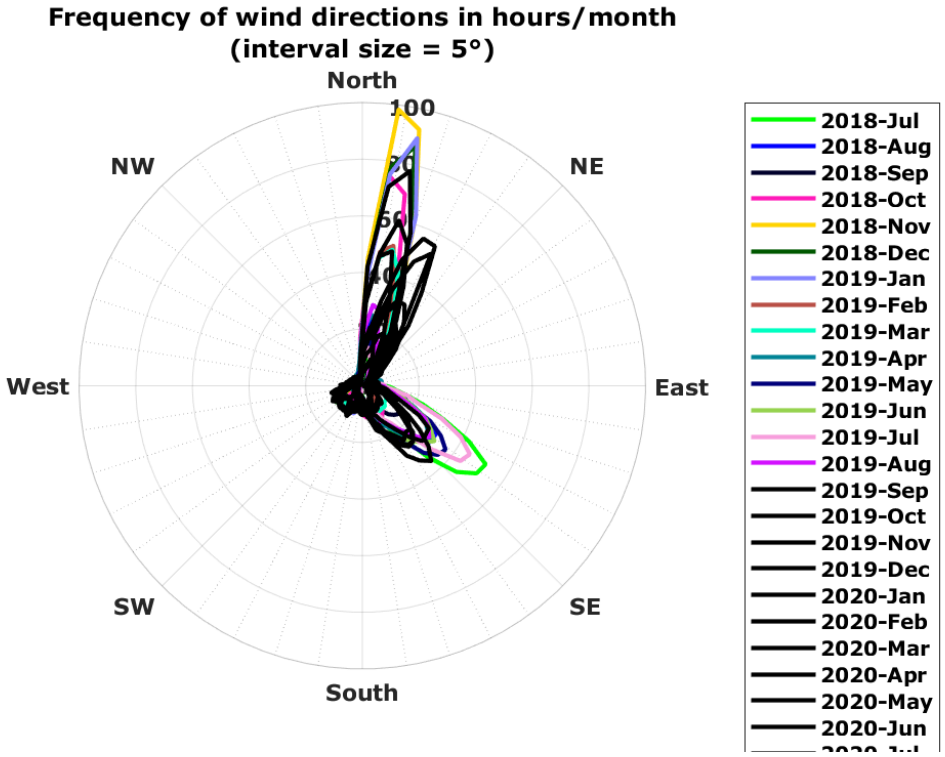

Figure 18: Wind direction distribution 2018-07 to 2020-07

Figure 18 shows the frequency distribution of wind direction in 1-minute time resolution. Two clear main wind directions are visible: From southeast during the months May to July, North-northeast from October to March, with transitionary months which show both prevailing wind directions in August, September and April. Figure 19 shows that additionally to the two main wind directions, the few high wind gusts >14 m/s also occurred from West and South-west directions.

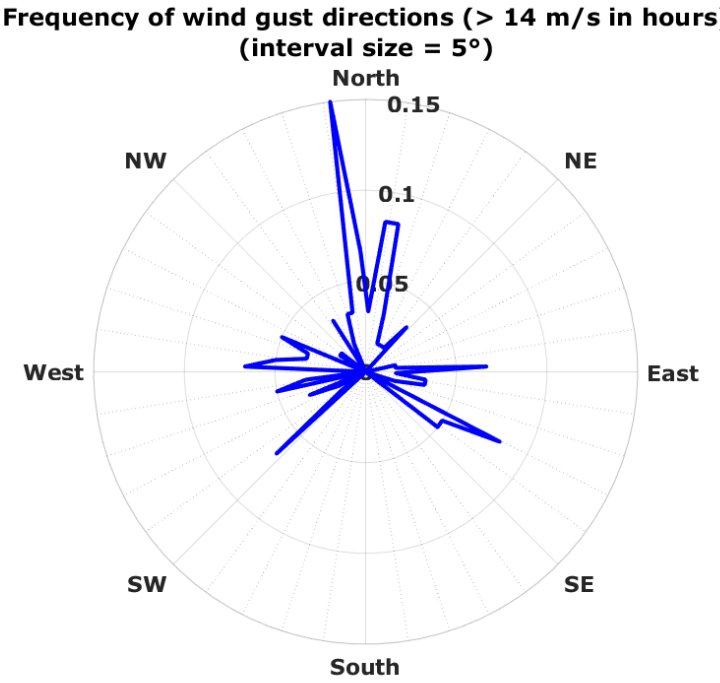

Figure 19: Wind gust direction distribution 2018-07 to 2020-07

5 On-site maintenance and irradiance sensor cleaning

The maintenance on site was done by local personnel. They were contracted and specially trained for this task upon installation of the station. The maintenance on site consisted mainly of visual inspection of the equipment, verifying the sensor alignment and cleaning the irradiance sensors and PV modules. The cleaning was scheduled to be performed on a work-daily basis, which was almost always adhered to throughout the whole measurement campaign with a ramp-up phase in the beginning of the campaign. Overall, 83% of all days had a cleaning event. The exact cleaning dates and times are recorded in the monthly measurement reports and in the measurement data.

Table 6 gives an overview of the maintenance frequency per month.

Table 6: Number of maintenance visits by local staff per month

Month	Maintenance visits
Jul 2018	10
Aug 2018	23
Sep 2018	12
Oct 2018	23
Nov 2018	29
Dec 2018	27
Jan 2019	17
Feb 2019	18
Mar 2019	29
Apr 2019	29
May 2019	29
Jun 2019	29
Jul 2019	28
Aug 2019	30
Sep 2019	27
Oct 2019	24
Nov 2019	29
Dec 2019	29
Jan 2020	28
Feb 2020	26
Mar 2020	29
Apr 2020	25
May 2020	28
Jun 2020	25
Jul 2020	26

6 Irradiance sensor soiling rates and soiling behavior

6.1 Soiling rates of DNI sensor (pyrheliometer)

All data from the pyrheliometer was corrected for sensor soiling by applying a linearly interpolated cleanliness factor[1] to the measurement data where applicable and necessary, i.e. only where cleanliness factor at cleaning was not 1. It has to be noted that cleanliness factors can only be determined under certain conditions:

- The cleaning is performed correctly and swiftly (no influencing of sensors except during a few seconds in the cleaning process)
- The irradiation conditions are stable enough to distinguish signal increase resulting from dust removal from natural fluctuations
- The signal increase resulting from dust removal is sufficiently large to be detectable

If no analysis is possible, soiling correction is not applied.

Table 7 on the next page shows

- Simplified average sensor cleanliness factors of the pyrheliometer DNI sensor detected at the above described cleaning events
- Simplified average daily soiling rate of the pyrheliometer. This rate expresses how much the irradiance sensor signal is reduced each day without cleaning. Simplified in this context means that the rate is a simple average of the change of cleanliness factors over all days of the month
- The minimum cleanliness factors (i.e., maximum sensor soiling) observed just before the sensor cleaning. Especially on/after strong wind occasions such as e.g. dust storms, high singular soiling rates can be observed. The daily cleaning ensures that these single events with high soiling do not influence long periods of data (usually only up to one day) and were mostly well corrigible

[1] Sensor cleanliness factor is defined as the dimensionless factor by which the recorded measurement value has to be divided in order to obtain the soiling-corrected value. E.g., if at cleaning a signal increase of 3% has been detected, the factor before the cleaning is 1/(1+0.03) = 0.97, after the cleaning (clean sensors) = 1.

Table 7: Average sensor cleanliness factors (pyrheliometer)

Month	Average sensor cleanliness	Minimum cleanliness factor	Average daily soiling rate
Jul 2018	1.00	1.00	0.0 %
Aug 2018	1.00	1.00	0.0 %
Sep 2018	1.00	1.00	0.0 %
Oct 2018	1.00	1.00	0.0 %
Nov 2018	1.00	1.00	0.0 %
Dec 2018	1.00	0.99	0.0 %
Jan 2019	1.00	0.99	0.1 %
Feb 2019	0.99	0.97	0.2 %
Mar 2019	1.00	0.99	0.0 %
Apr 2019	1.00	1.00	0.0 %
May 2019	1.00	0.99	0.0 %
Jun 2019	1.00	1.00	0.0 %
Year 1	**1.00**	**0.97**	**0.0 %**
Jul 2019	1.00	1.00	0.0 %
Aug 2019	1.00	1.00	0.0 %
Sep 2019	1.00	1.00	0.0 %
Oct 2019	1.00	1.00	0.0 %
Nov 2019	1.00	1.00	0.0 %
Dec 2019	1.00	0.99	0.0 %
Jan 2020	1.00	0.98	0.1 %
Feb 2020	1.00	1.00	0.0 %
Mar 2020	1.00	1.00	0.0 %
Apr 2020	1.00	1.00	0.0 %
May 2020	1.00	1.00	0.0 %
Jun 2020	1.00	1.00	0.0 %
Jul 2020	1.00	1.00	0.0 %
Year 2	**1.00**	**0.98**	**0.0 %**

The average soiling influence on the measurement data (after correction) was negligible, and only few singular events of notable pyrheliometer soiling were detected. Summarizing, it can be said that pyrheliometer soiling was not an issue in this measurement campaign, mostly because the sensor cleaning schedule was well adhered to during the entire measurement campaign and soiling correction was applied to the data.

6.2 Soiling rates of GHI and DHI sensors (pyranometers)

Due to the work-daily cleaning and the ventilation units that largely keep dust from settling on the pyranometer glass domes, soiling of the pyranometers was not an issue.

Further, due to the geometry of the sensor window (hemispheric glass dome), dust deposition is usually not uniformly distributed over the sensor field of view. For example, with wind coming from a certain direction, the glass dome may be dust-covered on the windward side only, lacking any dust cover on the leeward side. Thickness of the soiling layer may also vary over the height of the glass dome. Figure 20 shows an extreme example of this characteristic (from a site in a different country).

Such asymmetric distribution of soiling, when present, leads to different cleanliness factors of the sensor during the course of the day depending of the elevation angle of the sun (azimuth angle is constant on tracked systems). This asymmetric distribution is unknown and signal increase can only be observed at the time of cleaning.

Meaningful cleanliness factors can therefore not be obtained and sensor soiling correction is generally not applied to thermopile pyranometer measurements by CSP Services.

Figure 20: Asymmetric pyranometer glass dome soiling (exemplary picture)

7 Measurement accuracy and uncertainty

The overall data availability is 100% and the local maintenance (irradiance sensor cleaning and visual check) was done mostly on schedule and according to the defined procedures. Cleaning was usually done work-daily. All ground measurement data was subject to a multi-step data quality control process:

- Transmission of measurement data to CSP Services' server in near-real time
- Daily application of automatic data screening routines (e.g. gap test, step test, physical limits, consistency of solar irradiance components)
- Daily visual inspection of measurement data curves by experienced operators
- Soiling correction of irradiance values measured with pyrheliometer, similar to the method developed by [2]
- Continuous comparison of redundant measurements
- Verification of pyranometer calibration with traveling standard

The documentation of the ground measurement data includes:

- Report for weather station installation (including the calibration certificates of solar sensors)
- Maintenance visit report for the regular inspection visit
- Documentation of each sensor cleaning with time and date through a maintenance button on the automatic weather stations, pressed by the operator after sensor cleaning (included in the measurement data)

7.1 Coincidence of DNI measurements

The DNI measured by the pyrheliometer can be compared to DNI values calculated from the measured GHI and DHI values and the solar zenith angle (DNI_{calc}). DNI_{calc} and the coincidence between the two DNI values can be determined along the following formulas[2]:

$$DNI_{calc} = \frac{GHI - DHI}{\cos(SZA)}, \qquad \text{with } SZA\text{: Solar Zenith Angle} \qquad (1)$$

$$DNI_{coincidence} = DNI - DNI_{calc} \qquad (2)$$

This DNI coincidence is an indicator for the accuracy of the irradiance measurement, the deviation between the measured and calculated DNI should stay within reasonable limits. The usual limits are ±20 W/m² or 2-3% of the measured DNI for instantaneous values for higher sun elevations and high DNI values; high deviations of DNI_{calc} for low sun elevations are normal due to the cosine effect (close to sun elevation of zero, cos(SZA) converges to zero, thus dividing by cos(SZA) results in very high DNI_{calc} values). The comparison of DNI_{calc} and the measured DNI is used continuously for the daily irradiance measurement data quality control.

[2] F. Wolfertstetter, K. Pottler, N. Geuder, R. Affolter, A.A. Merrouni, A. Mezrhab, R. Pitz-Paal: Monitoring of mirror and sensor soiling with TraCS for improved quality of ground-based irradiance measurements. Energy Procedia 49 (2014), 2422-2432. doi:10.1016/j.egypro.2014.03.257.

Figure 21 shows the correlation of DNI and DNI_{calc} in a scatterplot of 1min and 10min resolution measurement values. The following effects can be seen:

- For low DNI values, spread is partly due to the cosine effect as explained above.
- The majority of values are distributed in a narrow range around the bisecting line and almost symmetrical with a small bias toward higher DNI_{calc} values.
- In the 1min-resolution graph (left), a few values that seem to form along lines different from the bisecting line can be observed. This may be partly attributable to short periods with incorrect tracker alignment which is not improved by the sun sensor, which has a tracking improvement effect only at DNI>300 W/m².
- Other outliers can be explained by sensor shading and to a small amount by the effect of the cleaning of the sensors by the operators
- In 10min time resolution, the spread is much less due to averaging effects

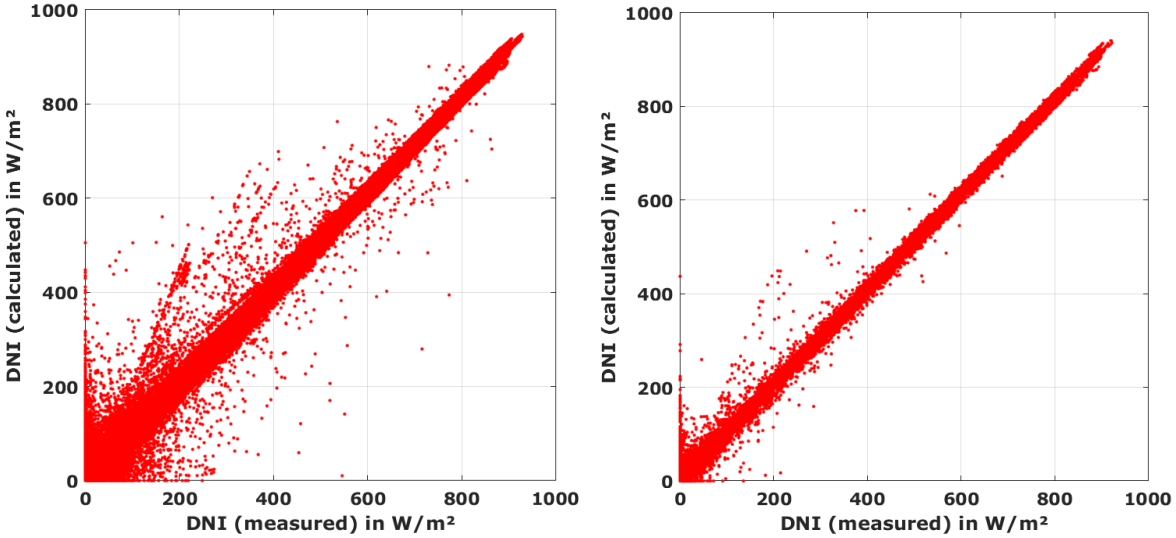

Figure 21: Correlation of DNI_{calc} and DNI (Left: 1min resolution. Right: 10min resolution)

In general, the coincidence can be considered as good, which is a consequence of the stringent maintenance procedures, high-quality sun tracker with active sun tracking, high sensor quality and accurate calibration. For the further use of the measurement data, data points with DNI coincidence values outside ±20 W/m² or 2-3% of the measured DNI are recommended to be filtered and discharged.

7.2 Coincidence of GHI measurements

Using the same formula (1) and replacing DNI_{calc} with the measured DNI, the coincidence of GHI can be calculated from the DNI and DHI measurement. Analogue to DNI, GHI coincidence is defined as measured GHI minus calculated GHI.

Figure 22 shows the correlation of calculated and measured GHI. Again, the correlation can be considered as good with only few outliers which (as for the DNI coincidence) are mostly due to maintenance influences, shading occurrences and short periods with non-ideal tracker alignment.

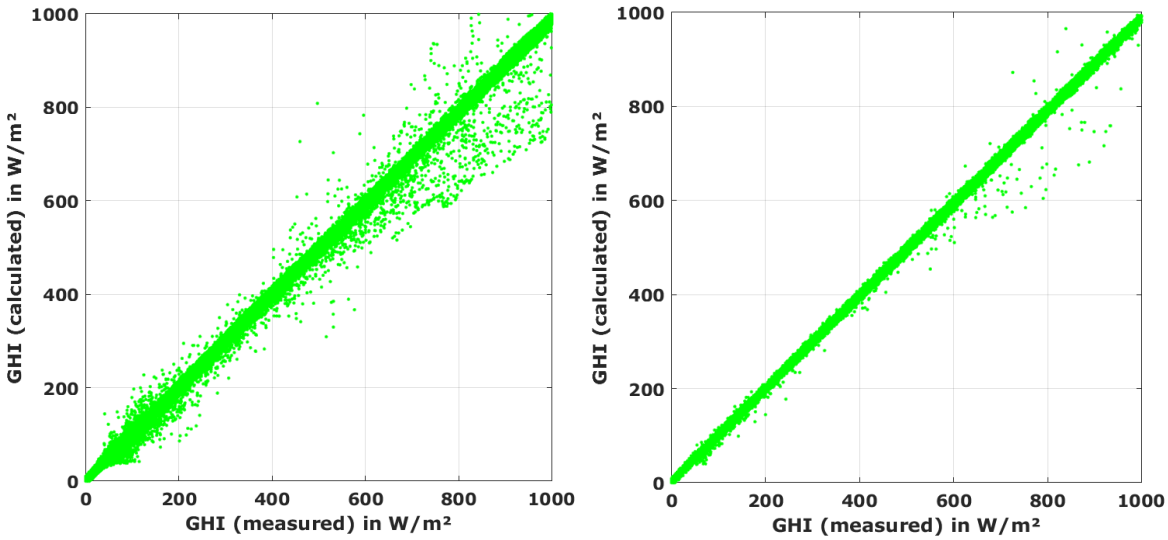

Figure 22: Correlation of GHI_{calc} and GHI (Left: 1min resolution. Right: 10min resolution)

7.3 Measurement uncertainty

The measurement uncertainty was assessed along the guideline in the NREL Best Practices Handbook for the Collection and Use of Solar Resource Data for Solar Energy Applications [1].

Best practices guidelines for selection of equipment, calibration, installation as well as operation and maintenance were followed and maintenance performance was assessed to include potential additional uncertainty contributions that could have occurred.

Two stages with related uncertainty contributions can be identified according to [1]:

- Instrument calibration (laboratory calibration by manufacturer): Uncertainty of calibration is specified in individual calibration certificates.
- Sources of uncertainty in field measurement are
    - Instrument-related (e.g. datalogger precision, pyrheliometer temperature response)
    - Installation-related (e.g. tracker alignment accuracy)
    - Operation-related (mainly frequency and thoroughness of cleaning)

DNI measurements

In the NREL Best Practices Handbook [1], typical calibration uncertainties for pyrheliometers are estimated with ±1.8% (at 95% level of confidence). The calibration certificate for the installed CHP1 pyrheliometer states a lower value of ±1.1%. Since this is well justified and the calibration verification did not give any reason of doubt, this lower value is assumed to be applicable.

In the field, much focus was given on using high-class measurement equipment (high-accuracy sensors, sun tracker and datalogger), excellent installation and alignment and regular maintenance and cleaning. The handbook estimates high-quality final measurement campaign DNI uncertainty with ±2.0% to ±2.5% for pyrheliometers for sub-hourly values (at 95% confidence interval).

For this measurement campaign, a measurement uncertainty of ±2.0% (at 95% confidence interval) for DNI values is estimated (after filtering and excluding values with bad coincidence as described above).

GHI and DHI measurements

In the literature, pyranometer calibration uncertainty is estimated with ±3.2% for solar zenith angles (SZA) between 30° and 60°. This is composed of an uncertainty of ±1.2% at a fixed, narrow incidence angle and a higher contribution of ±2.0% at a broader range of incidence angles [1]. Field measurements in well-maintained measurement campaigns can be estimated with uncertainties of ±3.0% for SZA between 30° and 60° and up to ±7.0% to ±10.0%for SZA>60° for GHI. For DHI, the uncertainty contribution resulting from SZA is irrelevant, since the direct irradiance is blocked by the shading ball assembly.

The calibration certificates for the installed CMP21 pyranometers state a value of ±1.35%. Calibration in the laboratory is done at a fixed incidence angle, thus this value replaces the literature estimate of ±1.2%. Since this is well justified and calibration verification did not give any reason of doubt, the value of ±1.35% is accepted.

The CMP21 pyranometers have an additional individual characterization for incidence angle and temperature sensitivity, and an incidence angle and temperature correction was applied to the GHI measurement values. Thus, the uncertainty resulting from broader incidence angles is much reduced. For the DHI, the temperature correction was applied. Therefore, the lower boundary of the literature values is assumed.

For this measurement campaign, a measurement uncertainty (at 95% confidence interval) of

- ±3.0% for all GHI values at SZA between 30° and 60°
- ±7.0% for all GHI values at SZA below 30° or above 60°
- ±2.0% for all DHI values

is estimated (after filtering and excluding values with bad coincidence as described above).

8 Conclusion

25 months of meteorological measurement data were collected at the site on IOE Dharan campus with a Tier1 automatic weather station between July 2018 and July 2020. The data was measured with a tracked pyrheliometer, ventilated pyranometers and additional meteorological sensors.

- Except for minor measurement problems, there were no significant operational difficulties
- Local maintenance and irradiance sensor cleaning were carried out on a work-daily schedule with few exceptions, each visit was recorded and documented
- Three regular (preventive) maintenance visits to the station were performed
- The measurement data was monitored on a daily basis by CSP Services operators, applying automatic quality assessment routines according to international best practices guidelines and visual inspection of the data by experienced operators
- The deviation between the installed irradiance sensors (redundant thermopile measurements) was within the expected limits
- The shading of the sensors was limited
- The calibration of the used thermopile irradiance sensors was successfully validated upon a field calibration verification campaign in October 2019 and October 2020. For the field calibration verification, traveling standard sensors calibrated at the WRC in Davos, Switzerland, were used as calibration reference.
- Measurement uncertainty is found to be within the expectable range given in best-practices literature

The 2-year measurement campaign at the site was successfully carried out, yielding a time series of on-site solar and meteorological measurement data in high quality. All measurement data was submitted to the World Bank in regular intervals by uploading to the energydata.info website. Additionally, the installation and maintenance reports as well as all calibration certificates and detailed descriptions of the measurement equipment were submitted to the World Bank.

9 References

[1] M. Sengupta, A. Habte, C. Gueymard, S. Wilbert and D. Renné, *Best Practices Handbook for the Collection and Use of Solar Resource Data for Solar Energy Applications: Second Edition,* Golden, Colorado: National Renewable Energy Laboratory, 2017.

[2] F. Wolfertstetter, , K. Pottler, A. Alami, A. Mezrhab and R. Pitz-Paal, "A novel method for automatic real-time monitoring of mirror soiling rates," in *SolarPACES 2012*, Marrakesh, Morocco, 2012.

CSP Services GmbH, Köln, Germany

CSPS Technical Documentation

Client: The World Bank

Selection #: 1230234

- Solar Resource Measurement Campaign Nepal –

24-Month Site Measurement Report Jumla, Nepal

Birk Kraas
Anne Forstinger

CSP Services GmbH
Friedrich-Ebert-Ufer 30
51143 Köln/Cologne, Germany
Email: b.kraas@cspservices.de

Version 04 December 2020

CSP Services
CONCENTRATING SOLAR POWER SERVICES

CSP Services GmbH, Köln, Germany

24-Month Station Operation Report

Table 1: Site and installation information

Site and Installation Information	
Site:	Hotel Kanjirowa, Jumla
Coordinates, Elevation:	29.27237°N, 82.19351°E (WGS84), 2368 m
Station Type:	ESMAP Tier1 automatic weather station
Date of installation:	2018-07-28
Date of maintenance visits:	2018-11-04, 2019-10-21

CSP Services GmbH
Friedrich-Ebert-Ufer 30
51143 Köln · Germany
T: +49 2203 959 0030
F: +49 2203 180 2528
www.cspservices.de

Geschäftsführer
(Managing Directors):
Dr. Klaus Pottler
Dr.-Ing. Steffen Ulmer

Sitz der Gesellschaft
(Registered Office): Köln
Amtsgericht Köln
HRB 61644
USt-ID-No: DE814904840

Bank Account:
IBAN: DE18 5001 0060 0049 6816 08
BIC (Swift-Code): PBNKDEFF
Postbank · Frankfurt-Main · Germany

1 Contents

2 Executive summary

24 months of meteorological measurement data was collected at the measurement site in Jumla between August 2018 and July 2020. This report summarizes the station operation during the reported measurement period.

Figure 1: Site location at Jumla (Image: Google Earth)

The Tier1 meteorological measurement station was installed at the site in Jumla on 28 July 2018 and visited for regular maintenance visit on 04 November 2018 and 21 October 2019.

A calibration verification was performed upon the second maintenance visit performed on 20 and 21 October 2019. Further scheduled maintenance visits and the planned solar irradiance sensor calibration in 2020 could not be conducted due to the lockdown and travel restrictions imposed or risk of travel resulting from the COVID-19 pandemic.

The station was operating correctly, the data availability was 100% (no data gaps) and the local maintenance (work-daily sensor cleaning and visual check) was done mostly on schedule and according to the defined procedures.

The measurement data collected after the reporting period is not subject of this report.

3 Equipment description and functionality, sensor calibration

3.1 Measurement equipment

The Tier1 automatic weather station is equipped with a datalogger and a GSM modem, a sun tracker equipped with an ISO9060 First Class pyrheliometer for DNI measurement and ISO9060 Secondary Standard pyranometers for measurement of GHI and DHI. As additional meteorological sensors, an anemometer and a wind vane for wind speed and direction measurement on 10 m height, a barometric pressure sensor, a tipping bucket rain gauge and a temperature and humidity sensor are installed. The exact types of sensor/equipment and serial numbers are listed in the tables below.

Table 2: Equipment and serial numbers

Equipment and serial numbers		
Automatic Weather Station	CSP Services MHP Automatic Weather Station	CSPS.MT.18.206
Main Control Box	CSP Services	CSPS.CA.18.202.0005
Datalogger	Campbell CR1000	E12055
Datalogger peripherals	CFM100 CF Module	14206
Sun Tracker	K&Z Solys2	180411
Sun Sensor	K&Z Sun Sensor Kit	170324
GSM Modem	Sierra Wireless Xtend	
GPS Module	Garmin 16x HVS	1A4250272
Power Supply	4x100 W PV modules, 4x150 Ah solar battery	Connected as 200 W, 300 Ah @24VDC

Table 3: Measured Parameters and Sensors

Measured parameter	Unit	Sensor type	Serial number
GHI	W/m²	K&Z CMP21, w. CVF4 ventilation unit	170868
DHI	W/m²	K&Z CMP21, w. CVF4 ventilation unit	170869
DNI	W/m²	K&Z CHP1	180584
Temperature	°C	Campbell CS215	E20181
Humidity	%	Campbell CS215	E20181
Pressure	hPa	Setra 278	7225866
Precipitation	mm	Young 52203	TB 14420
Wind Speed	m/s	NRG #40C anemometer	1795-00303671
Wind direction	°N	NRG #200P wind vane	1799-00019699

3.2 Equipment functionality

After an initial alignment problem of the sun tracker in July 2018, the functionality of the equipment was good, the station was operating without significant problems.

On several occasions, dew or droplets on the pyrheliometer was noticed. This presumably happened at fog events or in the morning. Impact on the data was negligible since the dew evaporated quickly.

Notable events at the station are listed in Table 4.

Table 4: Notable events during operation

Date	Event
2018-10-04	Dew on pyrheliometer front window
2018-11-04	Station maintenance (regular maintenance visit)
2018-11-07 to -11	Tracking device misaligned, DHI replaced with data from closest possible day with similar weather pattern, DNI calculated
2018-11-11	Station maintenance (improvement of sun tracker alignment)
2019-03-20, 2019-04-20, -24, 2019-05-13, -25, 2019-08-19, 2019-08-23, 2019-08-28, 2019-09-21, 2019-09-29, 2019-10-15, 2020-03-14, 2020-03-15, 2020-05-08	Dew on pyrheliometer front window

3.3 Sensor calibrations

Factory calibrations

All sensors were calibrated before deployment in the field. The thermopile pyranometers and pyrheliometers were calibrated in the factory by the manufacturer according to applicable ISO standards. Other meteorological sensors (wind speed sensor, barometric pressure sensors) were also calibrated by the respective manufacturer. Calibration certificates were handed over with the installation report.

Pyrheliometer and pyranometer field calibration verification

Upon the second regular maintenance visit, an irradiance sensor comparison against traveling standard sensors was performed. The travelling standard sensors were calibrated against the World Radiometric Reference (WRR) at Davos (Switzerland) prior to their delivery to Nepal.

This calibration comparison and its result were reported in the 12-month site measurement report. In the second year of operation, the on-site sensor comparison could not be repeated due to the COVID-19 pandemic which made visit of the site unfeasible.

4 Measurement results

Table 5 shows the monthly summary values of all measurement variables at this weather station. Each parameter is discussed in more detail in the following sections.

Table 5: Monthly irradiation sums and average meteorological data

Month	Irradiance sums [kWh/m²]			Avg. Temp. [°C]	Avg. RH [%]	Avg. WS [m/s]	Avg. Press [hPa]	Sum Rain [mm]	Usable data
	GHI	DNI	DHI						
Aug 2018	146	53	104	18.4	88	1.5	762	175	100 %
Sep 2018	165	155	58	17.3	80	2.0	766	54	100 %
Oct 2018	182	266	25	10.5	60	2.7	769	0	100 %
Nov 2018	136	225	24	6.8	49	2.2	769	0	100 %
Dec 2018	125	227	20	2.7	47	2.1	767	1	100 %
Jan 2019	111	151	38	2.1	65	1.8	767	47	100 %
Feb 2019	110	119	44	3.5	73	1.6	767	91	100 %
Mar 2019	190	224	48	7.9	58	2.6	767	14	100 %
Apr 2019	205	214	52	13.4	64	2.7	767	51	100 %
May 2019	215	192	68	15.0	59	2.7	766	26	100 %
Jun 2019	203	175	70	18.5	66	2.7	763	59	100 %
Jul 2019	158	84	93	18.6	84	1.7	762	145	100 %
Year 1	**1946**	**2085**	**644**	**11.2**	**66**	**2.2**	**766**	**663**	**100 %**
Aug 2019	162	97	90	18.7	85	1.7	763	97	100 %
Sep 2019	149	109	74	17.5	84	1.6	766	30	100 %
Oct 2019	164	210	42	12.4	68	2.3	769	0	100 %
Nov 2019	124	184	31	8.7	56	2.2	769	0	100 %
Dec 2019	122	214	21	2.4	58	1.7	768	43	100 %
Jan 2020	108	146	38	2.2	71	1.7	766	42	100 %
Feb 2020	147	210	31	4.7	59	2.3	767	21	100 %
Mar 2020	183	216	46	7.5	66	2.4	767	57	100 %
Apr 2020	200	191	64	11.5	65	2.6	767	99	100 %
May 2020	204	181	67	14.6	67	2.6	765	27	100 %
Jun 2020	166	103	89	18.1	78	2.1	763	81	100 %
Jul 2020	167	82	107	19.3	83	2.0	763	102	100 %
Year 2	**1896**	**1943**	**700**	**11.5**	**70**	**2.1**	**766**	**599**	**100 %**

4.1 Solar irradiance

Figure 2 shows the measured monthly irradiance sums in a bar chart. Some seasonal dependency of the irradiation sums is visible. Monthly global irradiance sums are generally higher in the summer season whereas the DNI monthly sums are generally higher in winter, with diffuse irradiance behaving the opposite way to direct irradiance. This can be explained with the monsoon season that reduced DNI during the monsoon months with strong cloud cover. GHI is still high in these months because of the longer daylight duration per day and high sun elevation. In winter (dry season), the sky is more often showing clear-sky conditions leading to higher DNI values.

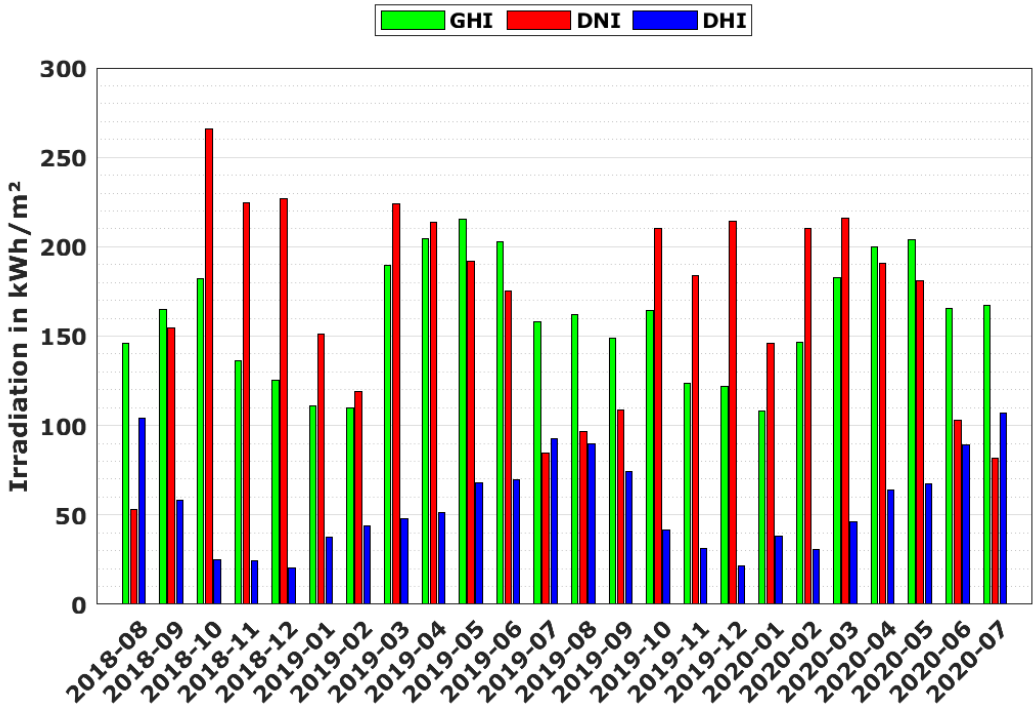

Figure 2: Monthly irradiation sums 2018-08 to 2020-07

The frequency distribution of hourly irradiance values (Figure 3) shows clear occurrence peaks for DNI (scale on the left axis) and DHI (scale on the right axis). The frequency distribution of GHI values (scale on left axis) is broader with no expressed occurrence peak. The peak for DNI values is just below 1000 W/m² and generally, DNI values above 600 W/m² are frequent. The diffuse irradiance frequency peaks at around 100 W/m². The frequency distributions indicate a clear-sky dominated climate with high irradiance values at this site.

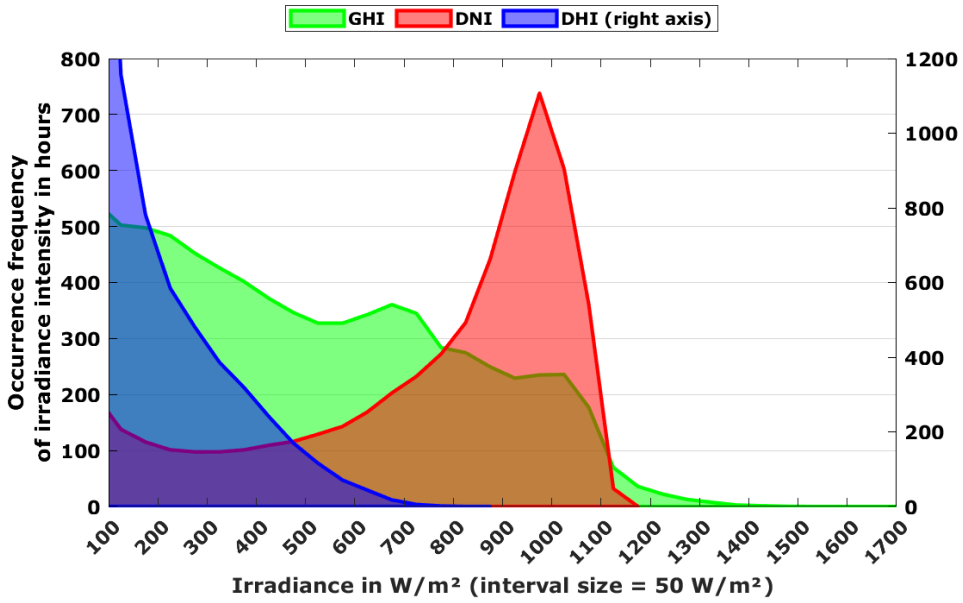

Figure 3: Frequency distribution of hourly irradiance averages 2018-08 to 2020-07

Figure 4 and Figure 5 show the irradiance intensity for GHI and DNI over the 24-months measurement period. The irradiation intensity and the length of the days vary with the seasons.

GHI is strongest during the spring and summer period (Figure 4), corresponding to the high solar elevation periods. Cloudy periods with low GHI values occur mostly in the monsoon period.

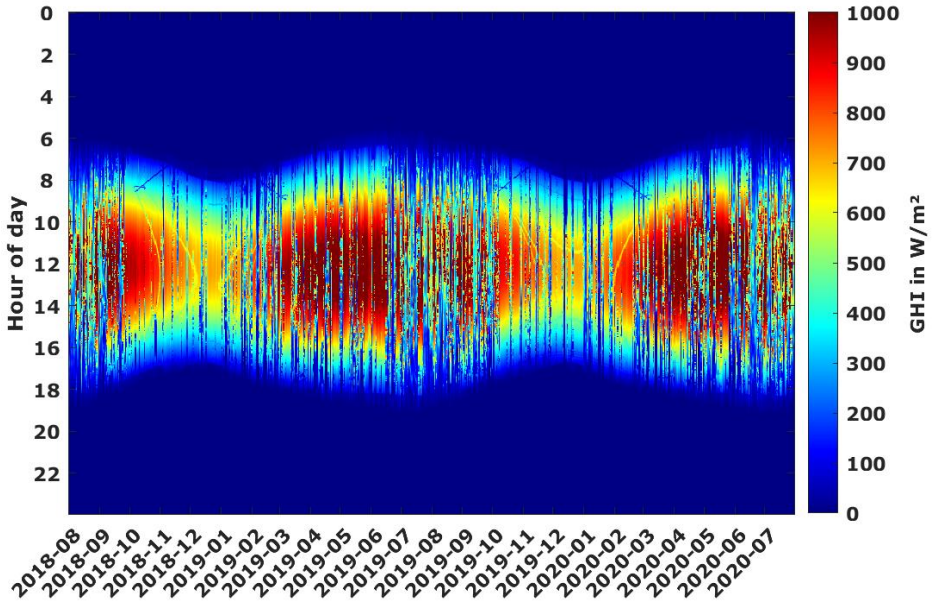

Figure 4: GHI irradiance intensity 2018-08 to 2020-07

The DNI values show high irradiance intensities of above 800 W/m² with a high stability throughout the winter and spring months (Figure 5). Periods with lower DNI (cloud cover or aerosol load) occur mainly in monsoon season. Due to the higher sensitivity of DNI to reductions by light cloud cover or aerosols, low DNI periods occur more often than for GHI, hence the slightly more fragmented appearance of the DNI plot.

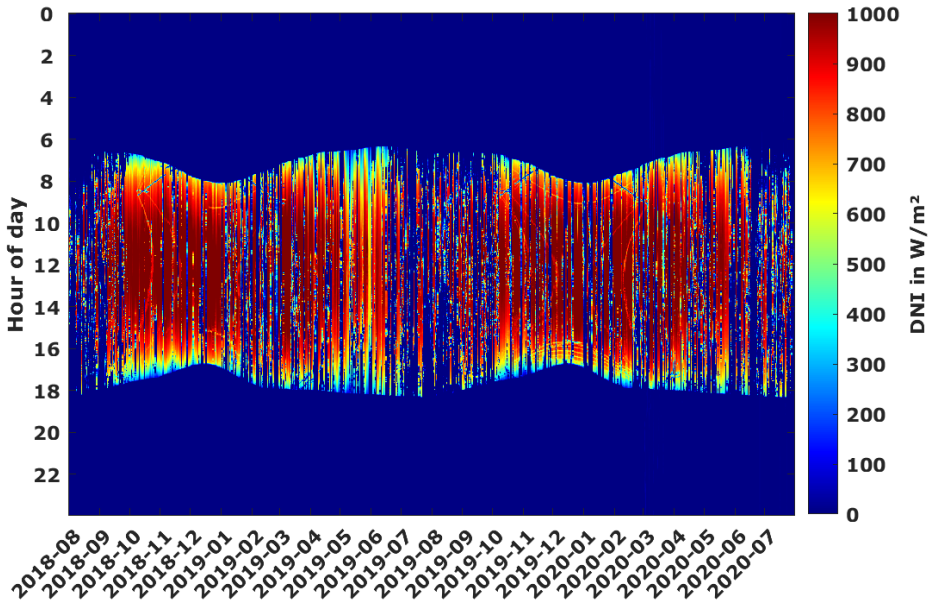

Figure 5: DNI irradiance intensity 2018-08 to 2020-07

Shading impact on solar irradiance measurement

In the intensity plot of the GHI as well as the DNI, visible shadings from the power line crossing the field of vision of the sensors can be identified. These shadings are now discussed in more detail.

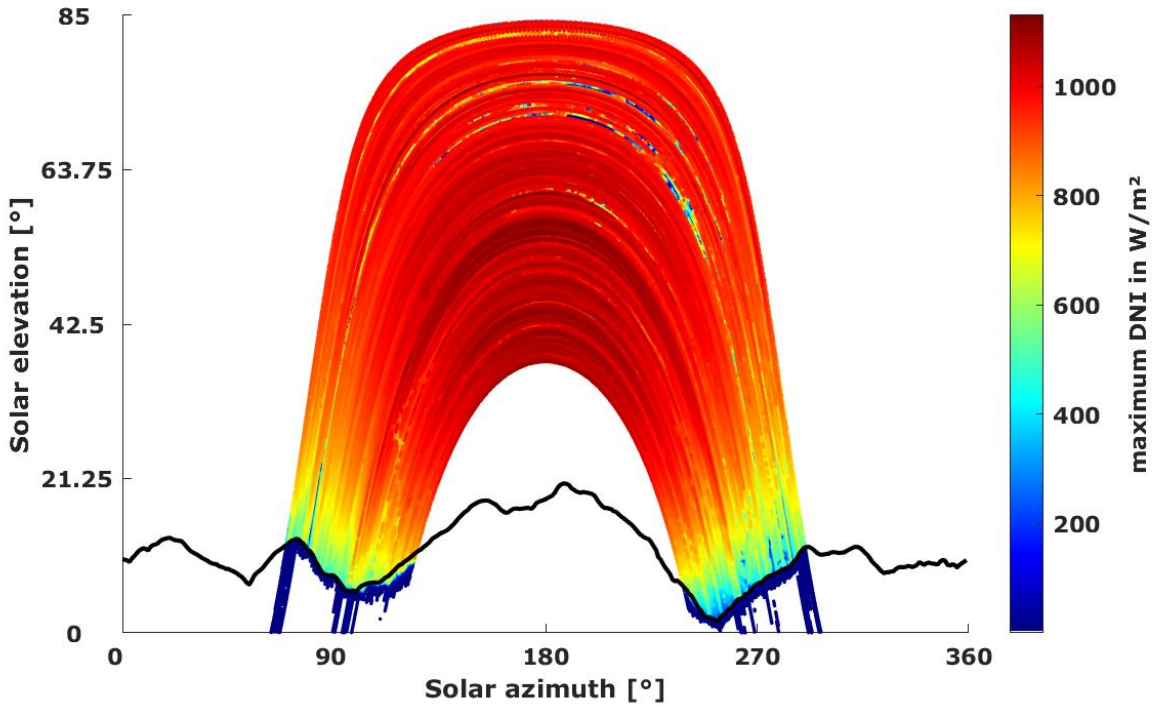

Figure 6: Measured maximum DNI at distinct sun positions (black line: horizon line from SRTM digital elevation model)

Figure 6 shows the maximum DNI values (in 1-minute resolution) recorded at the respective sun position (azimuth and elevation angle). In this graph, the clear "cut" in the morning and evening which results from the natural horizon (mountain ridge) can be seen very well. The horizon line is plotted in black and is obtained from the Shuttle Radar Topography Mission (SRTM). The blue values below horizon line can be ignored.

Other obstacles (power line and its supporting masts) are difficult to see in this graph.

However, some obstacles are visible in the following plots (same as Figure 4 and Figure 5, with zoom into specific period).

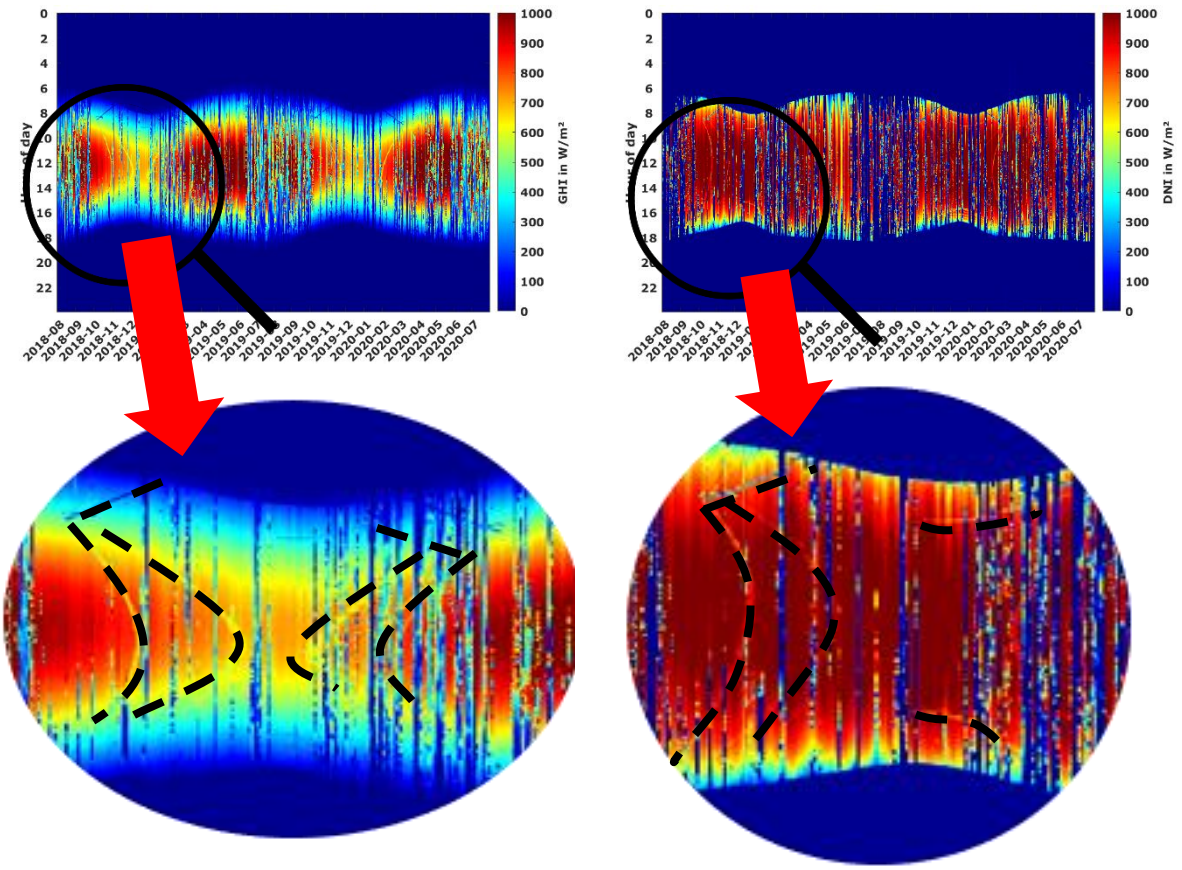

Figure 7: GHI (left) / DNI (right) intensity with visible shadings from powerline

Figure 7 again shows the GHI and DNI intensities with a zoom on the period of October 2018 to February 2019. It can be seen that there are visible lines formed by values that are lower than those immediately before and after (marked with black dashed lines in zoom image). The masts and wires affect each sensor at individually different times, as the shadows cast by these obstacles wander across the tracker and the attached instruments. The same patterns repeat in the second year of measurement, as the obstacles are persistent.

Figure 8 shows a panoramic view with a centered south view, taken from behind the sun tracker upon installation of the station. Blue crosshair markers show the cardinal directions at horizon height. The sun paths at different months are also displayed. It is obvious that the shadings are resulting from the surrounding mountains and the crossing power line

Figure 8: Panoramic View from Pyranometer Sensor Height with Sun Paths and Horizon

Compared to the shading analysis from the installation report, the exact time of shading is slightly different since at the time of the installation, the panoramic image on which analysis was based was taken from behind the tracker, not from exact instrument position.

4.2 Temperature and humidity

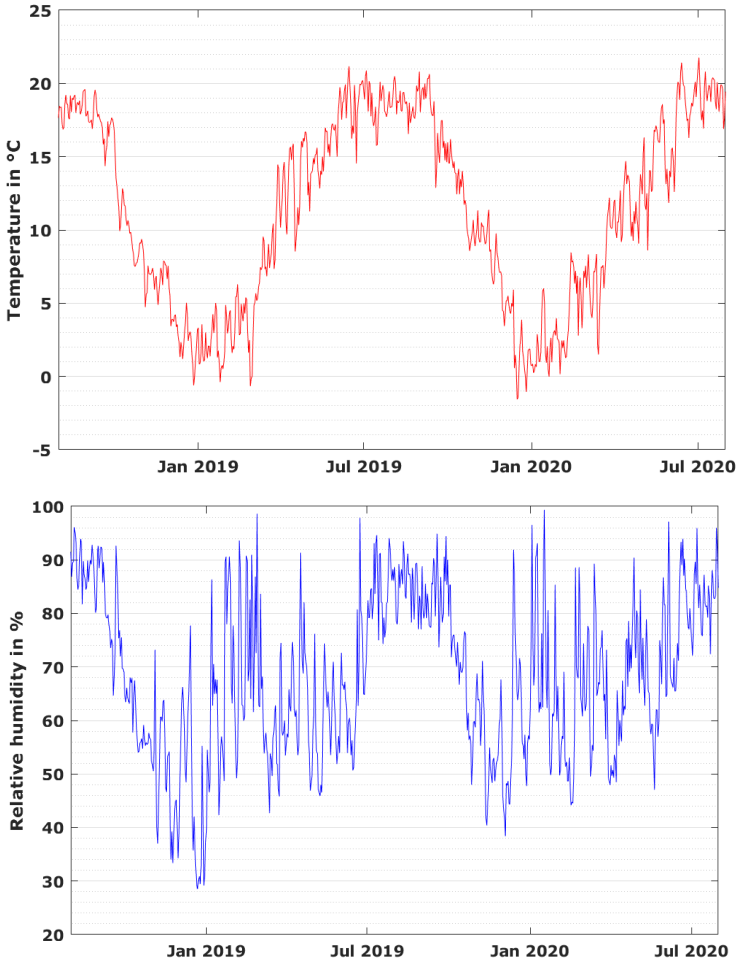

Figure 9: Daily temperature and relative humidity averages (1-minute resolution)

Figure 9 shows daily averages of temperate and relative humidity. A seasonal dependency is visible. Temperature is lowest in the northern hemisphere winter months (November to February) and high in the summer months. The month with the highest average temperature is June, the coldest monthly average temperature was in January. The most frequent temperature is 17°C and the relative humidity is commonly between 95 % and 100% (Figure 10). Daily relative humidity averages were highly variable, with tendentially lower humidity in the winter months (which were also the months with highest DNI sums) and high humidity during the monsoon season.

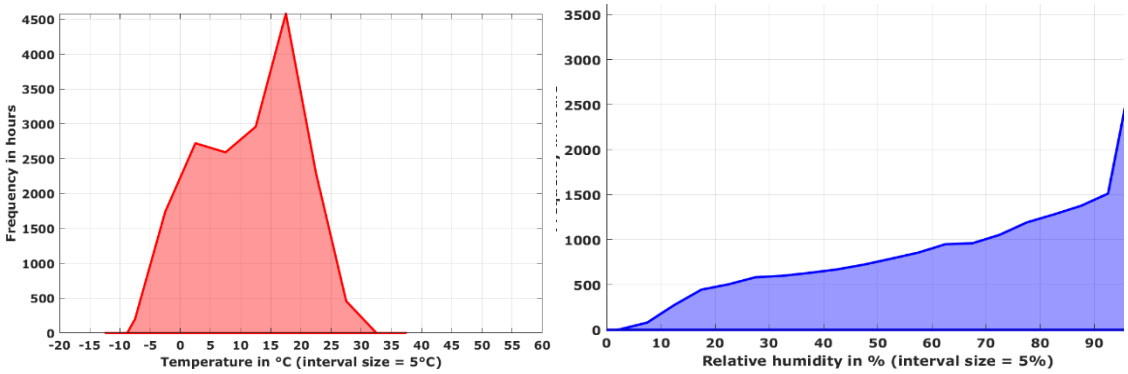

Figure 10: Frequency distribution of temperature and relative humidity (1-minute resolution)

4.3 Barometric pressure

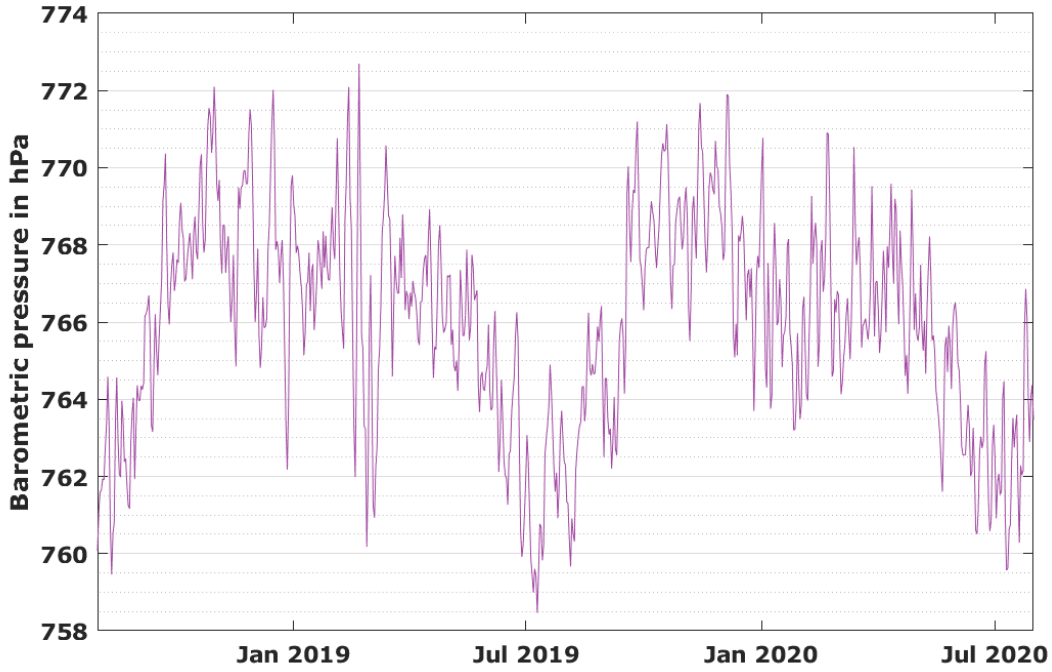

Figure 11: Daily averages of barometric pressure

Figure 11 shows daily averages of barometric pressure. Again, a clear seasonal dependence is visible: Higher pressure in the winter months and lower pressure in the summer months. Figure 12 shows the frequency distribution of recorded 1-minute resolution barometric pressure values.

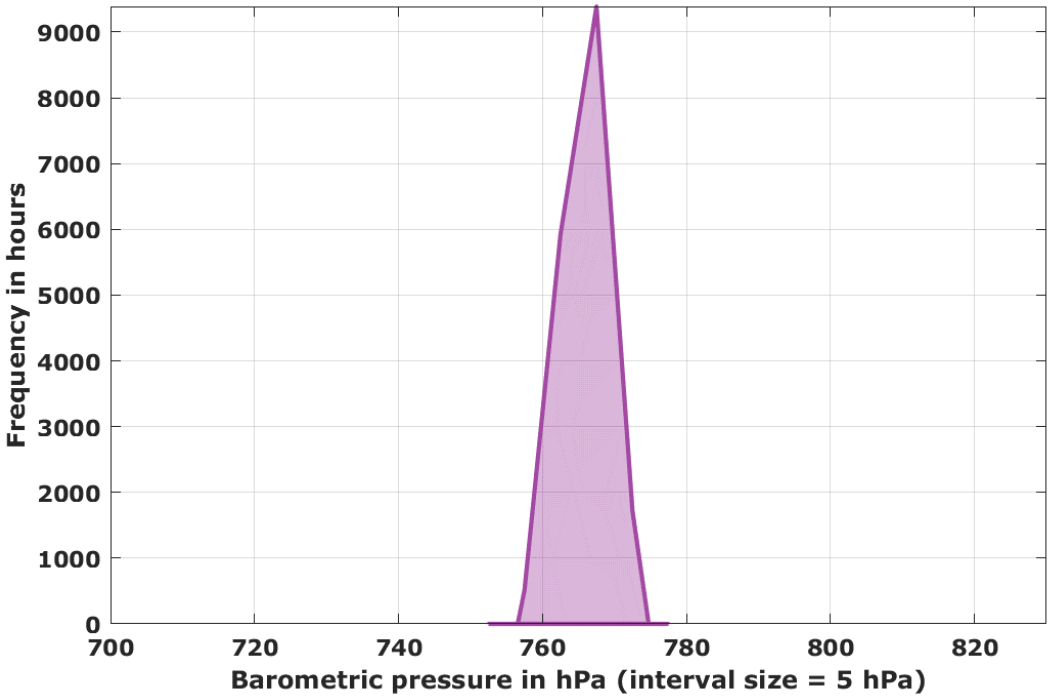

Figure 12: Frequency distribution of barometric pressure (1-minute resolution)

4.4 Precipitation

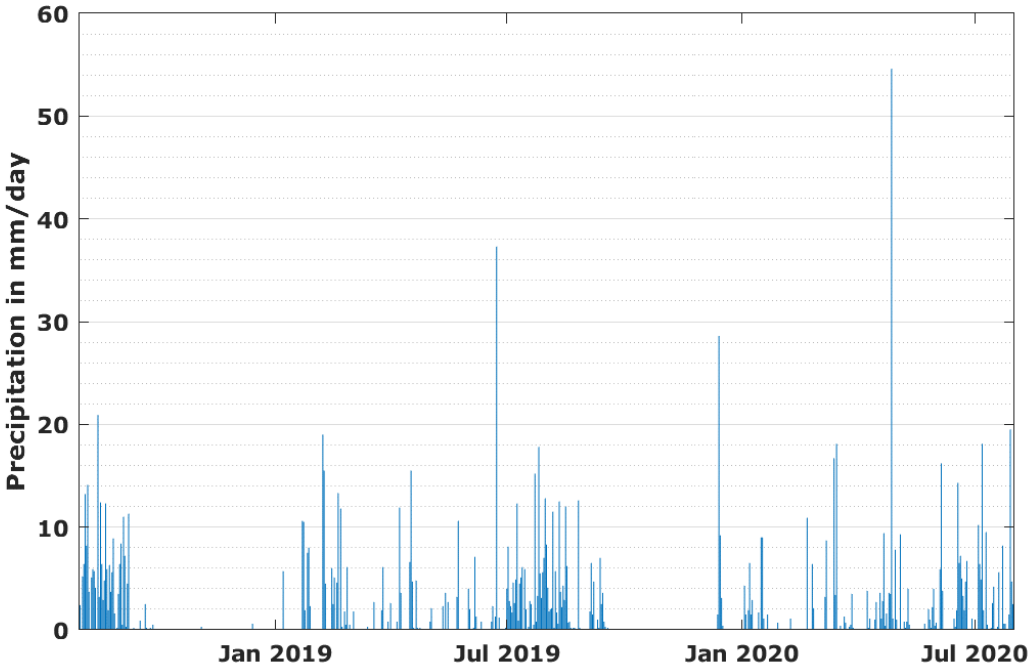

Figure 13: Daily sums of precipitation

Figure 13 shows the daily sums of precipitation. Again, a clear seasonal variability was observed with a dry period with no precipitation from November to January and an expressed rainy season in the months of June to September. The same periods were observed in both years of the measurement campaign.

4.5 Wind speed and direction

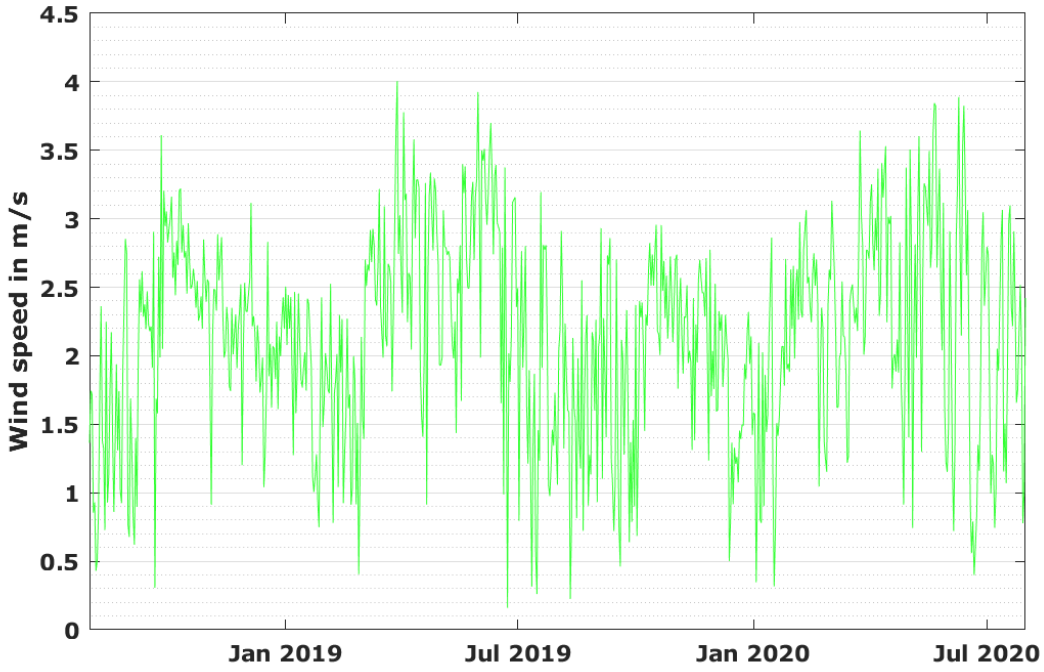

Figure 14: Daily averages of wind speed

Figure 14 shows the daily averages of wind speed. They are continuously low and almost no seasonal dependency was observed. The frequency distribution, shown in Figure 15, emphasize that wind speeds of <4 m/s are common and wind gusts of up to only 12 m/s were observed.

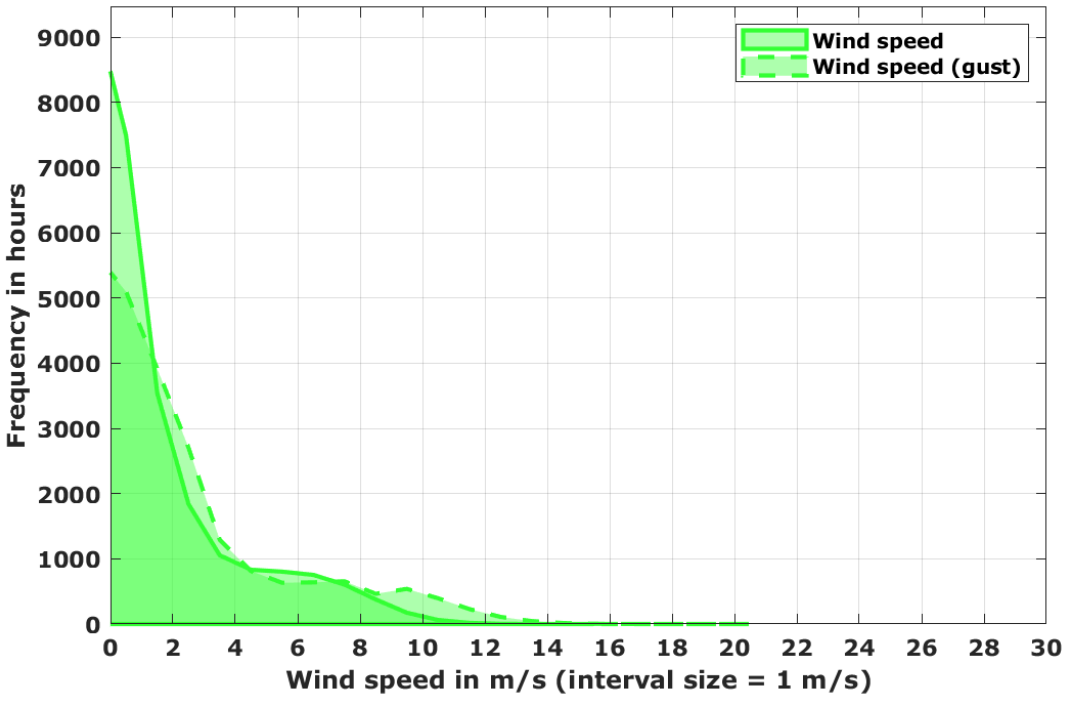

Figure 15: Frequency distribution of wind speeds (1-minute values)

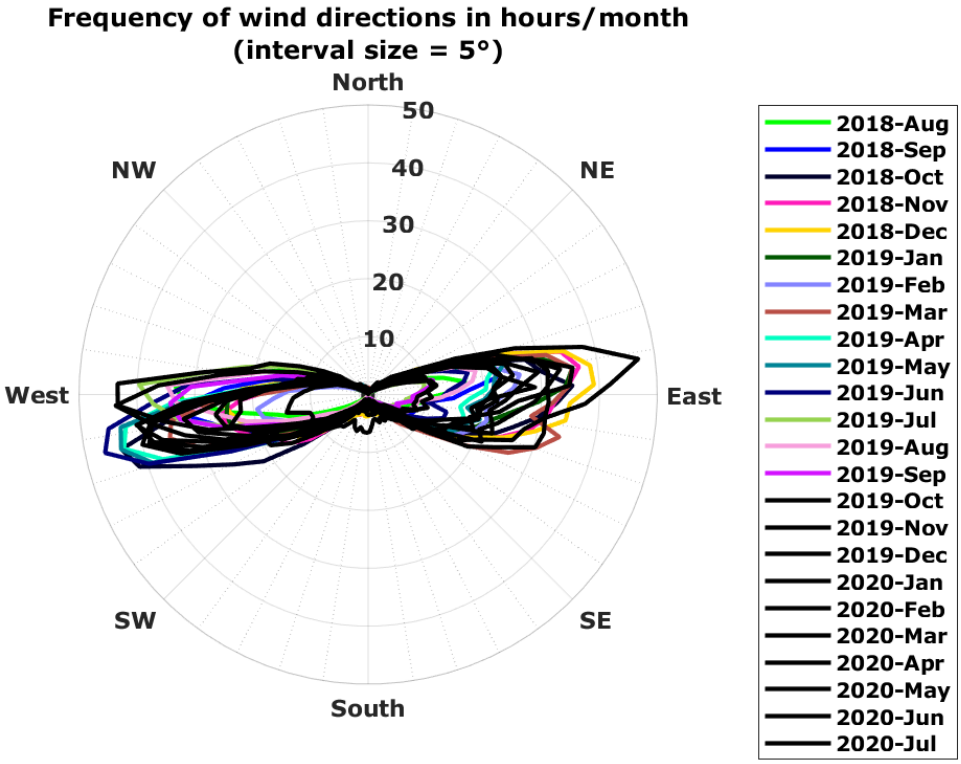

Figure 16: Wind direction distribution 2018-08 to 2020-07

Figure 16 shows the frequency distribution of wind direction in 1-minute time resolution. Two clear main wind directions are visible: From west in the summer time and from the east in the winter months.

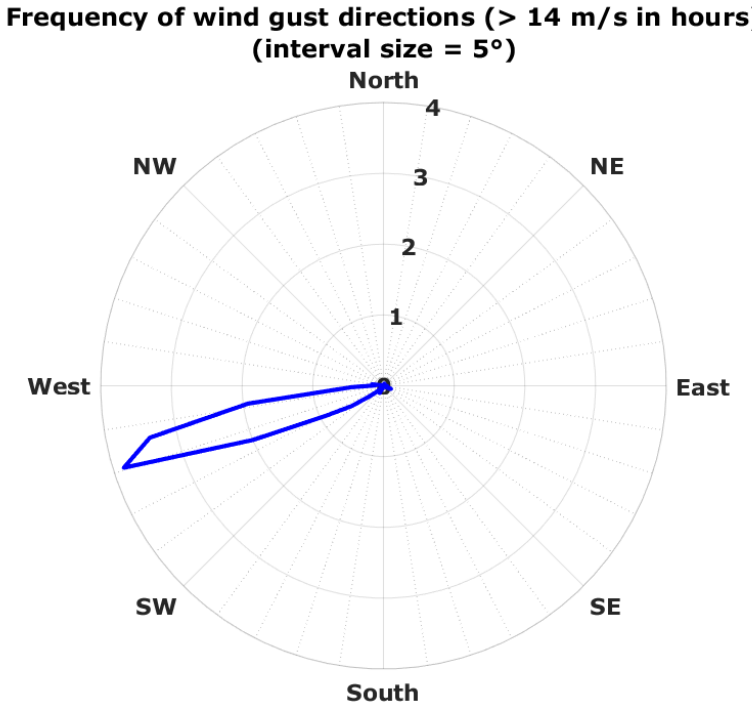

Figure 17: Wind gust direction distribution 2018-08 to 2020-07

5 On-site maintenance and irradiance sensor cleaning

The maintenance on site was done by local personnel. They were contracted and specially trained for this task upon installation of the station. The maintenance on site consisted mainly of visual inspection of the equipment, verifying the sensor alignment and cleaning the irradiance sensors and PV modules. The cleaning was scheduled to be performed on a work-daily basis, which was almost always adhered to throughout the whole measurement campaign with a ramp-up phase in the beginning of the campaign. Overall, 68% of all days had a cleaning event. The less frequent cleanings in 2020 can be credited to the Corona pandemic and the subsequent local lock-down. The exact cleaning dates and times are recorded in the monthly measurement reports and in the measurement data.

Table 6 gives an overview of the maintenance frequency per month.

Table 6: Number of maintenance visits by local staff per month

Month	Maintenance visits
Aug 2018	22
Sep 2018	22
Oct 2018	30
Nov 2018	28
Dec 2018	27
Jan 2019	26
Feb 2019	21
Mar 2019	26
Apr 2019	27
May 2019	23
Jun 2019	25
Jul 2019	17
Aug 2019	26
Sep 2019	22
Oct 2019	21
Nov 2019	19
Dec 2019	17
Jan 2020	13
Feb 2020	11
Mar 2020	17
Apr 2020	17
May 2020	17
Jun 2020	13
Jul 2020	11

6 Irradiance sensor soiling rates and soiling behavior

6.1 Soiling rates of DNI sensor (pyrheliometer)

All data from the pyrheliometer was corrected for sensor soiling by applying a linearly interpolated cleanliness factor[1] to the measurement data where applicable and necessary, i.e. only where cleanliness factor at cleaning was not 1. It has to be noted that cleanliness factors can only be determined under certain conditions:

- The cleaning is performed correctly and swiftly (no influencing of sensors except during a few seconds in the cleaning process)
- The irradiation conditions are stable enough to distinguish signal increase resulting from dust removal from natural fluctuations
- The signal increase resulting from dust removal is sufficiently large to be detectable

If no analysis is possible, soiling correction is not applied.

Table 7 on the next page shows

- Simplified average sensor cleanliness factors of the pyrheliometer DNI sensor detected at the above described cleaning events
- Simplified average daily soiling rate of the pyrheliometer. This rate expresses how much the irradiance sensor signal is reduced each day without cleaning. Simplified in this context means that the rate is a simple average of the change of cleanliness factors over all days of the month
- The minimum cleanliness factors (i.e., maximum sensor soiling) observed just before the sensor cleaning. Especially on/after strong wind occasions such as e.g. dust storms, high singular soiling rates can be observed. The daily cleaning ensures that these single events with high soiling do not influence long periods of data (usually only up to one day) and were mostly well corrigible

[1] Sensor cleanliness factor is defined as the dimensionless factor by which the recorded measurement value has to be divided in order to obtain the soiling-corrected value. E.g., if at cleaning a signal increase of 3% has been detected, the factor before the cleaning is 1/(1+0.03) = 0.97, after the cleaning (clean sensors) = 1.

Table 7: Average sensor cleanliness factors (pyrheliometer)

Month	Average sensor cleanliness	Minimum cleanliness factor	Average daily soiling rate
Aug 2018	1.00	1.00	0.0%
Sep 2018	1.00	0.99	0.1%
Oct 2018	0.99	0.98	1.4%
Nov 2018	1.00	0.98	0.6%
Dec 2018	0.99	0.94	1.7%
Jan 2019	1.00	0.98	0.4%
Feb 2019	1.00	1.00	0.0%
Mar 2019	1.00	0.98	0.6%
Apr 2019	1.00	0.98	0.8%
May 2019	0.99	0.95	1.2%
Jun 2019	0.99	0.97	0.9%
Jul 2019	0.99	0.95	0.3%
Year 1	**1.00**	**0.94**	**0.7 %**
Aug 2019	1.00	1.00	0.0%
Sep 2019	1.00	0.97	0.1%
Oct 2019	1.00	0.98	0.4%
Nov 2019	0.99	0.97	0.8%
Dec 2019	1.00	0.97	0.3%
Jan 2020	1.00	1.00	0.0%
Feb 2020	1.00	1.00	0.0%
Mar 2020	1.00	0.99	0.0%
Apr 2020	0.99	0.95	0.3%
May 2020	0.99	0.97	0.5%
Jun 2020	0.99	0.95	0.3%
Jul 2020	1.00	1.00	0.0%
Year 2	**1.00**	**0.95**	**0.3 %**

In several months, there have been notable sensor soiling rates at the site. However, the soiling influence on the measurement data (after correction) was small, and only few singular events of notable pyrheliometer soiling were detected. Summarizing, it can be said that pyrheliometer soiling is not an issue to data quality, because the sensor cleaning schedule was well adhered to during the entire measurement campaign and soiling correction was applied to the data.

6.2 Soiling rates of GHI and DHI sensors (pyranometers)

Due to the work-daily cleaning and the ventilation units that largely keep dust from settling on the pyranometer glass domes, soiling of the pyranometers was not an issue.

Further, due to the geometry of the sensor window (hemispheric glass dome), dust deposition is usually not uniformly distributed over the sensor field of view. For example, with wind coming from a certain direction, the glass dome may be dust-covered on the windward side only, lacking any dust cover on the leeward side. Thickness of the soiling layer may also vary over the height of the glass dome. Figure 18 shows an extreme example of this characteristic (from a site in a different country).

Such asymmetric distribution of soiling, when present, leads to different cleanliness factors of the sensor during the course of the day depending of the elevation angle of the sun (azimuth angle is constant on tracked systems). This asymmetric distribution is unknown and signal increase can only be observed at the time of cleaning.

Meaningful cleanliness factors can therefore not be obtained and sensor soiling correction is generally not applied to thermopile pyranometer measurements by CSP Services.

Figure 18: Asymmetric pyranometer glass dome soiling (exemplary picture)

7 Measurement accuracy and uncertainty

The overall data availability is 100% and the local maintenance (irradiance sensor cleaning and visual check) was done mostly on schedule and according to the defined procedures. Cleaning was usually done work-daily. All ground measurement data was subject to a multi-step data quality control process:

- Transmission of measurement data to CSP Services' server in near-real time
- Daily application of automatic data screening routines (e.g. gap test, step test, physical limits, consistency of solar irradiance components)
- Daily visual inspection of measurement data curves by experienced operators
- Soiling correction of irradiance values measured with pyrheliometer, similar to the method developed by [1]
- Continuous comparison of redundant measurements
- Verification of pyranometer calibration with traveling standard

The documentation of the ground measurement data includes:

- Report for weather station installation (including the calibration certificates of solar sensors)
- Maintenance visit report for the regular inspection visit
- Documentation of each sensor cleaning with time and date through a maintenance button on the automatic weather stations, pressed by the operator after sensor cleaning (included in the measurement data)

7.1 Coincidence of DNI measurements

The DNI measured by the pyrheliometer can be compared to DNI values calculated from the measured GHI and DHI values and the solar zenith angle (DNI_{calc}). DNI_{calc} and the coincidence between the two DNI values can be determined along the following formulas[2]:

$$DNI_{calc} = \frac{GHI - DHI}{\cos(SZA)}, \qquad \text{with } SZA\text{: Solar Zenith Angle} \tag{1}$$

$$DNI_{coincidence} = DNI - DNI_{calc} \tag{2}$$

This DNI coincidence is an indicator for the accuracy of the irradiance measurement, the deviation between the measured and calculated DNI should stay within reasonable limits. The usual limits are ±20 W/m² or 2-3% of the measured DNI for instantaneous values for higher sun elevations and high DNI values; high deviations of DNI_{calc} for low sun elevations are normal due to the cosine effect (close to sun elevation of zero, cos(SZA) converges to zero, thus dividing by cos(SZA) results in very high DNI_{calc} values). The comparison of DNI_{calc} and the measured DNI is used continuously for the daily irradiance measurement data quality control.

[2] F. Wolfertstetter, K. Pottler, N. Geuder, R. Affolter, A.A. Merrouni, A. Mezrhab, R. Pitz-Paal: Monitoring of mirror and sensor soiling with TraCS for improved quality of ground-based irradiance measurements. Energy Procedia 49 (2014), 2422-2432. doi:10.1016/j.egypro.2014.03.257.

Figure 19 shows the correlation of DNI and DNI_{calc} in a scatterplot of 1min and 10min resolution measurement values. The following effects can be seen:

- For low DNI values, the spread is partly due to the cosine effect as explained above.
- The majority of values are distributed in a narrow range around the bisecting line and almost symmetrical with a small bias toward higher DNI_{calc} values.
- In the 1min-resolution graph (left), a lot of outliers in a cone around the bisection line can be observed. This may be partly attributable to short periods with incorrect tracker alignment which is not improved by the sun sensor, which has a tracking improvement effect only at DNI>300 W/m².
- There are many outliers that are far away from the bisecting line. This can mostly be explained by sensor shading by obstacles (small shadow from power masts or lines influencing one instrument, then the other) and to a small amount by the effect of the cleaning of the sensors by the operators
- In 10min time resolution, the spread is much less due to averaging effects

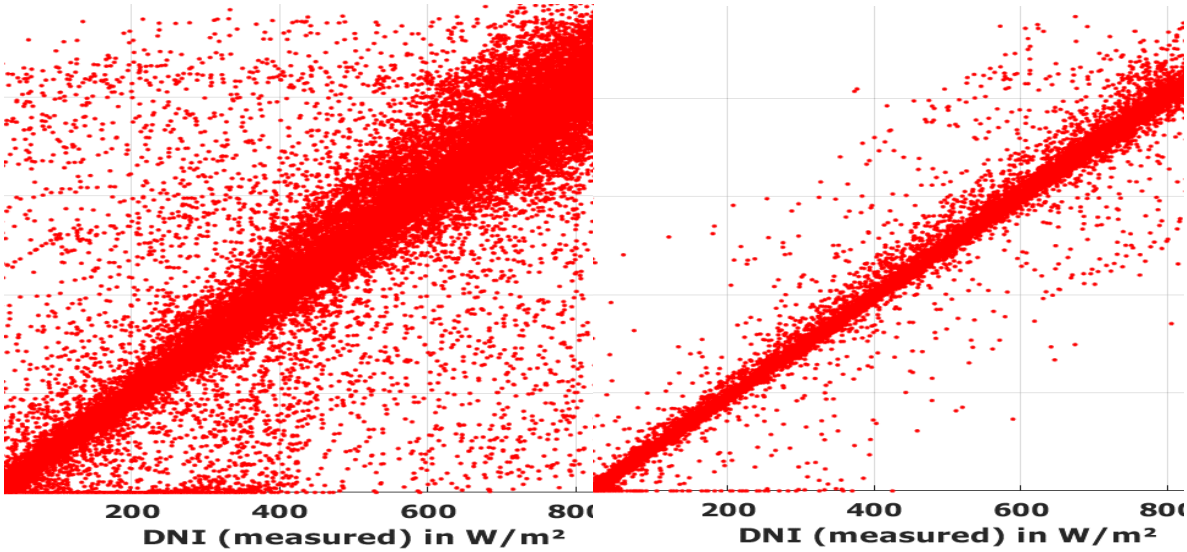

Figure 19: Correlation of DNI_{calc} and DNI (Left: 1min resolution. Right: 10min resolution)

In general, the coincidence can still be considered as good. The large amount of outliers due to shading of sensors is a consequence of the site location, which was a compromise between site availability and site suitability. Other than external influences that could not be avoided, the data quality benefits of the stringent maintenance procedures, good sun tracker with active sun tracking, high sensor quality and accurate calibration.

For the further use of the measurement data, data points with DNI coincidence values outside ±20 W/m² or 2-3% of the measured DNI as well as clear outliers are recommended to be filtered and discharged.

7.2 Coincidence of GHI measurements

Using the same formula (1) and replacing DNI_{calc} with the measured DNI, the coincidence of GHI can be calculated from the DNI and DHI measurement. Analogue to DNI, GHI coincidence is defined as measured GHI minus calculated GHI.

Figure 20 shows the correlation of calculated and measured GHI. Again, the large amount of outliers can be seen in the one-minute resolution data. In the 10-minute averages, the correlation looks much better.

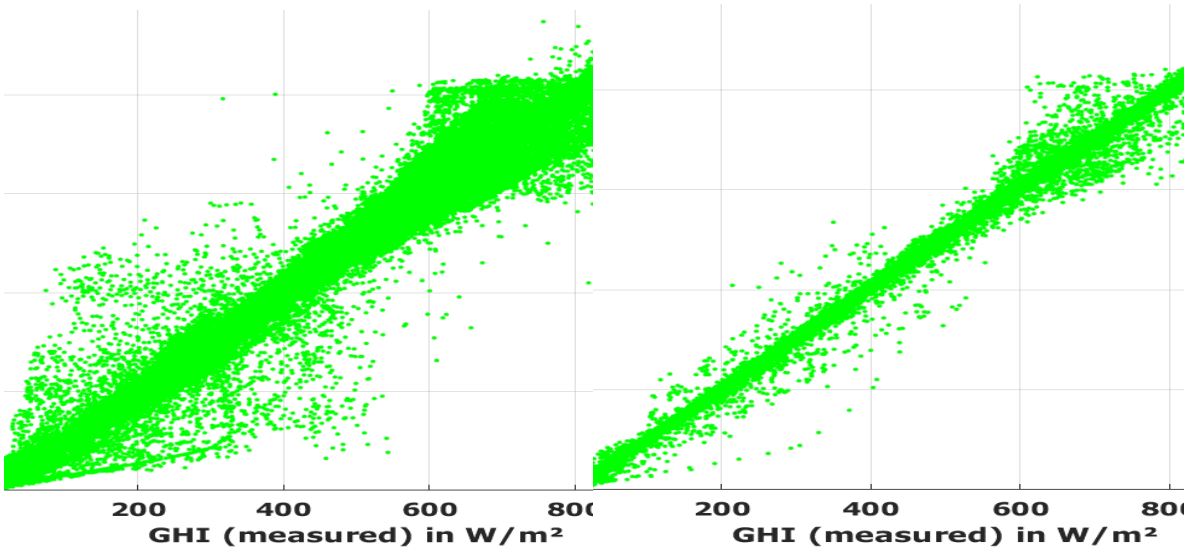

Figure 20: Correlation of GHI_{calc} and GHI (Left: 1min resolution. Right: 10min resolution)

7.3 Measurement uncertainty

The measurement uncertainty was assessed along the guideline in the NREL Best Practices Handbook for the Collection and Use of Solar Resource Data for Solar Energy Applications [2].

Best practices guidelines for selection of equipment, calibration, installation as well as operation and maintenance were followed and maintenance performance was assessed to include potential additional uncertainty contributions that could have occurred.

Two stages with related uncertainty contributions can be identified according to [2]:

- Instrument calibration (laboratory calibration by manufacturer): Uncertainty of calibration is specified in individual calibration certificates.
- Sources of uncertainty in field measurement are
    - Instrument-related (e.g. datalogger precision, pyrheliometer temperature response)
    - Installation-related (e.g. tracker alignment accuracy)
    - Operation-related (mainly frequency and thoroughness of cleaning)

DNI measurements

In the NREL Best Practices Handbook [2], typical calibration uncertainties for pyrheliometers are estimated with ±1.8% (at 95% level of confidence). The calibration certificate for the installed CHP1 pyrheliometer states a lower value of ±1.1%. Since this is well justified and the calibration verification did not give any reason of doubt, this lower value is assumed to be applicable.

In the field, much focus was given on using high-class measurement equipment (high-accuracy sensors, sun tracker and datalogger), excellent installation and alignment and regular maintenance and cleaning. The handbook estimates high-quality final measurement campaign DNI uncertainty with ±2.0% to ±2.5% for pyrheliometers for sub-hourly values (at 95% confidence interval).

For this measurement campaign, a measurement uncertainty of ±2.0% (at 95% confidence interval) for DNI values is estimated (after filtering and excluding values with bad coincidence as described above).

GHI and DHI measurements

In the literature, pyranometer calibration uncertainty is estimated with ±3.2% for solar zenith angles (SZA) between 30° and 60°. This is composed of an uncertainty of ±1.2% at a fixed, narrow incidence angle and a higher contribution of ±2.0% at a broader range of incidence angles [2]. Field measurements in well-maintained measurement campaigns can be estimated with uncertainties of ±3.0% for SZA between 30° and 60° and up to ±7.0% to ±10.0%for SZA>60° for GHI. For DHI, the uncertainty contribution resulting from SZA is irrelevant, since the direct irradiance is blocked by the shading ball assembly.

The calibration certificates for the installed CMP21 pyranometers state a value of ±1.35%. Calibration in the laboratory is done at a fixed incidence angle, thus this value replaces the literature estimate of ±1.2%. Since this is well justified and calibration verification did not give any reason of doubt, the value of ±1.35% is accepted.

The CMP21 pyranometers have an additional individual characterization for incidence angle and temperature sensitivity, and an incidence angle and temperature correction was applied to the GHI measurement values. Thus, the uncertainty resulting from broader incidence angles is much reduced. For the DHI, the temperature correction was applied. Therefore, the lower boundary of the literature values is assumed.

For this measurement campaign, a measurement uncertainty (at 95% confidence interval) of

- ±3.0% for all GHI values at SZA between 30° and 60°
- ±7.0% for all GHI values at SZA below 30° or above 60°
- ±2.0% for all DHI values

is estimated (after filtering and excluding values with bad coincidence as described above).

8 Conclusion

24 months of meteorological measurement data were collected at the site at Hotel Kanjirowa with a Tier1 automatic weather station between August 2018 and July 2020. The data was measured with a tracked pyrheliometer, ventilated pyranometers and additional meteorological sensors.

- Except for minor measurement problems, there were no significant operational difficulties
- The surroundings of the station are introducing a number of adverse effects on measurement data, namely sensor shading by surrounding mountains and an overhead power line crossing south of the station. This has been known in advance and must be considered when using the measurement data, e.g. by excluding outliers by means of filtering for instrument coincidence
- Local maintenance and irradiance sensor cleaning were carried out on a work-daily schedule with acceptably few exceptions, each visit was recorded and documented
- Two regular (preventive) maintenance visits to the station were performed
- The measurement data was monitored on a daily basis by CSP Services operators, applying automatic quality assessment routines according to international best practices guidelines and visual inspection of the data by experienced operators
- The deviation between the installed irradiance sensors (redundant thermopile measurements) was within the expected limits
- The calibration of the used thermopile irradiance sensors was successfully validated upon a field calibration verification campaign in October 2019. For the field calibration verification, traveling standard sensors calibrated at the WRC in Davos, Switzerland, were used as calibration reference
- Measurement uncertainty is found to be within the expectable range given in best-practices literature

The 2-year measurement campaign at the site was successfully carried out, yielding a time series of on-site solar and meteorological measurement data in high quality. All measurement data was submitted to the World Bank in regular intervals by uploading to the energydata.info website. Additionally, the installation and maintenance reports as well as all calibration certificates and detailed descriptions of the measurement equipment were submitted to the World Bank.

9 References

[1] F. Wolfertstetter, , K. Pottler, A. Alami, A. Mezrhab and R. Pitz-Paal, "A novel method for automatic real-time monitoring of mirror soiling rates," in *SolarPACES 2012*, Marrakesh, Morocco, 2012.

[2] M. Sengupta, A. Habte, C. Gueymard, S. Wilbert and D. Renné, *Best Practices Handbook for the Collection and Use of Solar Resource Data for Solar Energy Applications: Second Edition,* Golden, Colorado: National Renewable Energy Laboratory, 2017.

CSP Services GmbH, Köln, Germany

CSPS Technical Documentation

Client: The World Bank

Selection #: 1230234

- Solar Resource Measurement Campaign Nepal –

24-Month Site Measurement Report Kathmandu, Nepal

Birk Kraas
Anne Forstinger

CSP Services GmbH
Friedrich-Ebert-Ufer 30
51143 Köln/Cologne, Germany
Email: b.kraas@cspservices.de

Version 04 December 2020

CSP Services
CONCENTRATING SOLAR POWER SERVICES

CSP Services GmbH, Köln, Germany

24-Month Station Operation Report

Table 1: Site and installation information

Site and Installation Information	
Site:	Institute of Engineering, Pulchowk Campus, Kathmandu
Coordinates, Elevation:	27.68157°N, 85.31868°E (WGS84), 1315 m
Station Type:	ESMAP Tier1 automatic weather station
Date of installation:	2018-06-15
Date of maintenance visits:	2018-10-10, 2019-10-11, 2020-09-28 to 29

CSP Services GmbH
Friedrich-Ebert-Ufer 30
51143 Köln · Germany
T: +49 2203 959 0030
F: +49 2203 180 2528
www.cspservices.de

Geschäftsführer
(Managing Directors):
Dr. Klaus Pottler
Dr.-Ing. Steffen Ulmer

Sitz der Gesellschaft
(Registered Office): Köln
Amtsgericht Köln
HRB 61644
USt-ID-No: DE814904840

Bank Account:
IBAN: DE18 5001 0060 0049 6816 08
BIC (Swift-Code): PBNKDEFF
Postbank · Frankfurt-Main · Germany

1 Contents

2 Executive summary

24 months of meteorological measurement data was collected at the measurement site in in Kathmandu between July 2018 and June 2020. This report summarizes the station operation during the reported measurement.

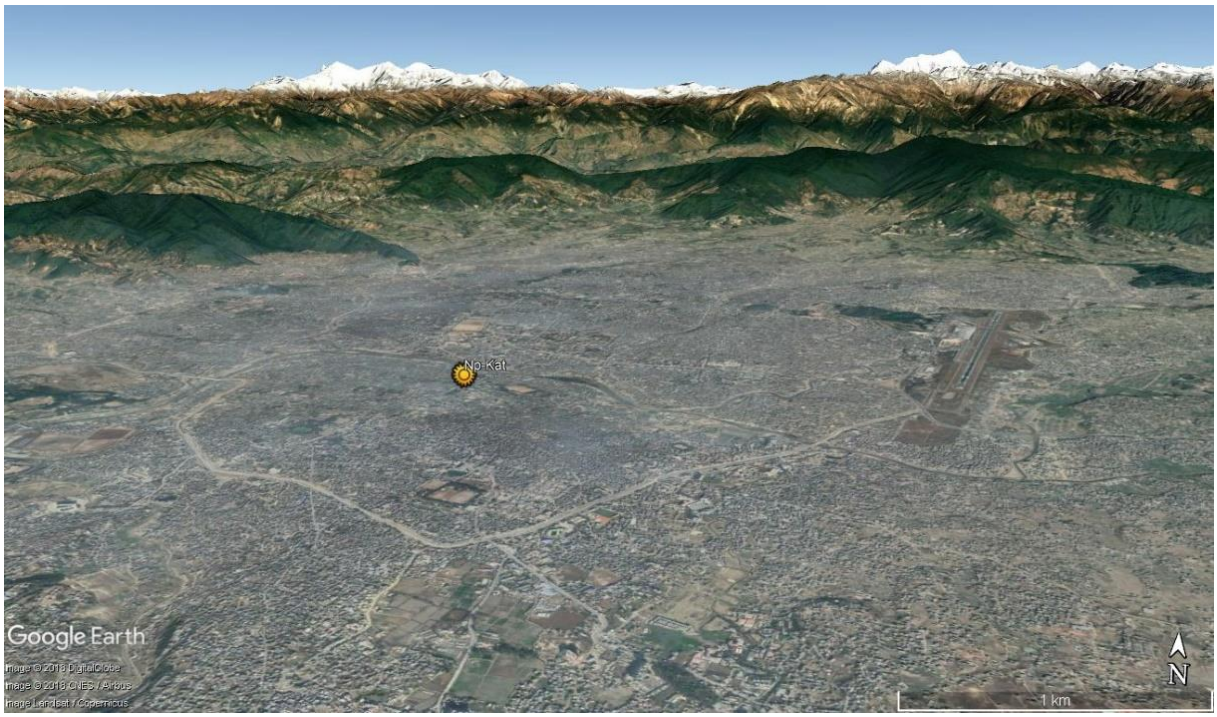

Figure 1: Site location in Kathmandu valley (Image: Google Earth)

The Tier1 meteorological measurement station was installed at the site on Pulchowk Campus of IOE on 15 June 2018 and visited for regular maintenance visit on 10 October 2018 and 11 October 2019.

Further scheduled maintenance visits in spring 2020 could not be conducted due to the lockdown and travel restrictions imposed resulting from the COVID-19 pandemic. One final maintenance visit with solar irradiance sensor comparison to reference sensors was conducted in September 2020, after the 24-month measurement period. Sensor comparison results are also reported in this document.

The station was operating correctly, the data availability was 100% (no data gaps) and the local maintenance (work-daily sensor cleaning and visual check) was done mostly on schedule and according to the defined procedures.

The measurement data collected after the reporting period is not subject of this report.

3 Equipment description and functionality, sensor calibration

3.1 Measurement equipment

The Tier1 automatic weather station is equipped with a datalogger and a GSM modem, a sun tracker equipped with an ISO9060 First Class pyrheliometer for DNI measurement and ISO9060 Secondary Standard pyranometers for measurement of GHI and DHI. As additional meteorological sensors, an anemometer and a wind vane for wind speed and direction measurement on 10 m height, a barometric pressure sensor, a tipping bucket rain gauge and a temperature and humidity sensor are installed. The exact types of sensor/equipment and serial numbers are listed in the tables below.

Table 2: Equipment and serial numbers

Equipment and serial numbers		
Automatic Weather Station	CSP Services MHP Automatic Weather Station	CSPS.MT.18.202
Main Control Box	CSP Services	CSPS.CA.18.202.0001
Datalogger	Campbell CR1000	E12050
Datalogger peripherals	CFM100 CF Module	14202
Sun Tracker	K&Z Solys2	180409
Sun Sensor	K&Z Sun Sensor Kit	170320
GSM Modem	Sierra Wireless Xtend	
GPS Module	Garmin 16x HVS	1A4250248
Power Supply	4x100 W PV modules, 4x150 Ah solar battery	Connected as 200 W, 300 Ah @24VDC

Table 3: Measured Parameters and Sensors

Measured parameter	Unit	Sensor type	Serial number
GHI	W/m²	K&Z CMP21, w. CVF4 ventilation unit	170860
DHI	W/m²	K&Z CMP21, w. CVF4 ventilation unit	170861
DNI	W/m²	K&Z CHP1	170570
Temperature	°C	Campbell CS215	E20177
Humidity	%	Campbell CS215	E20177
Pressure	hPa	Setra 278	7217843
Precipitation	mm	Young 52203	TB14377
Wind Speed	m/s	NRG #40C anemometer	1795-00303666
Wind direction	°N	NRG #200P wind vane	1799-00019685

3.2 Equipment functionality

The functionality of the equipment was good, the station was operating without significant problems.

On some occasions, the sun tracker was not well aligned. This may have been due to changes of alignment resulting from loosening bolts or similar. Where possible, data was corrected by modeling/interpolating DHI and calculating DNI from the modeled DHI.

On some occasions, dew or droplets on the pyrheliometer was noticed. This presumably happened at morning fog events. Impact on the data was negligible since the dew evaporated quickly.

Notable events at the station are listed in Table 4.

Table 4: Notable events during operation

Date	Event
2018-07-26, -28	Dew or rain on pyrheliometer front window
2018-09-02 to -14	Sun tracker misaligned
2018-09-14	Station maintenance (improvement of sun tracker alignment)
2018-10-09 to -10	Station maintenance (regular maintenance visit)
2018-11-25	Dew on pyrheliometer front window
2018-12-10, -16, -20, -23, -24, -25	Dew on pyrheliometer front window
2019-01-02	Dew on pyrheliometer front window
2019-02-10	Dew on pyrheliometer front window
2019-02-16 to 2019-03-02	Sun tracker misaligned in the morning; DHI modeled, DNI calculated from GHI and modeled DHI
2019-03-02	Station maintenance (improvement of sun tracker alignment)
2019-04-07	Dew on pyrheliometer front window
2019-04-20 to -21, -24, -25	Sun tracker misaligned in the morning; DHI modeled, DNI calculated from GHI and modeled DHI
2019-05-30 to 2019-06-01	Sun tracker misaligned in the morning; DHI modeled, DNI calculated from GHI and modeled DHI
2019-06-23	Pyrheliometer misaligned in the morning; DNI calculated from GHI and DHI
2019-10-11	Station maintenance (regular maintenance visit)
2019-12-04, -18, -22 2020-01-06	Dew on pyrheliometer front window
2020-01-07	Sun tracker misaligned in the morning; DHI modeled, DNI calculated from GHI and modeled DHI

Date	Event
2020-01-10 to 2020-01-15	
2020-01-19, -20	Dew on pyrheliometer front window
2020-03-06	Sun tracker misaligned in the morning; DHI modeled, DNI calculated from GHI and modeled DHI
2020-05-04, -08	Dew on pyrheliometer front window

3.3 Sensor calibrations

Factory calibrations

All sensors were calibrated before deployment in the field. The thermopile pyranometers and pyrheliometers were calibrated in the factory by the manufacturer according to applicable ISO standards. Other meteorological sensors (wind speed sensor, barometric pressure sensors) were also calibrated by the respective manufacturer. Calibration certificates were handed over with the installation report.

Pyrheliometer and pyranometer field calibration verification

Upon the second and third maintenance visits, an irradiance sensor comparison against traveling standard sensors was performed. The travelling standard sensors were calibrated against the World Radiometric Reference (WRR) at Davos (Switzerland) prior to their delivery to Nepal. The following equipment was installed for the comparison measurement:

- An additional pyrheliometer mounting clamp for a travelling standard reference pyrheliometer on the sun tracker
- An instrument table with mounting place for a reference pyranometer (to have the reference pyranometer installed on the same height as the other pyranometers on the ventilation units)
- Reference sensors at the described additional mounting places:
    - CHP1 Pyrheliometer SN 180580, Sensitivity: 8.096 µV/Wm²
    - CMP21 Pyranometer SN 170858, Sensitivity: 8.84 µV/Wm²

  Calibration certificates from PMOD WRC are attached to this report.

Figure 2: Tracker with regular (1) and reference pyrheliometer (2), reference pyranometer (3)

Figure 3: Tracker with DHI pyranometer (4) GHI pyranometer (5), reference pyranometer (3)

All sensors were measured with 1 Hz resolution, and the measurements were stored on the datalogger in 1 min averages.

3.4 Comparison method - pyrheliometer

The comparison measurement for pyrheliometers was set up following the measurement set-up procedures and recommendations described in ISO 9059 as closely as possible. *Please note: This cross-comparison is not an ISO-compatible calibration, as this was not the scope of the cross-comparison. The ISO standard was only followed as far as possible to obtain comparable results while adhering to best practices procedures.*

If both pyrheliometers are calibrated correctly, the observed deviation between the compared instruments should be within the combined calibration uncertainty. For the installed CHP1 sensor, Kipp&Zonen specifies a calibration uncertainty of ±1.1%. For the reference sensor, a calibration uncertainty of ±0.32 % is specified by PMOD (both at 95% coverage probability, stated in the calibration certificates). The combined calibration uncertainty is therefore ±1.15%. No other additional uncertainty contributions are added, since both devices are of identical model and installed on the same sun tracker, using the same datalogger. The final combined uncertainty is therefore ±1.15%, which can be interpreted as a strict limit since instrument-specific uncertainty contributions such as instrument temperature or individual alignment are neglected.

The measurement data from both sensors (reference and sensor to be compared) was filtered as follows:

- Only data where no soiling correction was applied (perfectly clean sensor windows)
- Only values with DNI >700 W/m² were used (acc. to ISO 9059) where this was possible.
- Outliers filtered and discarded (e.g., temporary shading of a single instrument due to maintenance staff passing the station or similar)
- Stable irradiance conditions (ideally, clear-sky conditions), if possible

Enough data was available to apply these filter criteria and still have a sufficient amount of comparison data.

The graph in the result section shows the perfect fit (exact identical measurement of reference and tested sensor) as the angle bisector in red. Above and below the bisecting line is the corridor defined by adding/subtracting the combined calibration uncertainty. If the used calibration constant of the tested sensor is correct, the vast majority of all measurement values (shown as blue triangle markers and named as "DNI") must be within this corridor.

3.5 Comparison results - pyrheliometer

The results shown in this report refer only to the comparison in 9 September 2020. The previous comparison in 2019 was reported on in the 12 Month Site Measurement Report.

356 values (1-minute averages) remain after applying the filters. This is a solid amount of data for this comparison. The data are from two different days, 28 and 29 September 2020.

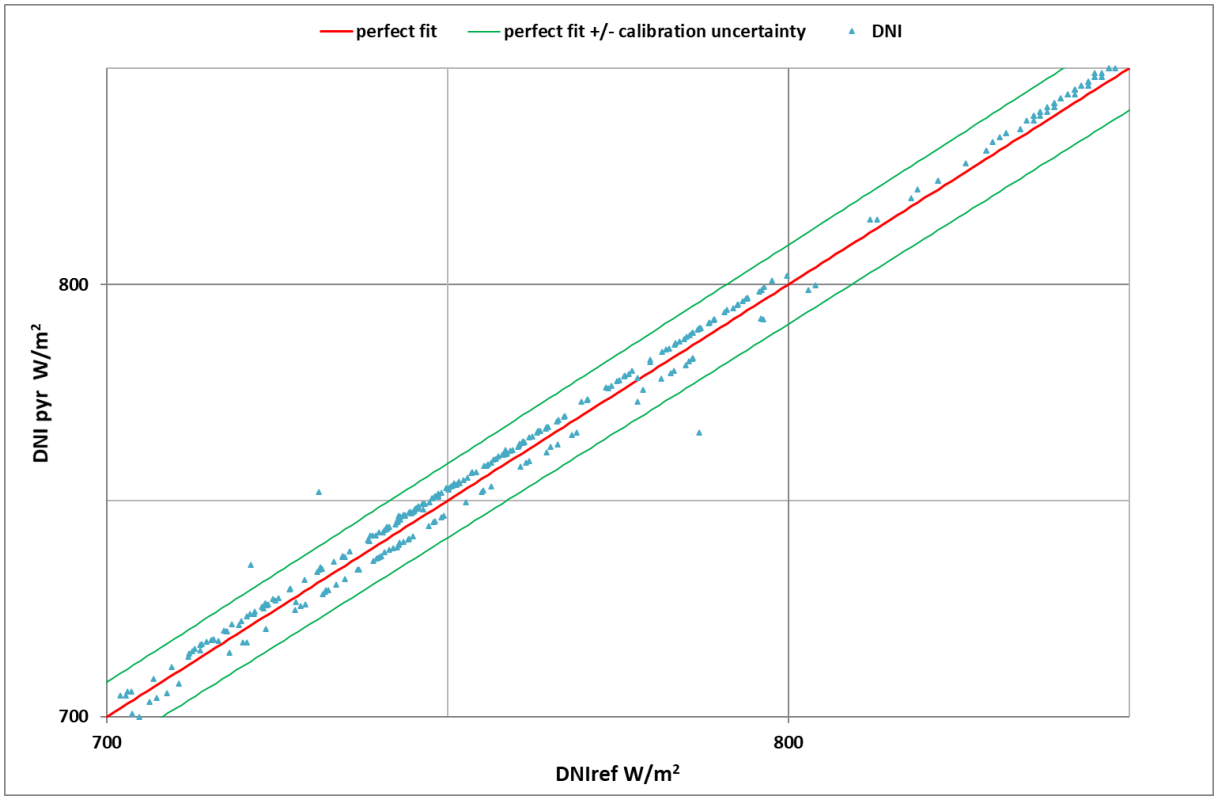

Figure 4: Comparison of pyrheliometer CHP1 SN170570 (vertical axis) to traveling standard pyrheliometer CHP1 SN180580 (horizontal axis)

All measurement values lie inside of the specified combined measurement uncertainty of ±1.15 %, except for a few outliers that are likely due to external influences like maintenance work ongoing.

The sensitivity calibration of this sensor is accepted as correct and valid.

3.6 Comparison method - pyranometers

The comparison measurement for pyranometers was set up following the measurement set-up procedures and recommendations described in ISO 9847 as closely as possible. *Please note: This cross-comparison is not an ISO-compatible calibration, as this was not the scope of the cross-comparison. The ISO standard was only followed as far as possible to obtain comparable results while adhering to best practices procedures.*

If both instruments are calibrated correctly, the observed deviation between the compared instruments should be within the combined calibration uncertainty. For the installed CMP21 pyranometers, Kipp&Zonen specifies a calibration uncertainty of ±1.35%. For the reference sensor, a calibration uncertainty of ±1.24 % is specified by PMOD (both at 95% coverage probability, stated in the calibration certificates). The combined calibration uncertainty is therefore ±1.83%. No other additional uncertainty contributions are added, since all devices are of identical model and installed on the same sun tracker, using the same datalogger. The final combined uncertainty is therefore ±1.83%, which can be interpreted as a strict limit since instrument-specific uncertainty contributions such as instrument temperature or individual alignment are neglected.

These values were determined at high incidence angles and with high global irradiance values. The uncertainty for lower sun elevations and lower GHI values may be significantly higher [1]. Therefore, only high sun elevation and high GHI values were utilized for the comparison.

The measurement data from all three sensors (reference and sensors to be compared) was filtered as follows:

- Only values with sun elevation > 20° were used (acc. to ISO 9847)
- Only values with GHI > 300 W/m² were used to exclude bad weather conditions
- Only series of minimum numbers of consecutive values were used for the comparison (following ISO 9847)
    - In periods with cloudless skies: min. 10 consecutive values
    - In periods with some clouds: min. 1-5 consecutive values
    - In cloudy sky (overcast): not used
- Outliers not considered (e.g., temporary shading of a single instrument due to maintenance staff cleaning the sensor or similar)

Enough data was available to apply these filter criteria and still have a sufficient amount of comparison data for all individual sensors.

The graphs in the result section show the perfect fit (exact identical measurement of reference and tested sensor) as the angle bisector in red. Above and below is the corridor defined by adding/subtracting the combined calibration uncertainty. If the calibration factor or the tested sensor is corrected, the vast majority of all measurement values (shown as blue triangle markers named as "GHI Pyranometer" or "DHI Pyranometer", the naming refers to the mounting place on the tracker and for which measurement these pyranometers are usually used) must be within this corridor.

3.7 Comparison results - pyranometers

The results shown in this report refer only to the comparison in 9 September 2020. The previous comparison in 2019 was reported on in the 12 Month Site Measurement Report.

For the GHI pyranometer, 612 values (1-minute averages) fulfilled the selection criteria. This is a solid amount of data for this comparison. Data from 28 and 29 October 2020 was used.

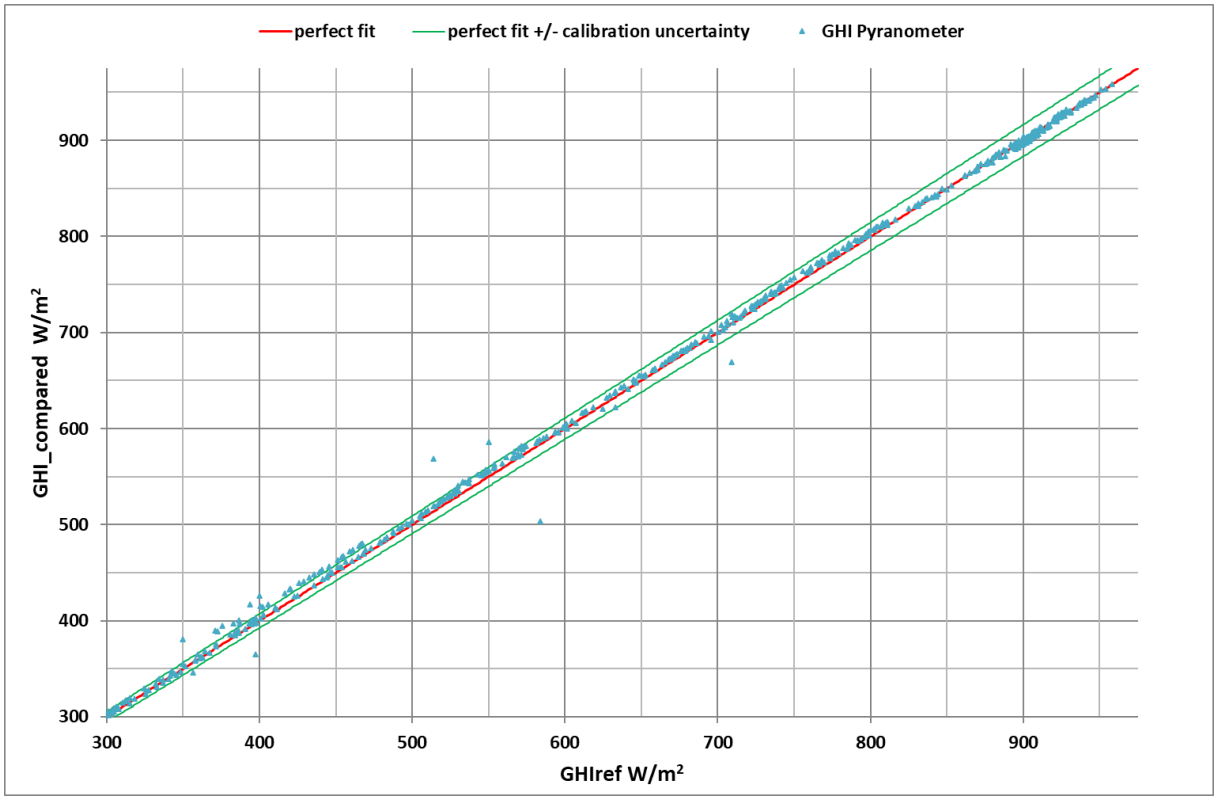

Figure 5: Comparison of GHI pyranometer CMP21 SN170860 (vertical axis) to traveling standard pyranometer CMP21 SN170585 (horizontal axis)

For the GHI pyranometer, the vast majority of measurement values, especially at high GHI levels, lie inside of the specified combined measurement uncertainty of ±1.83 %. The values outside this corridor are probably mostly due to maintenance work at the station. The sensitivity calibration of this sensor is accepted as correct and valid.

For the DHI pyranometer, some of the comparison period could not be used due to a sensor connection issue. Still, 261 values (1-minute averages) taken on 29 October 2020 fulfilled the selection criteria, including two consecutive periods of 106 and 55 minutes. This is a solid amount of data for this comparison.

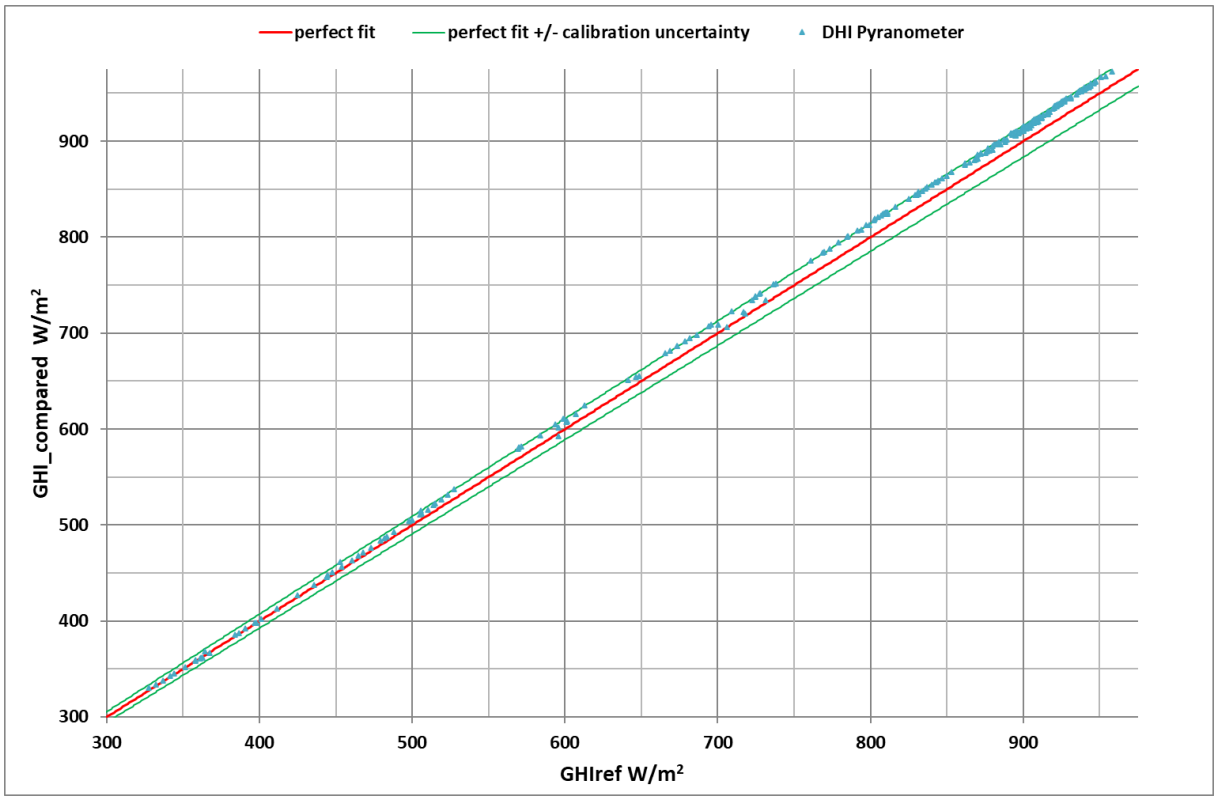

Figure 6: Comparison of DHI pyranometer CMP21 SN170861 (vertical axis) to traveling standard pyranometer CMP21 SN170585 (horizontal axis)

For the DHI pyranometer, the majority of measurement values lie inside of the specified combined measurement uncertainty of ±1.83 %. The sensitivity calibration of this sensor is accepted as correct and valid.

4 Measurement results

Table 5 shows the monthly summary values of all measurement variables at this weather station. Each parameter is discussed in more detail in the following sections.

Table 5: Monthly irradiation sums and average meteorological data

Month	Irradiance sums [kWh/m²]			Avg. Temp. [°C]	Avg. RH [%]	Avg. WS [m/s]	Avg. Press [hPa]	Sum Rain [mm]	Usable data
	GHI	DNI	DHI						
Jul 2018	136	48	95	24.1	83	0.9	860	282	100 %
Aug 2018	130	37	101	23.8	86	0.7	861	273	100 %
Sep 2018	149	92	93	23.7	80	1.0	866	38	100 %
Oct 2018	153	153	56	19.1	70	1.1	870	0	100 %
Nov 2018	120	141	41	15.0	71	1.0	871	0	100 %
Dec 2018	102	120	42	11.3	72	0.8	871	0	100 %
Jan 2019	100	97	48	10.4	72	0.8	871	13	100 %
Feb 2019	107	100	47	12.6	72	1.1	870	65	100 %
Mar 2019	166	149	64	16.2	64	1.4	868	30	100 %
Apr 2019	149	91	80	20.3	72	1.2	867	48	100 %
May 2019	181	127	83	23.5	63	1.5	864	100	100 %
Jun 2019	166	96	93	25.1	73	1.3	862	65	100 %
Year 1	**1659**	**1251**	**843**	**18.8**	**73**	**1.0**	**867**	**914**	**100 %**
Jul 2019	135	59	90	24.1	84	1.1	861	285	100 %
Aug 2019	155	90	89	24.9	81	1.1	862	124	100 %
Sep 2019	104	41	75	22.6	87	0.7	866	45	100 %
Oct 2019	141	122	61	20.0	78	1.0	870	1	100 %
Nov 2019	116	120	49	17.1	78	0.9	870	0	100 %
Dec 2019	109	139	37	11.0	76	0.9	871	22	100 %
Jan 2020	98	105	42	9.9	80	0.8	870	39	100 %
Feb 2020	115	94	58	12.5	76	1.1	870	7	100 %
Mar 2020	163	153	57	16.4	69	1.4	868	14	100 %
Apr 2020	152	107	71	19.2	68	1.3	868	54	100 %
May 2020	159	93	89	21.6	76	1.2	865	76	100 %
Jun 2020	138	61	91	23.5	84	0.9	862	168	100 %
Year 2	**1585**	**1184**	**809**	**18.6**	**78**	**1.0**	**867**	**835**	**100 %**

4.1 Solar irradiance

Figure 7 shows the measured monthly irradiance sums in a bar chart. A seasonal dependency of the irradiance sums is visible. Monthly global irradiance sums are generally higher in the summer season whereas the monthly direct irradiance sums are generally higher in winter, with diffuse irradiance behaving the opposite way to direct irradiance. This can be explained with the monsoon season that reduced DNI during the monsoon months with strong cloud cover. GHI is still high in these months because of the longer daylight duration per day and high sun elevation. In winter (dry season), the sky is more often showing clear-sky conditions leading to higher DNI values.

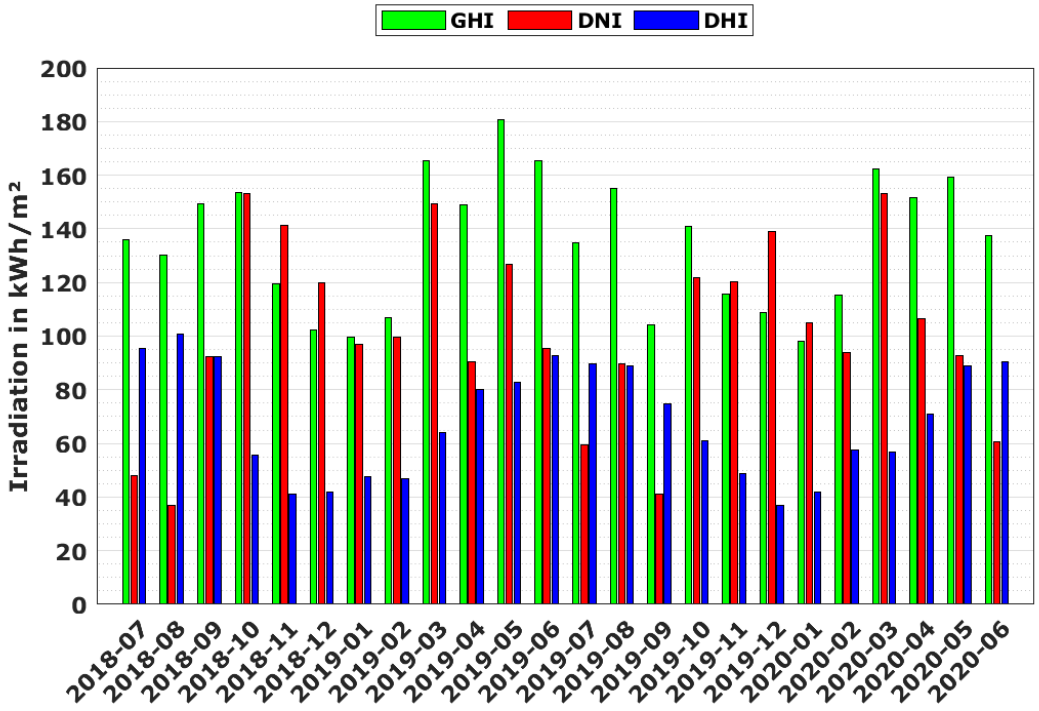

Figure 7: Monthly irradiation sums 2018-07 to 2020-06

The frequency distribution of hourly irradiance values (Figure 8) shows clear occurrence peaks for DNI (scale on the left axis) and DHI (scale on the right axis). The frequency distribution of GHI values (scale on left axis) is broader with a less expressed occurrence peak. The peak for DNI values is at 700 W/m² and generally, DNI values above 500 W/m² are frequent, but high values of more than 900 W/m² almost do not occur. The diffuse irradiance frequency peaks at around 150 W/m².

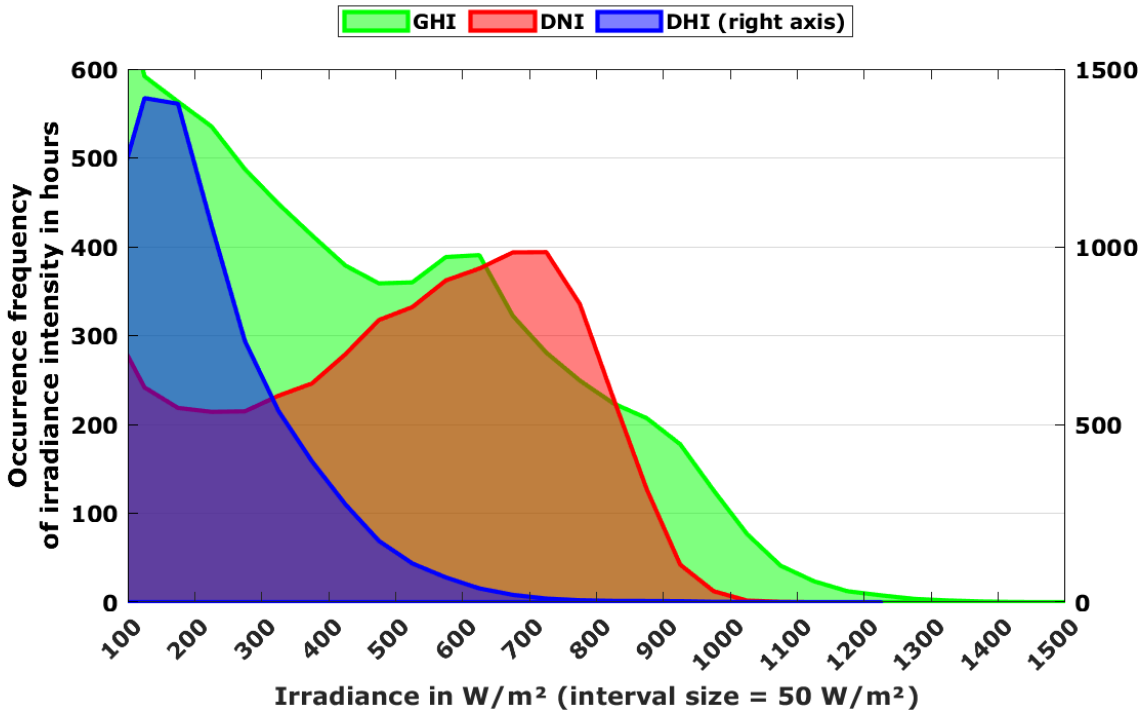

Figure 8: Frequency distribution of hourly irradiance averages 2018-07 to 2020-06

Figure 9 and Figure 10 show the irradiance intensity for GHI and DNI over the 24 months measurement period. The irradiation intensity and the length of the days vary with the seasons.

GHI is strongest during the summer period (Figure 9), corresponding to the high solar elevation periods. Cloudy periods with low GHI values occur mostly in the monsoon period.

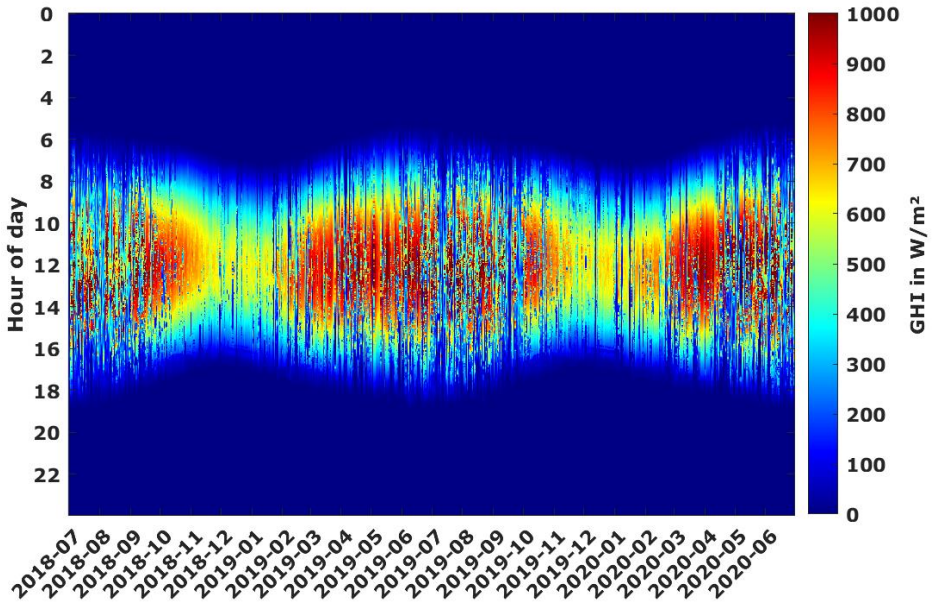

Figure 9: GHI irradiance intensity 2018-07 to 2020-06

The DNI values show high irradiance intensities of 700 W/m² and more with a high stability throughout the winter months (Figure 10). Periods with low or no DNI (cloud cover or aerosol load) occur mainly in monsoon season. Due to the higher sensitivity of DNI to reductions by light cloud cover or aerosols, low DNI periods occur more often than for GHI, hence the more fragmented appearance of the DNI plot.

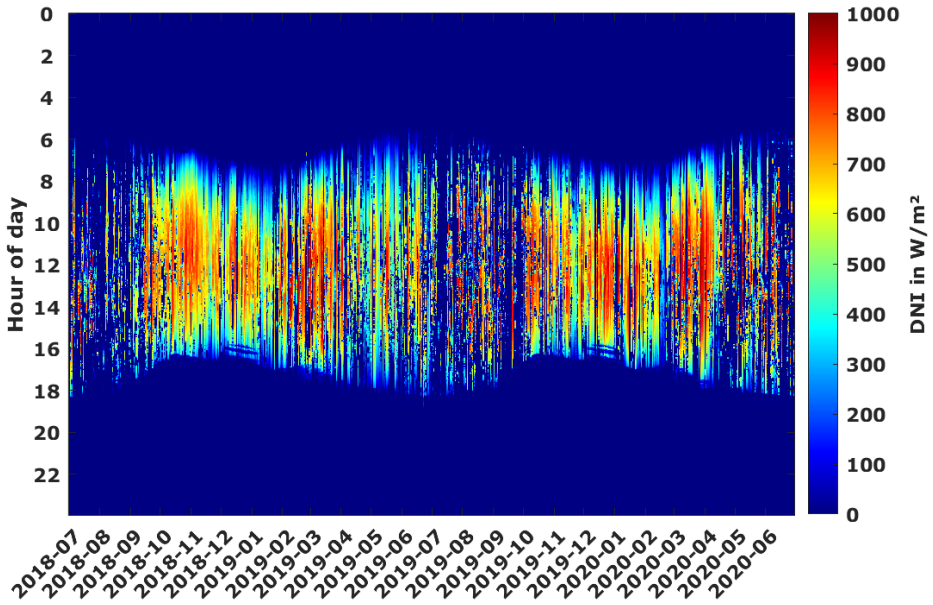

Figure 10: DNI irradiance intensity 2018-07 to 2020-06

4.2 Temperature and humidity

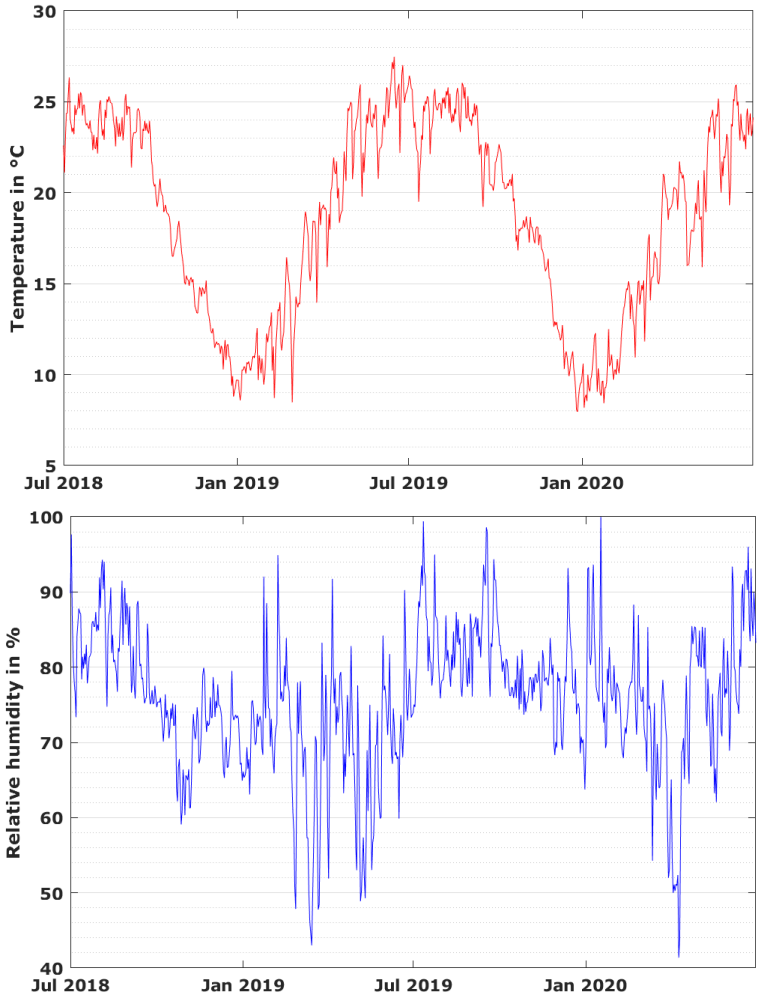

Figure 11: Daily temperature and relative humidity averages (1-minute resolution)

Figure 11 shows daily averages of temperate and relative humidity. A seasonal dependency is visible. Temperature is lowest in the northern hemisphere winter months (November to February) and high in the summer months. The month with the highest average temperature is June, the coldest monthly average temperature was in January. The most frequent temperature is 22°C (Figure 12). Daily relative humidity averages were highly variable, with tendentially lower humidity in the winter months (which were also the months with highest DNI sums) and high humidity during the monsoon season.

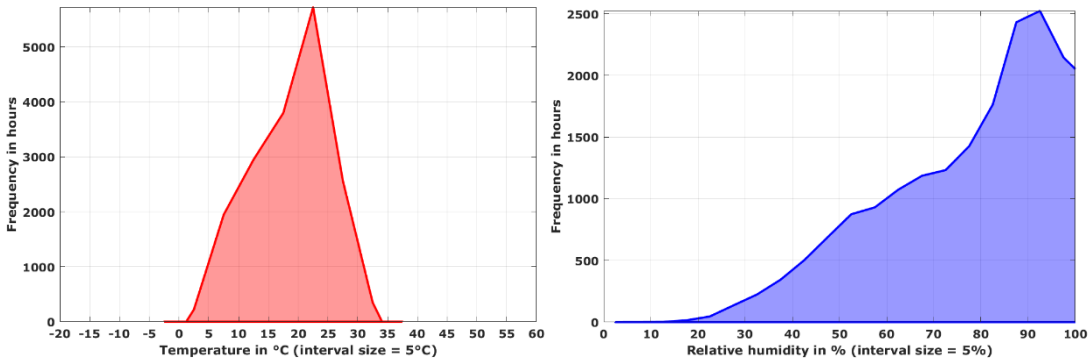

Figure 12: Frequency distribution of temperature and relative humidity (1-minute resolution)

4.3 Barometric pressure

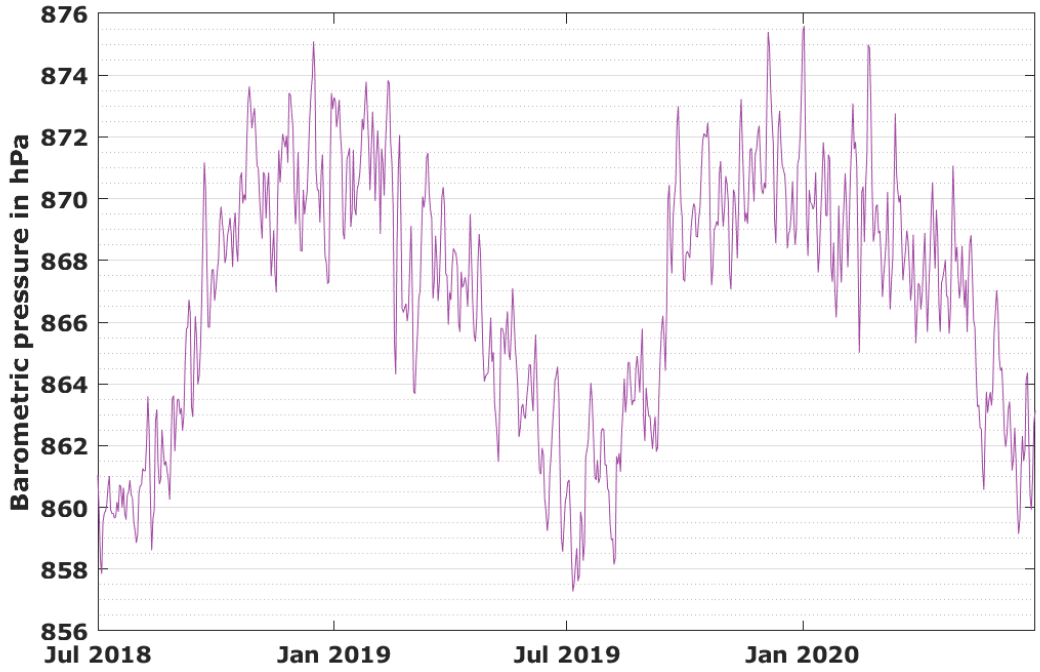

Figure 13: Daily averages of barometric pressure

Figure 13 shows daily averages of barometric pressure. Again, a clear seasonal dependence is visible: Higher pressure in the winter months and lower pressure in the summer months. Figure 14 shows the frequency distribution of recorded 1-minute resolution barometric pressure values.

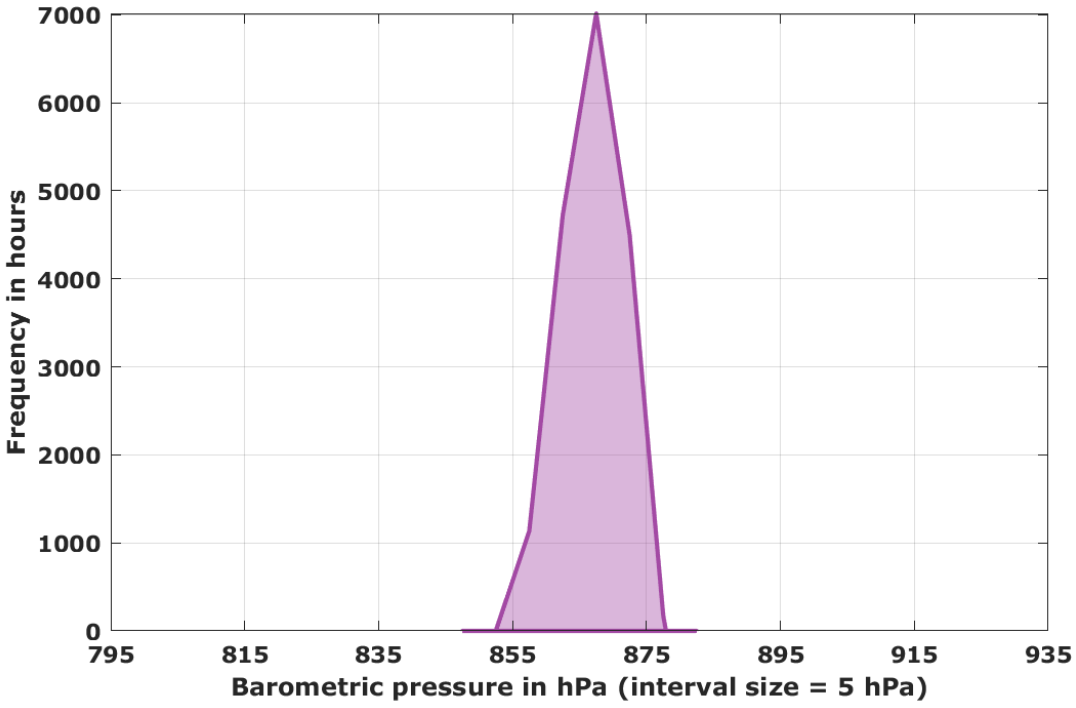

Figure 14: Frequency distribution of barometric pressure (1-minute resolution)

4.4 Precipitation

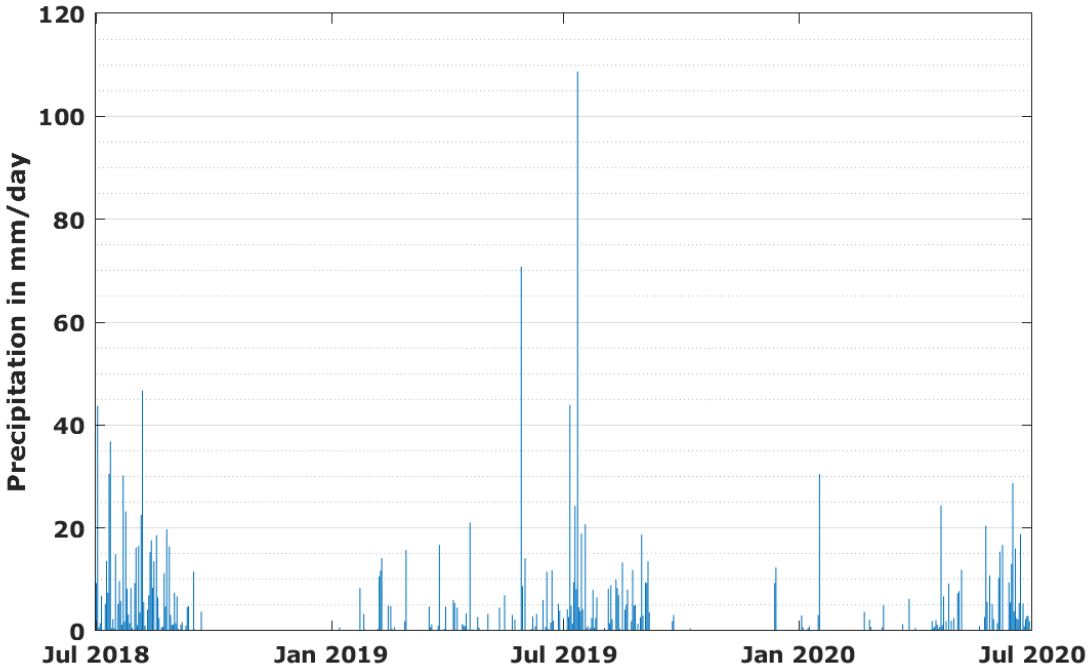

Figure 15: Daily sums of precipitation

Figure 15 shows the daily sums of precipitation. Again, a clear seasonal variability was observed with a dry period with no precipitation from November to January and an expressed rainy season in the months of May to September. The same periods were observed in both years of the measurement campaign.

4.5 Wind speed and direction

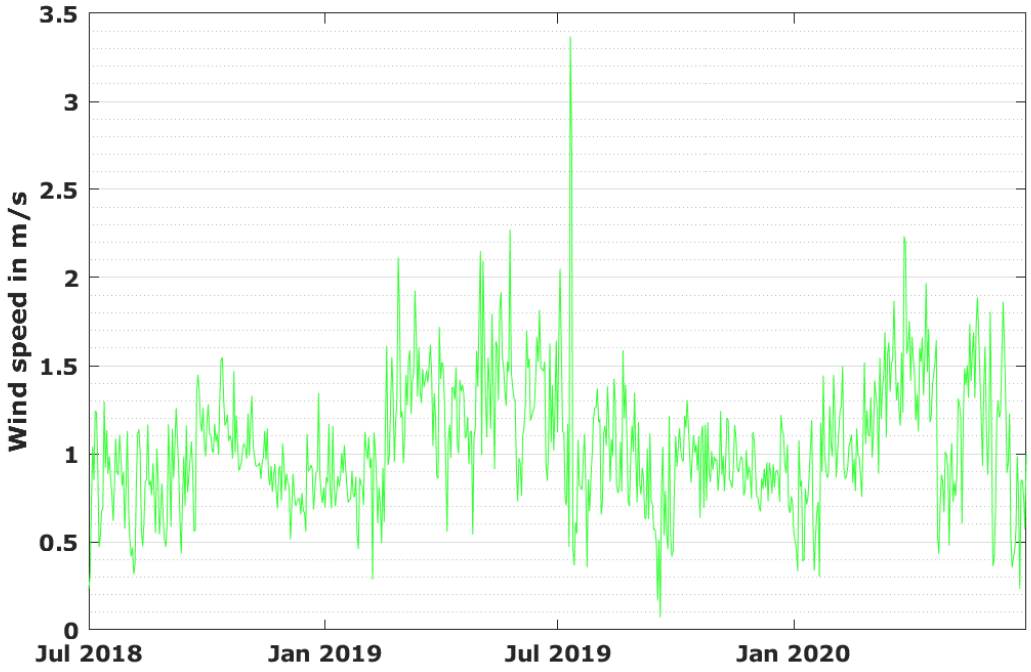

Figure 16: Daily averages of wind speed

Figure 16 shows the daily averages of wind speed. They are continuously low and almost no seasonal dependency was observed. The frequency distribution, shown Figure 17, emphasizes that wind speeds of <4 m/s are common and wind gusts of up to only 8 m/s were observed with any meaningful quantity.

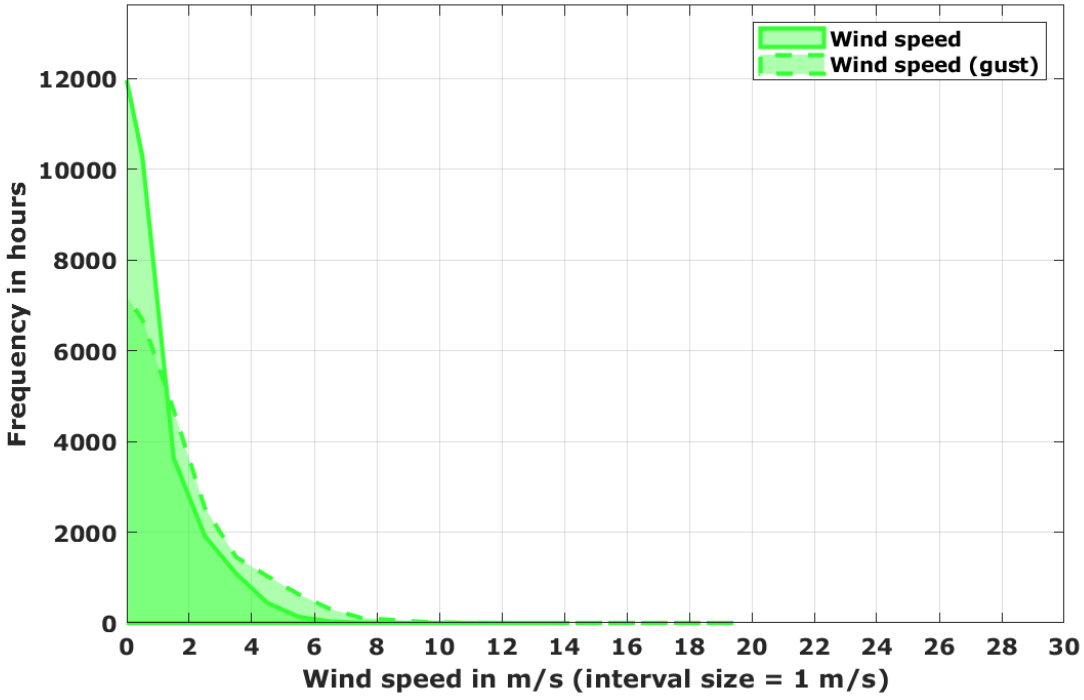

Figure 17: Frequency distribution of wind speeds (1-minute values)

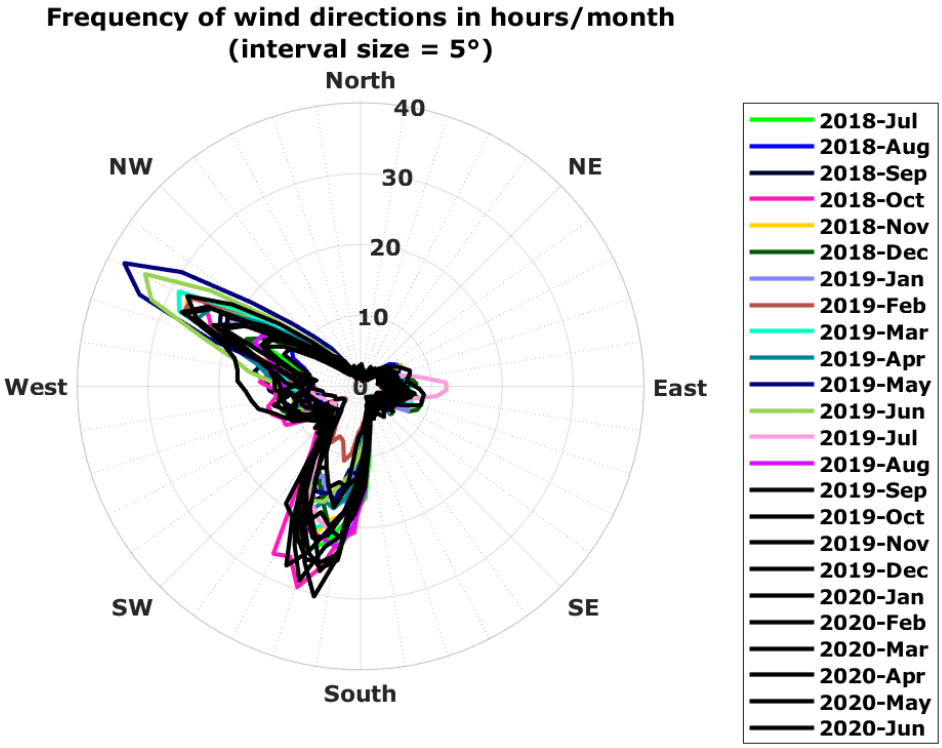

Figure 18: Wind direction distribution 2018-07 to 2020-06

Figure 18 shows the frequency distribution of wind direction in 1-minute time resolution. Two clear main wind directions are visible: From south-southwest during the summer months and from the west-northwest in the winter months and with transitionary months which show wind directions from the east and west for spring and autumn. Figure 19 shows that the few occasions of strong wind gusts >14m/s mainly originate from the west-north-west.

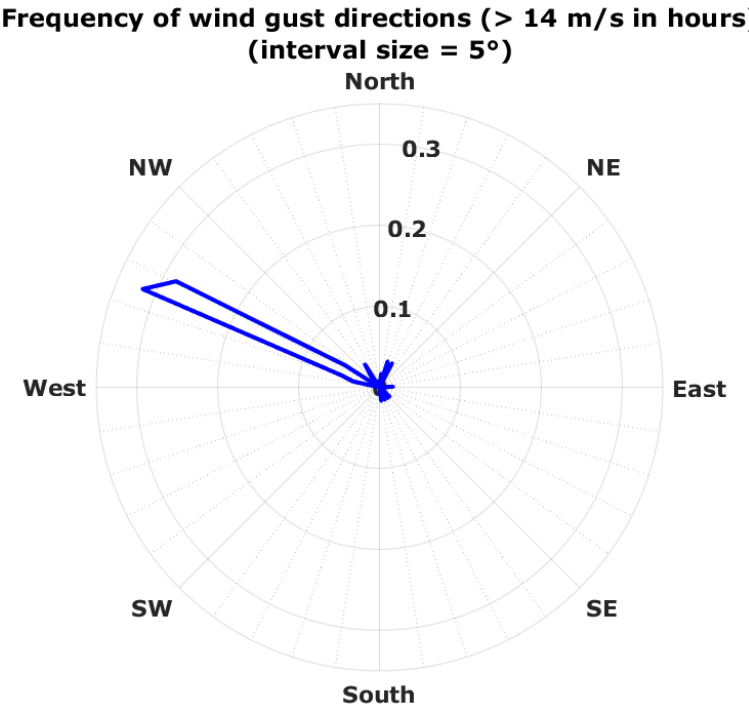

Figure 19: Wind gust direction distribution 2018-07 to 2020-06

5 On-site maintenance and irradiance sensor cleaning

The maintenance on site was done by local personnel. They were contracted and specially trained for this task upon installation of the station. The maintenance on site consisted mainly of visual inspection of the equipment, verifying the sensor alignment and cleaning the irradiance sensors and PV modules. The cleaning was scheduled to be performed on a work-daily basis, which was almost always adhered to throughout the whole measurement campaign with a ramp-up phase in the beginning of the campaign. Overall, 68% of all days had a cleaning event. The less frequent cleanings in 2020 can be credited to the Corona pandemic and the subsequent local lock-down. During some time, the campus was completely closed.

The exact cleaning dates and times are recorded in the monthly measurement reports and in the measurement data.

Table 6 gives an overview of the maintenance frequency per month.

Table 6: Number of maintenance visits by local staff per month

Month	Maintenance visits
Jul 2018	27
Aug 2018	24
Sep 2018	22
Oct 2018	20
Nov 2018	24
Dec 2018	23
Jan 2019	24
Feb 2019	19
Mar 2019	24
Apr 2019	23
May 2019	24
Jun 2019	22
Jul 2019	26
Aug 2019	25
Sep 2019	23
Oct 2019	22
Nov 2019	22
Dec 2019	26
Jan 2020	23
Feb 2020	19
Mar 2020	17
Apr 2020	0
May 2020	6
Jun 2020	11

6 Irradiance sensor soiling rates and soiling behavior

6.1 Soiling rates of DNI sensor (pyrheliometer)

All data from the pyrheliometer was corrected for sensor soiling by applying a linearly interpolated cleanliness factor[1] to the measurement data where applicable and necessary, i.e. only where cleanliness factor at cleaning was not 1. It has to be noted that cleanliness factors can only be determined under certain conditions:

- The cleaning is performed correctly and swiftly (no influencing of sensors except during a few seconds in the cleaning process)
- The irradiation conditions are stable enough to distinguish signal increase resulting from dust removal from natural fluctuations
- The signal increase resulting from dust removal is sufficiently large to be detectable

If no analysis is possible, soiling correction is not applied.

Table 7 on the next page shows

- Simplified average sensor cleanliness factors of the pyrheliometer DNI sensor detected at the above described cleaning events
- Simplified average daily soiling rate of the pyrheliometer. This rate expresses how much the irradiance sensor signal is reduced each day without cleaning. Simplified in this context means that the rate is a simple average of the change of cleanliness factors over all days of the month
- The minimum cleanliness factors (i.e., maximum sensor soiling) observed just before the sensor cleaning. Especially on/after strong wind occasions such as e.g. dust storms, high singular soiling rates can be observed. The daily cleaning ensures that these single events with high soiling do not influence long periods of data (usually only up to one day) and were mostly well corrigible

[1] Sensor cleanliness factor is defined as the dimensionless factor by which the recorded measurement value has to be divided in order to obtain the soiling-corrected value. E.g., if at cleaning a signal increase of 3% has been detected, the factor before the cleaning is 1/(1+0.03) = 0.97, after the cleaning (clean sensors) = 1.

Table 7: Average sensor cleanliness factors (pyrheliometer)

Month	Average sensor cleanliness	Minimum cleanliness factor	Average daily soiling rate
Aug 2018	1.00	1.00	0.0%
Sep 2018	1.00	1.00	0.0%
Oct 2018	1.00	1.00	0.0%
Nov 2018	1.00	0.98	0.1%
Dec 2018	1.00	0.97	0.1%
Jan 2019	1.00	0.96	0.3%
Feb 2019	1.00	0.97	0.3%
Mar 2019	1.00	0.98	0.2%
Apr 2019	1.00	0.99	0.0%
May 2019	1.00	0.99	0.1%
Jun 2019	1.00	0.98	0.2%
Jul 2019	1.00	1.00	0.0%
Year 1	**1.00**	**0.96**	**0.1 %**
Aug 2019	1.00	1.00	0.0%
Sep 2019	1.00	1.00	0.0%
Oct 2019	1.00	1.00	0.0%
Nov 2019	1.00	0.97	0.0%
Dec 2019	1.00	0.98	0.3%
Jan 2020	0.99	0.98	0.3%
Feb 2020	0.99	0.97	0.3%
Mar 2020	1.00	0.98	0.2%
Apr 2020	0.99	0.97	0.5%
May 2020	0.98	0.95	0.2%
Jun 2020	1.00	1.00	0.0%
Jul 2020	1.00	1.00	0.0%
Year 2	**1.00**	**0.95**	**0.3 %**

In several months, there have been notable sensor soiling rates at the site. However, the soiling influence on the measurement data (after correction) was small, and only few singular events of notable pyrheliometer soiling were detected. Summarizing, it can be said that pyrheliometer soiling is not an issue to data quality, because the sensor cleaning schedule was well adhered to and soiling correction was applied to the data. Even in the months with reduced sensor cleaning frequency (most affected: April and May 2020), no severe sensor soiling was detected, although the maximum single sensor soiling event occurred in May 2020.

6.2 Soiling rates of GHI and DHI sensors (pyranometers)

Due to the work-daily cleaning and the ventilation units that largely keep dust from settling on the pyranometer glass domes, soiling of the pyranometers was not an issue.

Further, due to the geometry of the sensor window (hemispheric glass dome), dust deposition is usually not uniformly distributed over the sensor field of view. For example, with wind coming from a certain direction, the glass dome may be dust-covered on the windward side only, lacking any dust cover on the leeward side. Thickness of the soiling layer may also vary over the height of the glass dome. Figure 20 shows an extreme example of this characteristic (from a site in a different country).

Such asymmetric distribution of soiling, when present, leads to different cleanliness factors of the sensor during the course of the day depending of the elevation angle of the sun (azimuth angle is constant on tracked systems). This asymmetric distribution is unknown and signal increase can only be observed at the time of cleaning.

Meaningful cleanliness factors can therefore not be obtained and sensor soiling correction is generally not applied to thermopile pyranometer measurements by CSP Services.

Figure 20: Asymmetric pyranometer glass dome soiling (exemplary picture)

7 Measurement accuracy and uncertainty

The overall data availability is 100% and the local maintenance (irradiance sensor cleaning and visual check) was done mostly on schedule and according to the defined procedures. Cleaning was usually done work-daily. All ground measurement data was subject to a multi-step data quality control process:

- Transmission of measurement data to CSP Services' server in near-real time
- Daily application of automatic data screening routines (e.g. gap test, step test, physical limits, consistency of solar irradiance components)
- Daily visual inspection of measurement data curves by experienced operators
- Soiling correction of irradiance values measured with pyrheliometer, similar to the method developed by [2]
- Continuous comparison of redundant measurements
- Verification of pyranometer calibration with traveling standard

The documentation of the ground measurement data includes:

- Report for weather station installation (including the calibration certificates of solar sensors)
- Maintenance visit report for the regular inspection visit
- Documentation of each sensor cleaning with time and date through a maintenance button on the automatic weather stations, pressed by the operator after sensor cleaning (included in the measurement data)

7.1 Coincidence of DNI measurements

The DNI measured by the pyrheliometer can be compared to DNI values calculated from the measured GHI and DHI values and the solar zenith angle (DNI_{calc}). DNI_{calc} and the coincidence between the two DNI values can be determined along the following formulas[2]:

$$DNI_{calc} = \frac{GHI - DHI}{\cos(SZA)}, \qquad \text{with } SZA\text{: Solar Zenith Angle} \tag{1}$$

$$DNI_{coincidence} = DNI - DNI_{calc} \tag{2}$$

This DNI coincidence is an indicator for the accuracy of the irradiance measurement, the deviation between the measured and calculated DNI should stay within reasonable limits. The usual limits are ±20 W/m² or 2-3% of the measured DNI for instantaneous values for higher sun elevations and high DNI values; high deviations of DNI_{calc} for low sun elevations are normal due to the cosine effect (close to sun elevation of zero, cos(SZA) converges to zero, thus dividing by cos(SZA) results in very high DNI_{calc} values). The comparison of DNI_{calc} and the measured DNI is used continuously for the daily irradiance measurement data quality control.

[2] F. Wolfertstetter, K. Pottler, N. Geuder, R. Affolter, A.A. Merrouni, A. Mezrhab, R. Pitz-Paal: Monitoring of mirror and sensor soiling with TraCS for improved quality of ground-based irradiance measurements. Energy Procedia 49 (2014), 2422-2432. doi:10.1016/j.egypro.2014.03.257.

Figure 21 shows the correlation of DNI and DNI_{calc} in a scatterplot of 1min and 10min resolution measurement values. The following effects can be seen:

- For low DNI values, the spread is larger than for higher values. This is partly due to the cosine effect as explained above.
- The majority of values are distributed in a narrow range around the bisecting line and almost symmetrical with a small bias toward higher DNI_{calc} values.
- In the 1min-resolution graph (left), a cluster of values below the bisecting line can be observed. This is attributable to the periods with incorrect tracker alignment.
- Other outliers can be explained by sensor shading from horizon at low sun elevations, dew on the pyrheliometer front window and the effect during the cleanings of the sensors by the operators
- In 10min time resolution, the spread is much less due to averaging effects

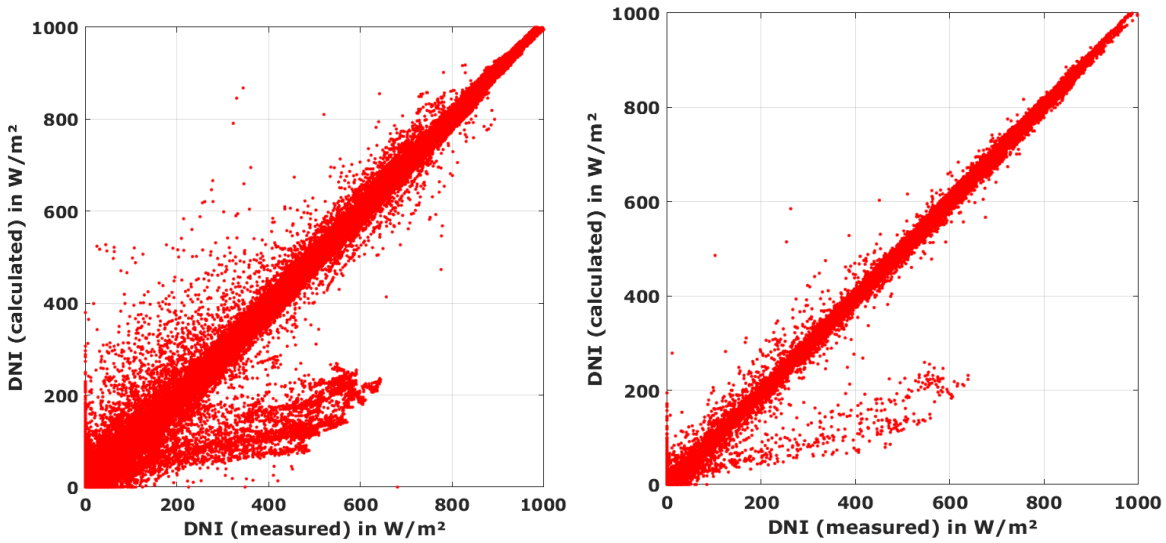

Figure 21: Correlation of DNI_{calc} and DNI (Left: 1min resolution. Right: 10min resolution)

In general, the coincidence can be considered as good. The data quality benefits of the stringent maintenance procedures, good sun tracker with active sun tracking, high sensor quality and accurate calibration.

For the further use of the measurement data, data points with DNI coincidence values outside ±20 W/m² or 2-3% of the measured DNI as well as clear outliers are recommended to be filtered and discharged.

7.2 Coincidence of GHI measurements

Using the same formula (1) and replacing DNI_{calc} with the measured DNI, the coincidence of GHI can be calculated from the DNI and DHI measurement. Analogue to DNI, GHI coincidence is defined as measured GHI minus calculated GHI.

Figure 22 shows the correlation of calculated and measured GHI. Again, the correlation can be considered as good with only few outliers and a cluster of values above the bisecting line which (as for the DNI coincidence) are mostly due to maintenance influences, shading occurrences and periods with non-ideal tracker alignment.

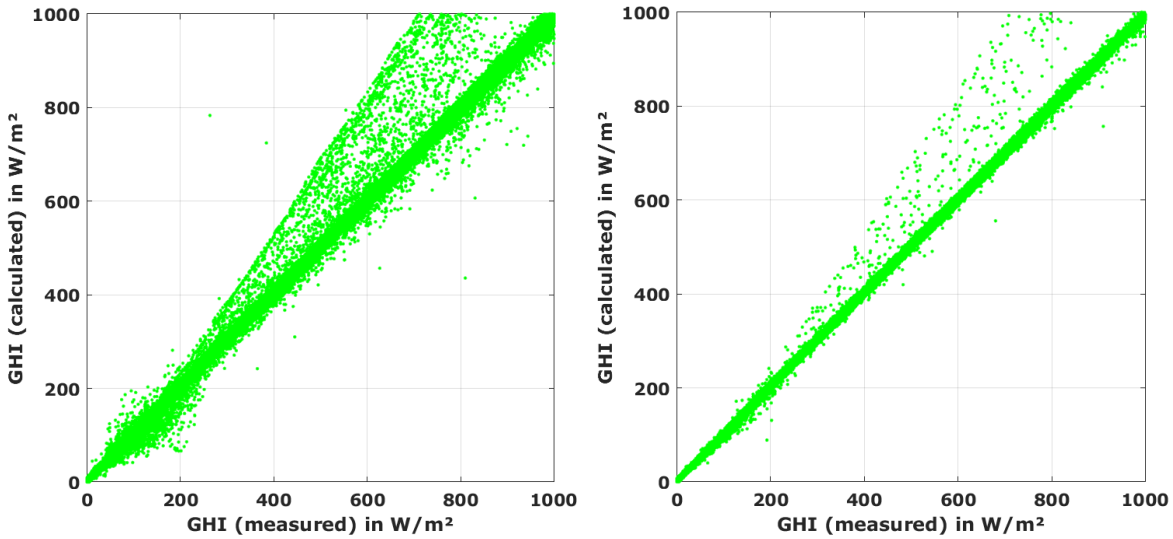

Figure 22: Correlation of GHI_{calc} and GHI (Left: 1min resolution. Right: 10min resolution)

7.3 Measurement uncertainty

The measurement uncertainty was assessed along the guideline in the NREL Best Practices Handbook for the Collection and Use of Solar Resource Data for Solar Energy Applications [1].

Best practices guidelines for selection of equipment, calibration, installation as well as operation and maintenance were followed and maintenance performance was assessed to include potential additional uncertainty contributions that could have occurred.

Two stages with related uncertainty contributions can be identified according to [1]:

- Instrument calibration (laboratory calibration by manufacturer): Uncertainty of calibration is specified in individual calibration certificates.
- Sources of uncertainty in field measurement are
    - Instrument-related (e.g. datalogger precision, pyrheliometer temperature response)
    - Installation-related (e.g. tracker alignment accuracy)
    - Operation-related (mainly frequency and thoroughness of cleaning)

DNI measurements

In the NREL Best Practices Handbook [1], typical calibration uncertainties for pyrheliometers are estimated with ±1.8% (at 95% level of confidence). The calibration certificate for the installed CHP1 pyrheliometer states a lower value of ±1.1%. Since this is well justified and the calibration verification did not give any reason of doubt, this lower value is assumed to be applicable.

In the field, much focus was given on using high-class measurement equipment (high-accuracy sensors, sun tracker and datalogger), excellent installation and alignment and regular maintenance and cleaning. The handbook estimates high-quality final measurement campaign DNI uncertainty with ±2.0% to ±2.5% for pyrheliometers for sub-hourly values (at 95% confidence interval).

For this measurement campaign, a measurement uncertainty of ±2.0% (at 95% confidence interval) for DNI values is estimated (after filtering and excluding values with bad coincidence as described above).

GHI and DHI measurements

In the literature, pyranometer calibration uncertainty is estimated with ±3.2% for solar zenith angles (SZA) between 30° and 60°. This is composed of an uncertainty of ±1.2% at a fixed, narrow incidence angle and a higher contribution of ±2.0% at a broader range of incidence angles [1]. Field measurements in well-maintained measurement campaigns can be estimated with uncertainties of ±3.0% for SZA between 30° and 60° and up to ±7.0% to ±10.0%for SZA>60° for GHI. For DHI, the uncertainty contribution resulting from SZA is irrelevant, since the direct irradiance is blocked by the shading ball assembly.

The calibration certificates for the installed CMP21 pyranometers state a value of ±1.35%. Calibration in the laboratory is done at a fixed incidence angle, thus this value replaces the literature estimate of ±1.2%. Since this is well justified and calibration verification did not give any reason of doubt, the value of ±1.35% is accepted.

The CMP21 pyranometers have an additional individual characterization for incidence angle and temperature sensitivity, and an incidence angle and temperature correction was applied to the GHI measurement values. Thus, the uncertainty resulting from broader incidence angles is much reduced. For the DHI, the temperature correction was applied. Therefore, the lower boundary of the literature values is assumed.

For this measurement campaign, a measurement uncertainty (at 95% confidence interval) of

- ±3.0% for all GHI values at SZA between 30° and 60°
- ±7.0% for all GHI values at SZA below 30° or above 60°
- ±2.0% for all DHI values

is estimated (after filtering and excluding values with bad coincidence as described above).

8 Conclusion

24-months of meteorological measurement data were collected at the site on IOE Pulchowk campus with a Tier1 automatic weather station between July 2018 and June 2020. The data was measured with a tracked pyrheliometer, ventilated pyranometers and additional meteorological sensors.

- Except for some periods with non-ideal tracker alignment and other minor measurement influences which have been recorded and documented, there were no significant operational difficulties
- Local maintenance and irradiance sensor cleaning were carried out on a work-daily schedule with acceptably little exceptions, each visit was recorded and documented
- One regular (preventive) maintenance visit to the station was performed, as well as two corrective visits for tracker realignment
- The measurement data was monitored on a daily basis by CSP Services operators, applying automatic quality assessment routines according to international best practices guidelines and visual inspection of the data by experienced operators
- The deviation between the installed irradiance sensors (redundant thermopile measurements) was within the expected limits in those periods where the tracker was well aligned
- The calibration of the used thermopile irradiance sensors was successfully validated upon a field calibration verification campaign after the measurement reporting period. For the field calibration verification, traveling standard sensors calibrated at the WRC in Davos, Switzerland, were used as calibration reference
- Measurement uncertainty is found to be within the expectable range given in best-practices literature

The 2-year measurement campaign at the site was successfully carried out, yielding a time series of on-site solar and meteorological measurement data in high quality. All measurement data was submitted to the World Bank in regular intervals by uploading to the energydata.info website. Additionally, the installation and maintenance reports as well as all calibration certificates and detailed descriptions of the measurement equipment were submitted to the World Bank.

9 References

[1] M. Sengupta, A. Habte, C. Gueymard, S. Wilbert and D. Renné, *Best Practices Handbook for the Collection and Use of Solar Resource Data for Solar Energy Applications: Second Edition,* Golden, Colorado: National Renewable Energy Laboratory, 2017.

[2] F. Wolfertstetter, , K. Pottler, A. Alami, A. Mezrhab and R. Pitz-Paal, "A novel method for automatic real-time monitoring of mirror soiling rates," in *SolarPACES 2012*, Marrakesh, Morocco, 2012.

CSP Services GmbH, Köln, Germany

CSPS Technical Documentation

Client: The World Bank

Selection #: 1230234

- Solar Resource Measurement Campaign Nepal –

24-Month Site Measurement Report Lumle, Nepal

Birk Kraas
Anne Forstinger

CSP Services GmbH
Friedrich-Ebert-Ufer 30
51143 Köln/Cologne, Germany
Email: b.kraas@cspservices.de
Version 04 December 2020

CSP Services
CONCENTRATING SOLAR POWER SERVICES

CSP Services GmbH, Köln, Germany

24-Month Station Operation Report

Table 1: Site and installation information

Site and Installation Information	
Site:	DHM Agro-Meteorological Station, Lumle
Coordinates, Elevation:	28.29666°N, 83.81800°E (WGS84), 1750 m
Station Type:	ESMAP Tier1 automatic weather station
Date of installation:	2018-06-22
Date of maintenance visits:	2018-10-12, 2019-10-25 & -26, 2020-10-03 & -04

CSP Services GmbH
Friedrich-Ebert-Ufer 30
51143 Köln · Germany
T: +49 2203 959 0030
F: +49 2203 180 2528
www.cspservices.de

Geschäftsführer
(Managing Directors):
Dr. Klaus Pottler
Dr.-Ing. Steffen Ulmer

Sitz der Gesellschaft
(Registered Office): Köln
Amtsgericht Köln
HRB 61644
USt-ID-No: DE814904840

Bank Account:
IBAN: DE18 5001 0060 0049 6816 08
BIC (Swift-Code): PBNKDEFF
Postbank · Frankfurt-Main · Germany

1 Contents

2 Executive summary

26 months of meteorological measurement data was collected at the measurement site at DHM agrometeorological station at Lumle between September 2018 and August 2020. This report summarizes the station operation during the reported measurement period as well as the results from the irradiance sensor calibration verification. This calibration verification was performed upon the second maintenance visit performed on 19 October 2019.

Figure 1: Site location west of Pokhara (Image: Google Earth)

The Tier1 meteorological measurement station was installed at the site in Lumle on 22 June 2018 and visited for regular maintenance visit on 12 October 2018, 19 October 2019 and 03+04 October 2020.

Further scheduled maintenance visits in spring 2020 could not be conducted due to the lockdown and travel restrictions imposed or risk of travel resulting from the COVID-19 pandemic.

After an initial phase with sun tracker misalignment, the station was operating correctly, the data availability was 100% (no data gaps) and the local maintenance (work-daily sensor cleaning and visual check) was done mostly on schedule and according to the defined procedures.

The measurement data collected after the reporting period is not subject of this report.

3 Equipment description and functionality, sensor calibration

3.1 Measurement equipment

The Tier1 automatic weather station is equipped with a datalogger and a GSM modem, a sun tracker equipped with an ISO9060 First Class pyrheliometer for DNI measurement and ISO9060 Secondary Standard pyranometers for measurement of GHI and DHI. As additional meteorological sensors, an anemometer and a wind vane for wind speed and direction measurement on 10 m height, a barometric pressure sensor, a tipping bucket rain gauge and a temperature and humidity sensor are installed. The exact types of sensor/equipment and serial numbers are listed in the tables below.

Table 2: Equipment and serial numbers

Equipment and serial numbers		
Automatic Weather Station	CSP Services MHP Automatic Weather Station	CSPS.MT.18.204
Main Control Box	CSP Services	CSPS.CA.18.202.0003
Datalogger	Campbell CR1000	E12052
Datalogger peripherals	CFM100 CF Module	14204
Sun Tracker	K&Z Solys2	180407
Sun Sensor	K&Z Sun Sensor Kit	170322
GSM Modem	Sierra Wireless Xtend	
GPS Module	Garmin 16x HVS	1A4250267
Power Supply	4x100 W PV modules, 4x150 Ah solar battery	Connected as 200 W, 300 Ah @24VDC

Table 3: Measured Parameters and Sensors

Measured parameter	Unit	Sensor type	Serial number
GHI	W/m²	K&Z CMP21, w. CVF4 ventilation unit	170864
DHI	W/m²	K&Z CMP21, w. CVF4 ventilation unit	170865
DNI	W/m²	K&Z CHP1	180582
Temperature	°C	Campbell CS215	E20180
Humidity	%	Campbell CS215	E20180
Pressure	hPa	Setra 278	7225863
Precipitation	mm	Young 52203	TB 14418
Wind Speed	m/s	NRG #40C anemometer	1795-00303669
Wind direction	°N	NRG #200P wind vane	1799-00019694

3.2 Equipment functionality

The tracking device was misaligned between 5 July 2018 and 12 October 2018. A site visit on 05 August 2018 to restore the tracker alignment was unsuccessful due to lack of direct irradiance, which is required to perform this task since the alignment optics are reliant on sufficient direct sunlight. An earlier second visit was not undertaken since due to the weather in this period, no period with sufficiently certain availability of direct irradiance to justify the effort of traveling from Kathmandu occurred.

After the alignment was restored, the functionality of the equipment was good, the station was operating without significant problems afterwards.

On few occasions, dew or droplets on the pyrheliometer was noticed. This presumably happened at morning fog events or rain spray. Impact on the data was negligible since the dew evaporated quickly.

Notable events at the station are listed in Table 4.

Table 4: Notable events during operation

Date	Event
2018-07-05 to 2018-10-12	Sun tracker misaligned; no DNI and DHI measurement data available in this period. Due to this misalignment, two months were added to total measurement duration
2018-10-12, -13	Station maintenance (regular maintenance visit)
2018-12-04, -09	Dew on pyrheliometer front window
2019-01-06	Dew on pyrheliometer front window
2019-06-07	Dew on pyrheliometer front window
2019-08-16, -19	Dew on pyrheliometer front window
2019-09-17	Dew on pyrheliometer front window
2019-10-21	New data logger program uploaded
2019-10-25, -26	Station maintenance (regular maintenance visit)
2019-11-01	Dew on pyrheliometer front window
2020-01-24	Dew on pyrheliometer front window
2020-05-22	New data logger program uploaded

3.3 Sensor calibrations

Factory calibrations

All sensors were calibrated before deployment in the field. The thermopile pyranometers and pyrheliometers were calibrated in the factory by the manufacturer according to applicable ISO standards. Other meteorological sensors (wind speed sensor, barometric pressure sensors) were also calibrated by the respective manufacturer. Calibration certificates were handed over with the installation report.

Pyrheliometer and pyranometer field calibration verification

Upon the second and third maintenance visits, an irradiance sensor comparison against traveling standard sensors was performed. The travelling standard sensors were calibrated against the World Radiometric Reference (WRR) at Davos (Switzerland) prior to their delivery to Nepal. The following equipment was installed for the comparison measurement:

- An additional pyrheliometer mounting clamp for a travelling standard reference pyrheliometer on the sun tracker
- An instrument table with mounting place for a reference pyranometer (to have the reference pyranometer installed on the same height as the other pyranometers on the ventilation units)
- Reference sensors at the described additional mounting places:
    - CHP1 Pyrheliometer SN 180580, Sensitivity: 8.096 µV/Wm²
    - CMP21 Pyranometer SN 170858, Sensitivity: 8.84 µV/Wm²

  Calibration certificates from PMOD WRC are attached to this report.

Figure 2: Tracker with regular (1) and reference pyrheliometer (2), reference pyranometer (3)

Figure 3: Tracker with DHI pyranometer (4) GHI pyranometer (5), reference pyranometer (3)

All sensors were measured with 1 Hz resolution, and the measurements were stored on the datalogger in 1 min averages.

3.4 Comparison method - pyrheliometer

The comparison measurement for pyrheliometers was set up following the measurement set-up procedures and recommendations described in ISO 9059 as closely as possible. *Please note: This cross-comparison is not a full ISO-compatible calibration, as this was not the scope of the cross-comparison. The ISO standard was only followed as far as possible to obtain comparable results while adhering to best practices procedures.*

If both pyrheliometers are calibrated correctly, the observed deviation between the compared instruments should be within the combined calibration uncertainty. For the installed CHP1 sensor, Kipp&Zonen specifies a calibration uncertainty of ±1.1%. For the reference sensor, a calibration uncertainty of ±0.32 % is specified by PMOD (both at 95% coverage probability, stated in the calibration certificates). The combined calibration uncertainty is therefore ±1.15%. No other additional uncertainty contributions are added, since both devices are of identical model and installed on the same sun tracker, using the same datalogger. The final combined uncertainty is therefore ±1.15%, which can be interpreted as a strict limit since instrument-specific uncertainty contributions such as instrument temperature or individual alignment are neglected.

The measurement data from both sensors (reference and sensor to be compared) was filtered as follows:

- Only data where no soiling correction was applied (perfectly clean sensor windows)
- Only values with DNI >700 W/m² were used (acc. to ISO 9059) where this was possible.
- Outliers filtered and discarded (e.g., temporary shading of a single instrument due to maintenance staff passing the station or similar)
- Stable irradiance conditions (ideally, clear-sky conditions), if possible

Enough data was available to apply these filter criteria and still have a sufficient amount of comparison data for all individual sensors.

The graph in the result section shows the perfect fit (exact identical measurement of reference and tested sensor) as the angle bisector in red. Above and below the bisecting line is the corridor defined by adding/subtracting the combined calibration uncertainty. If the used calibration constant of the tested sensor is correct, the vast majority of all measurement values (shown as blue triangle markers and named as "DNI") must be within this corridor.

3.5 Comparison results - pyrheliometer

The results shown in this report refer only to the comparison on 04 October 2020. The previous comparison in 2019 was reported on in the 12 Month Site Measurement Report.

110 values (1-minute averages) remain after applying the filters. This is a sufficient amount of data for a comparison.

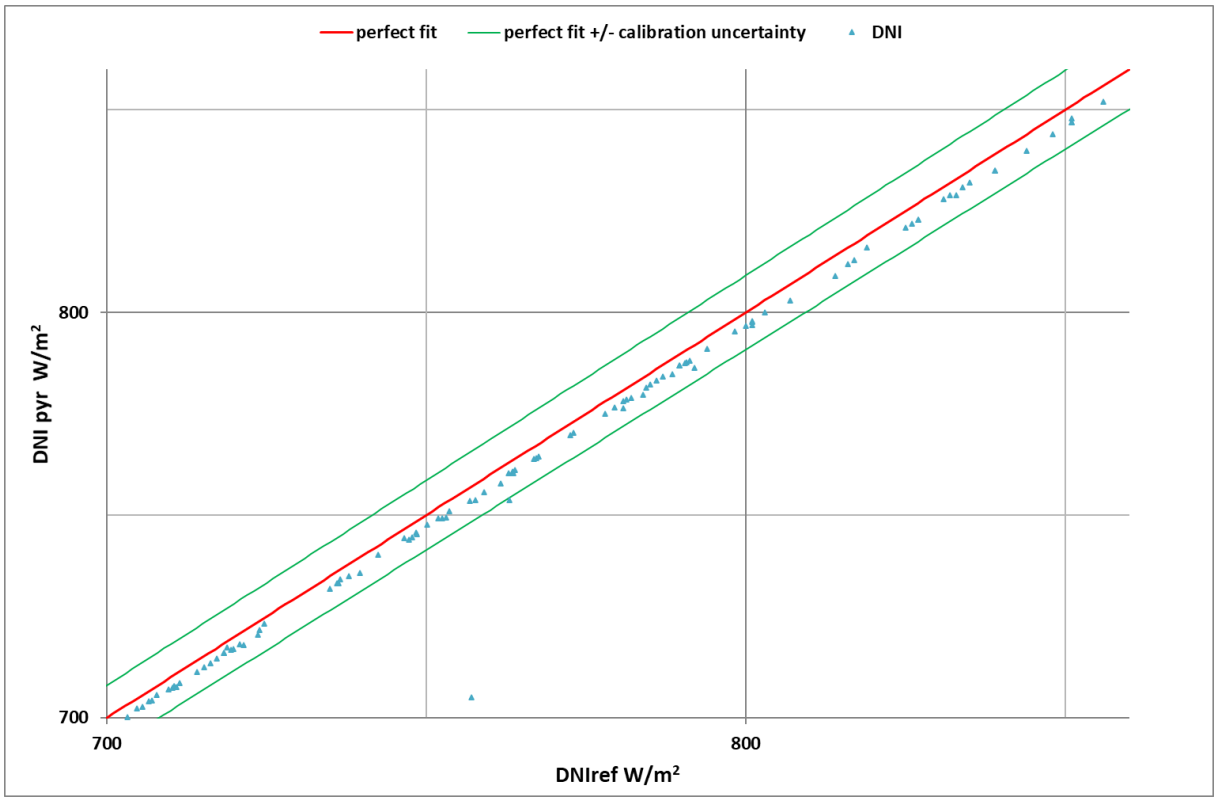

Figure 4: Comparison of pyrheliometer CHP1 SN180582 (vertical axis) to traveling standard pyrheliometer CHP1 SN180580 (horizontal axis)

All measurement values lie inside of the specified combined measurement uncertainty of ±1.15 %. The few outliers may be due to interactions of the staff working at the station during the maintenance visit.

The sensitivity calibration of this sensor is accepted as correct and valid.

3.6 Comparison method - pyranometers

The comparison measurement for pyranometers was set up following the measurement set-up procedures and recommendations described in ISO 9847 as closely as possible. *Please note: This cross-comparison is not a full ISO-compatible calibration, as this was not the scope of the cross-comparison. The ISO standard was only followed as far as possible to obtain comparable results while adhering to best practices procedures.*

If both instruments are calibrated correctly, the observed deviation between the compared instruments should be within the combined calibration uncertainty. For the installed CMP21 pyranometers, Kipp&Zonen specifies a calibration uncertainty of ±1.35%. For the reference sensor, a calibration uncertainty of ±1.24 % is specified by PMOD (both at 95% coverage probability, stated in the calibration certificates). The combined calibration uncertainty is therefore ±1.83%. No other additional uncertainty contributions are added, since all devices are of identical model and installed on the same sun tracker, using the same datalogger. The final combined uncertainty is therefore ±1.83%, which can be interpreted as a strict limit since instrument-specific uncertainty contributions such as instrument temperature or individual alignment are neglected.

These values were determined at high incidence angles and with high global irradiance values. The uncertainty for lower sun elevations and lower GHI values may be significantly higher [1]. Therefore, only high sun elevation and high GHI values were utilized for the comparison.

The measurement data from all three sensors (reference and sensors to be compared) was filtered as follows:

- Only values with sun elevation > 20° were used (acc. to ISO 9847)
- Only values with GHI > 300 W/m² were used to exclude bad weather conditions
- Only series of minimum numbers of consecutive values were used for the comparison (following ISO 9847)
    - In periods with cloudless skies: min. 10 consecutive values
    - In periods with some clouds: min. 1-5 consecutive values
    - In cloudy sky (overcast): not relevant due to 400 W/m²filter
- Outliers not considered (e.g., temporary shading of a single instrument due to maintenance staff cleaning the sensor or similar)

Enough data was available to apply these filter criteria and still have a sufficient amount of comparison data.

The graphs in the result section show the perfect fit (exact identical measurement of reference and tested sensor) as the angle bisector in red. Above and below is the corridor defined by adding/subtracting the combined calibration uncertainty. If the calibration factor or the tested sensor is corrected, the vast majority of all measurement values (shown as blue triangle markers named as "GHI Pyranometer" or "DHI Pyranometer", the naming refers to the mounting place on the tracker and for which measurement these pyranometers are usually used) must be within this corridor.

3.7 Comparison results - pyranometers

The results shown in this report refer only to the comparison on 4 October 2020. The previous comparison in 2019 was reported on in the 12 Month Site Measurement Report.

122 values (1-minute averages) on 4 October fulfilled the selection criteria. This is a sufficient amount of data for this comparison.

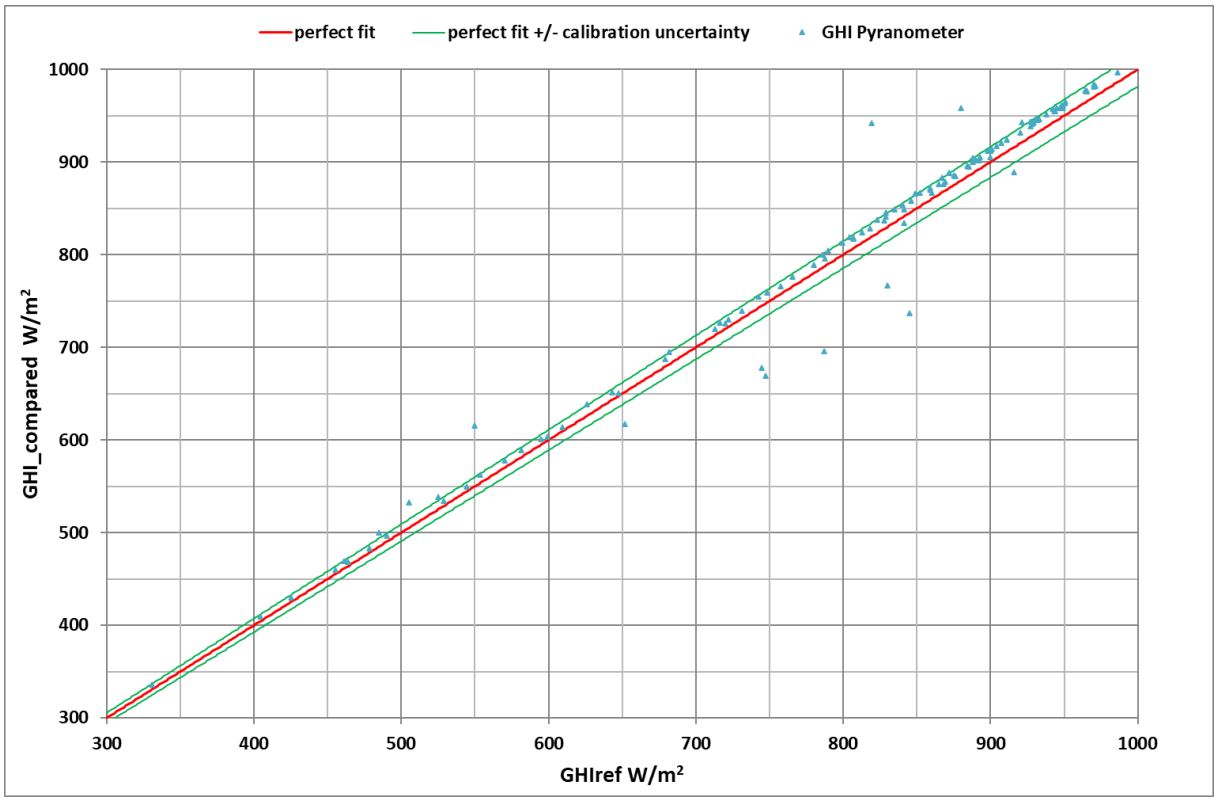

Figure 5: Comparison of GHI pyranometer CMP21 SN170864 (vertical axis) to traveling standard pyranometer CMP21 SN170585 (horizontal axis)

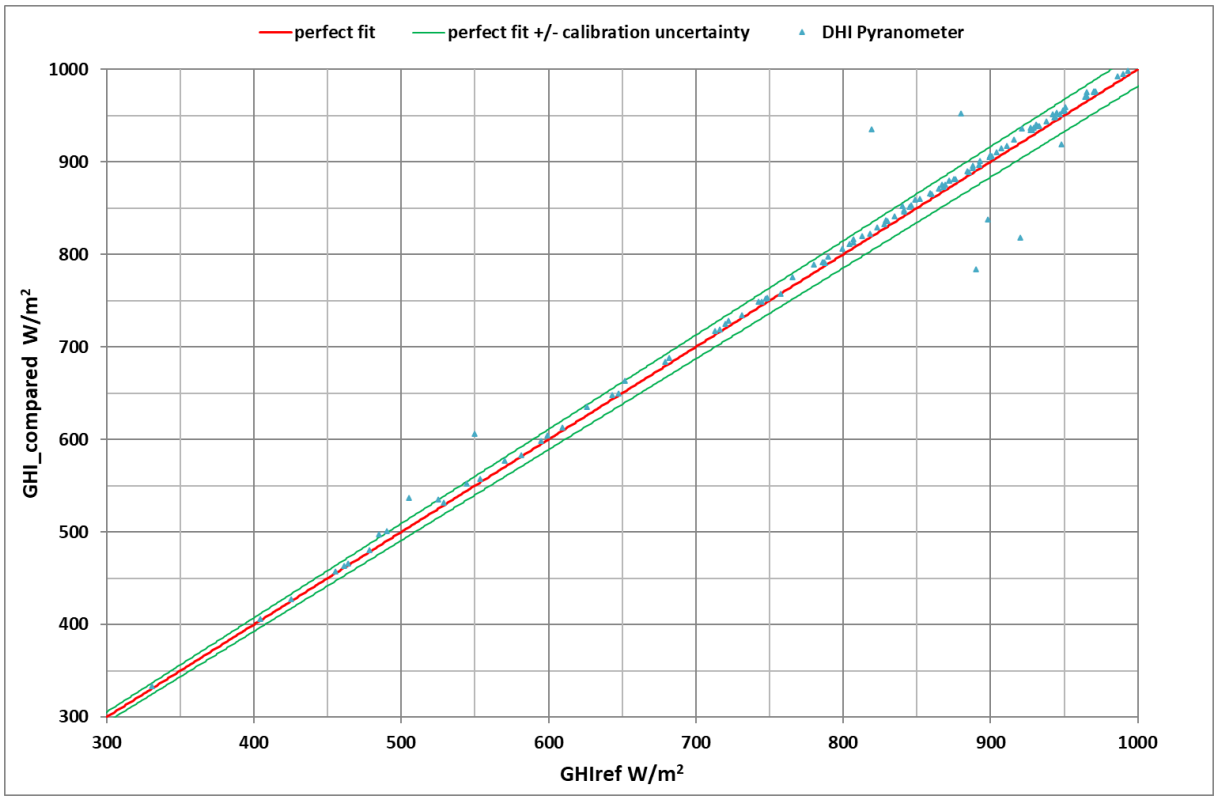

Figure 6: Comparison of DHI pyranometer CMP21 SN170865 (vertical axis) to traveling standard pyranometer CMP21 SN170585 (horizontal axis)

Except for a few outliers due to work on the station or external influence, all measurement values from the dataset lie inside of the specified combined measurement uncertainty of ±1.83 %. The sensitivity calibration of both sensors is accepted as correct and valid.

4 Measurement results

Table 5 shows the monthly summary values of all measurement variables at this weather station. Each parameter is discussed in more detail in the following sections.

Table 5: Monthly irradiation sums and average meteorological data

Month	Irradiance sums [kWh/m²]			Avg. Temp. [°C]	Avg. RH [%]	Avg. WS [m/s]	Avg. Press [hPa]	Sum Rain [mm]	Usable data
	GHI	DNI	DHI						
Jul 2018	119	-	-	20.2	96	1.4	820	1399	-
Aug 2018	113	-	-	20.0	97	1.2	821	1237	-
Sep 2018	116	-	-	19.3	97	1.4	825	608	100 %
Oct 2018	143	-	-	15.3	85	1.6	828	40	100 %
Nov 2018	115	127	47	12.5	84	1.7	828	6	100 %
Dec 2018	106	136	41	8.8	76	1.7	828	0	100 %
Jan 2019	112	130	45	8.0	73	1.8	828	59	100 %
Feb 2019	109	105	47	9.6	83	2.0	827	97	100 %
Mar 2019	165	160	56	13.0	72	2.0	826	65	100 %
Apr 2019	137	84	71	16.4	83	1.9	825	169	100 %
May 2019	187	132	78	18.8	76	2.1	824	192	100 %
Jun 2019	157	87	86	20.2	90	1.7	822	196	100 %
Jul 2019	125	43	89	20.2	96	1.3	820	711	100 %
Aug 2019	138	62	90	20.7	95	1.4	822	873	100 %
Year 1	**1610**	**-**	**-**	**15.2**	**84**	**1.7**	**825**	**3016**	
Sep 2019	101	37	75	18.9	96	1.2	825	826	100 %
Oct 2019	125	97	66	16.2	93	1.2	828	158	100 %
Nov 2019	109	97	53	14.0	89	1.5	828	14	100 %
Dec 2019	108	143	35	8.6	80	1.7	828	46	100 %
Jan 2020	102	110	41	7.4	84	1.6	827	69	100 %
Feb 2020	109	89	55	9.1	85	1.7	828	40	100 %
Mar 2020	166	163	54	12.8	79	1.9	826	103	100 %
Apr 2020	153	110	69	15.3	79	1.8	826	234	100 %
May 2020	150	82	84	17.5	87	1.6	824	211	100 %
Jun 2020	119	45	86	19.5	95	1.2	822	647	100 %
Jul 2020	94	21	77	19.7	98	1.2	821	1031	100 %
Aug 2020	113	37	85	20.4	97	1.2	821	782	100 %
Year 2	**1449**	**1031**	**780**	**15.0**	**89**	**1.5**	**825**	**4161**	**100 %**

July to August 2018 is not used for annual total or average values, additionally DNI and DHI of September and October 2018 is not used for the annual sum of the first measurement year due to tracker misalignment in that period. DNI and DHI values were not measured correctly. Therefore, the measurement period was extended by two months in order to obtain the required minimum data completeness including DNI and DHI values.

4.1 Solar irradiance

Figure 7 shows the measured monthly irradiance sums in a bar chart. Some seasonal dependency of the irradiation sums is visible. Monthly irradiation sums are generally higher in the summer season for the GHI whereas the DNI monthly sums are generally higher in winter.

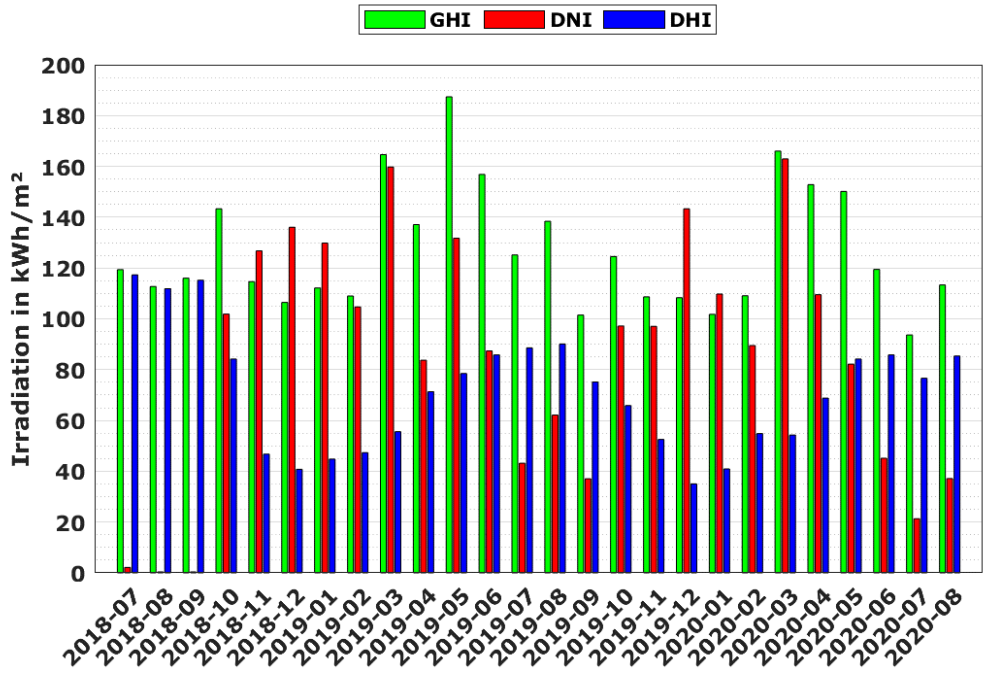

Figure 7: Monthly irradiation sums 2018-07 to 2020-08

As mentioned before, the sun tracker was misaligned until 18 October 2018. No DNI or DHI data is available for the period before. Therefore, in July to October 2018 DNI sum is small and DHI sum appears overly large because during most of the time, DHI was measured identical to GHI. The DNI and DHI bars in Figure 7 can therefore be ignored for July to October 2018.

The frequency distribution of hourly irradiance values (Figure 8) shows clear occurrence peaks for DNI (scale on the left axis) and DHI (scale on the right axis). The frequency distribution of GHI values (scale on left axis) is broader with a less expressed occurrence peak. The peak for DNI values is just above 900 W/m² and generally, DNI values above 800 W/m² are frequent. The diffuse hourly irradiance frequency peaks at around 100 W/m².

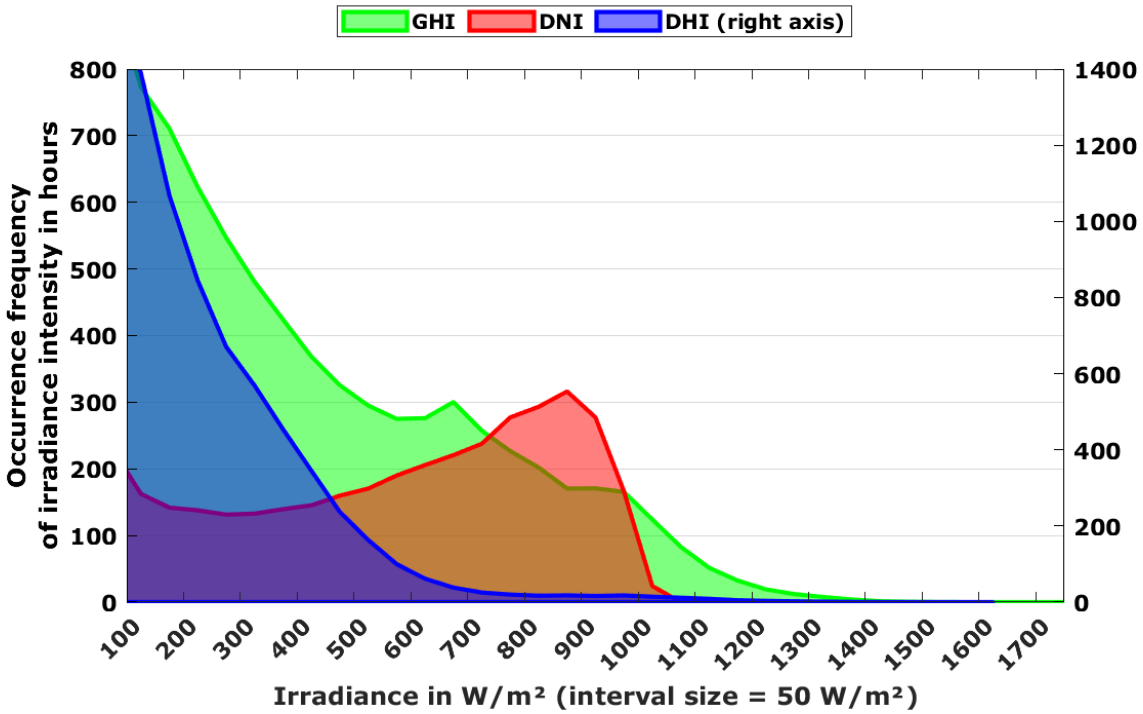

Figure 8: Frequency distribution of hourly irradiance averages 2018-07 to 2020-08

Figure 9 and Figure 10 show the irradiance intensity for GHI and DNI over the 26 months measurement period. The irradiation intensity and the length of the days vary with the seasons.

GHI is strongest during the summer period (Figure 9), corresponding to the high solar elevation periods. Cloudy periods with low GHI values occur mostly in the monsoon period. Indicated by the orange arrow in Figure 9 is shading that stems from a mast that was built after the first year of measurement. It is advised to exclude these measurement values from further use of the data.

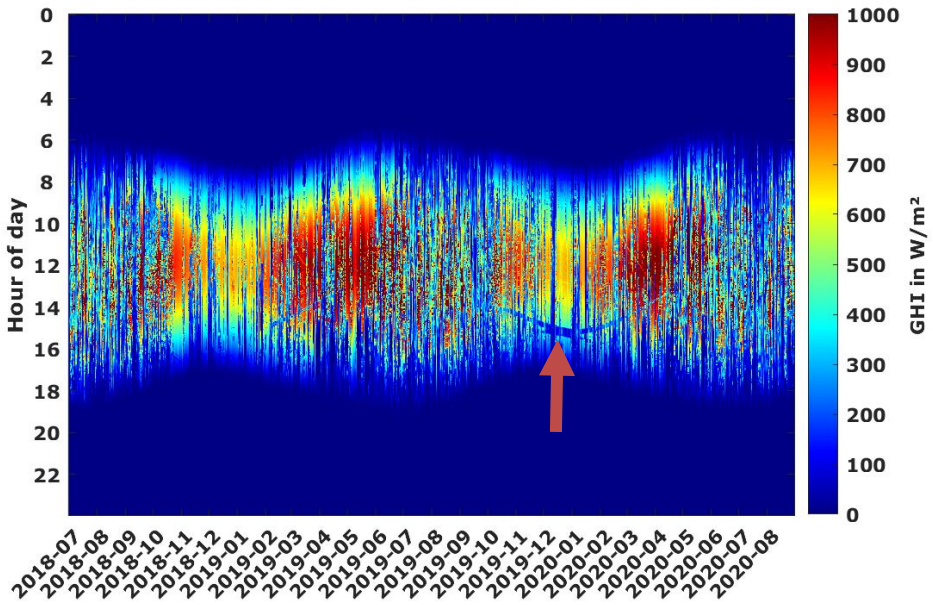

Figure 9: GHI irradiance intensity 2018-07 to 2020-08

The DNI values show high irradiance intensities of above 700 W/m² with a high frequency and over periods of several days to weeks throughout the winter months (Figure 10). Periods with low or no DNI (cloud cover or aerosol load) occur mainly in monsoon season. Due to the higher sensitivity of DNI to reductions by cloud cover or aerosols, low DNI periods occur more often than for GHI, hence the more fragmented appearance of the DNI plot.

In the beginning of the measurement campaign, the DNI was not measured, which is why Figure 10 shows zero value for that time period. Indicated by multiple orange arrows in Figure 10 are shadings from surrounding masts. It is advised to exclude these measurement values from further use of the data.

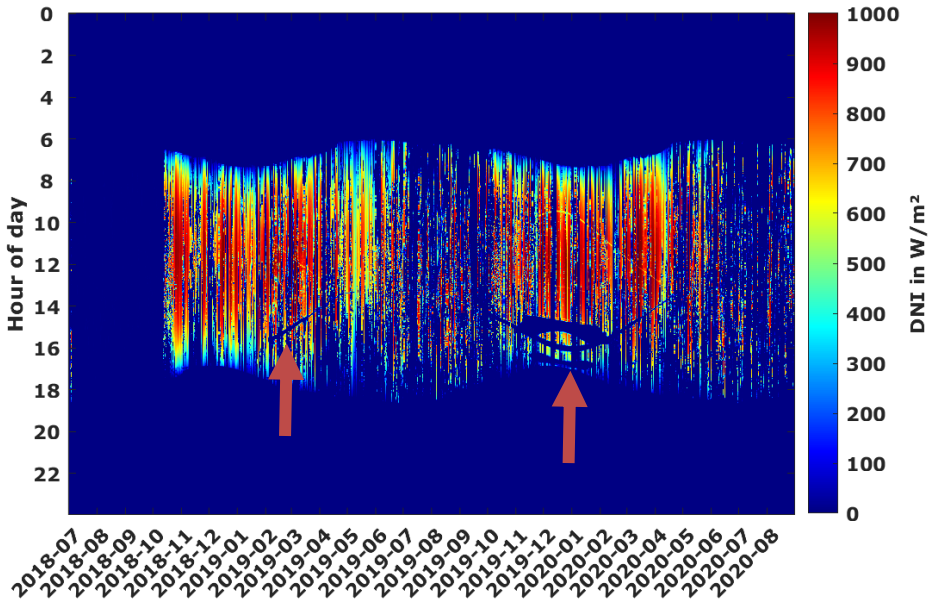

Figure 10: DNI irradiance intensity 2018-07 to 2020-08

Shading impact on solar irradiance measurement

The shading impacts observed in Figure 9 and Figure 10 are now discussed in more detail.

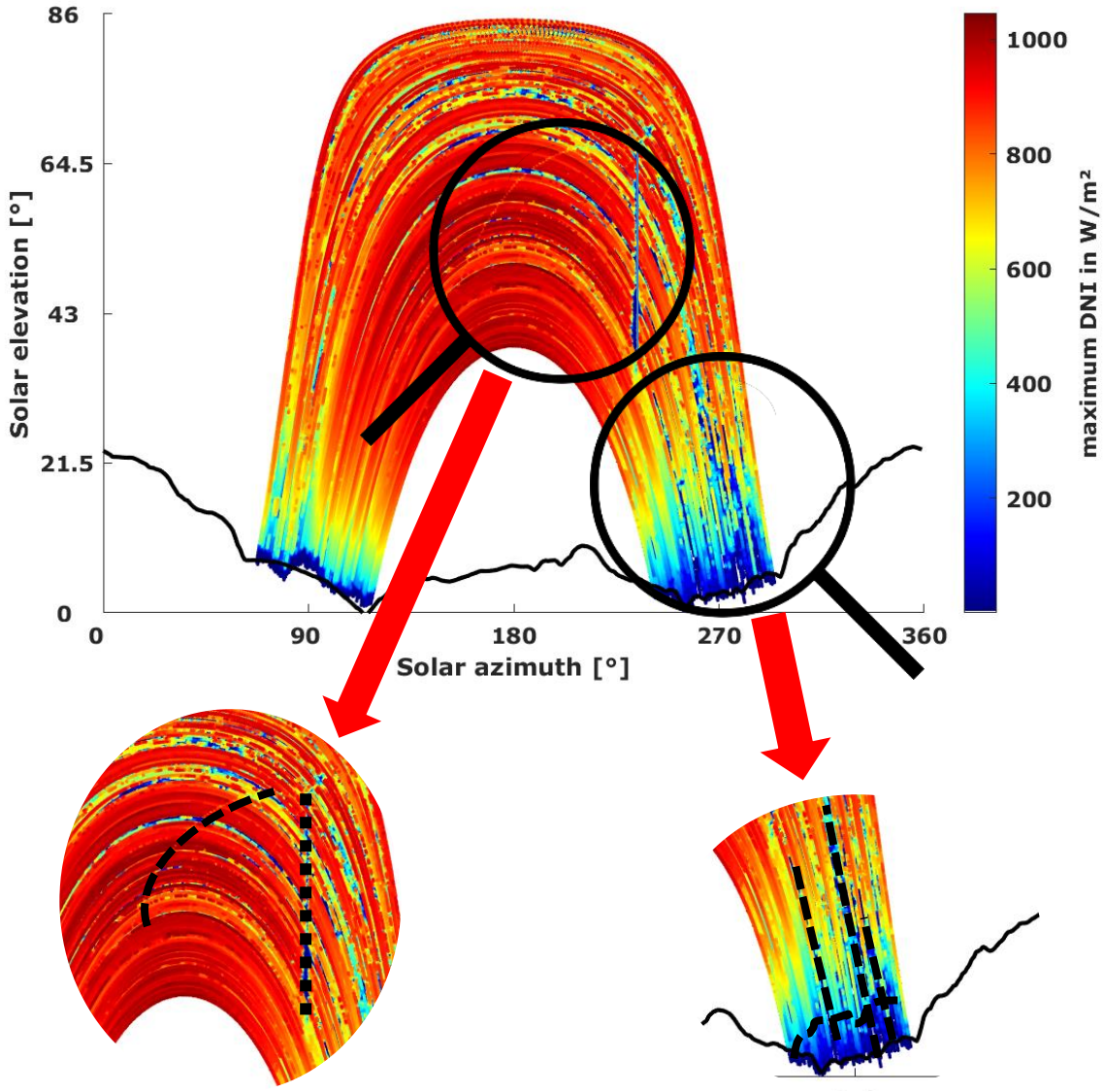

Figure 11: Measured maximum DNI at distinct sun positions (black line: horizon line from SRTM digital elevation model)

Figure 11 shows the maximum DNI values (in 1-minute resolution) recorded at the respective sun position (azimuth and elevation angle). In this graph, the clear "cut" in the morning and evening which results from the natural horizon (mountain ridge) can be seen very well. The horizon line plotted in black is obtained from the Shuttle Radar Topography Mission (SRTM) and corresponds well with the observed sunrise/sunset. The blue values below horizon line can be ignored.

Some obstacles are visible in the plot, contrasted against the surrounding pixels by differing color. In the zoom to the two most affected areas, the shadings are highlighted with dashed black lines.

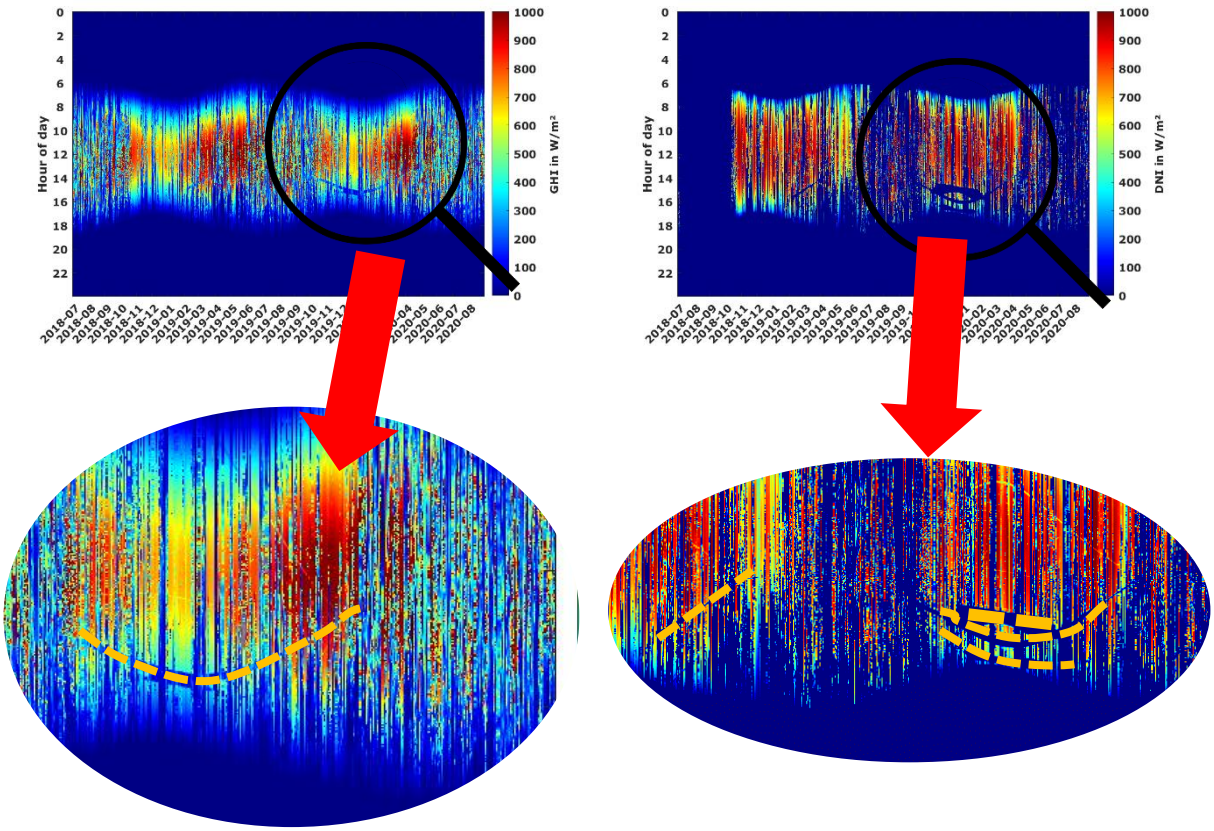

Figure 12: GHI (left) / DNI (right) intensity with visible shadings

Figure 12 again shows the GHI and DNI intensities with a zoom on the most affected periods. It can be seen that there are visible lines formed by values that are lower than those immediately before and after (marked with orange dashed lines in zoom image). The masts affect each sensor at individually different times, as the shadows cast by these obstacles wander across the tracker and the attached instruments.

The most severe shading appears after November 2019, resulting from some additional installation added to the DHM weather station during the measurement campaign.

Figure 13 shows a panoramic view with a centered south view, taken from behind the sun tracker upon the third maintenance visit in October 2020. Blue crosshair markers show the cardinal directions at horizon height. The sun paths at different months are also displayed. It is obvious that the shadings are from the surrounding mountains and the installed masts.

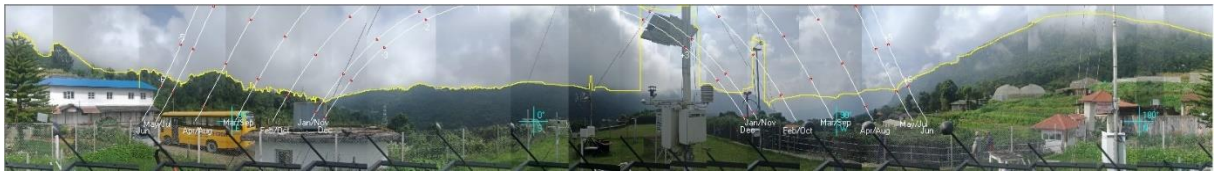

Figure 13: Panoramic View from Pyranometer Sensor Height with Sun Paths and Horizon

Overall, it is recommended that the measurements which are affected by shading are excluded from further use of the data.

4.2 Temperature and relative humidity

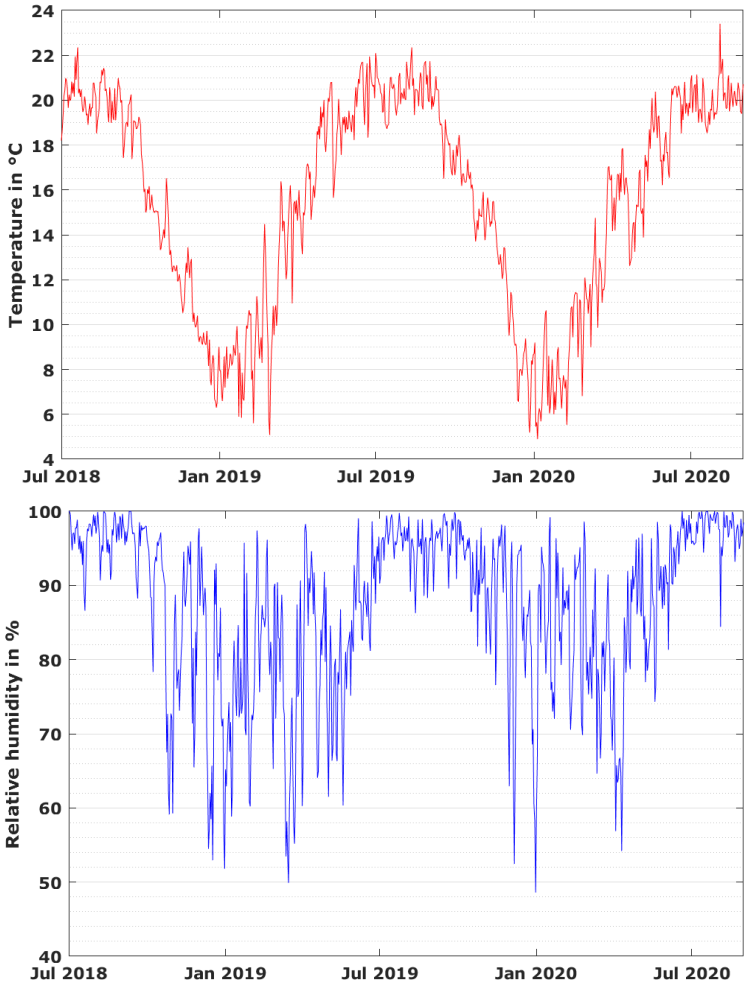

Figure 14: Daily temperature and relative humidity averages (1-minute resolution)

Figure 14 shows daily averages of temperate and relative humidity. A seasonal dependency is visible. Temperature is lowest in the northern hemisphere winter months (November to February) and high in the summer months. The month with the highest average temperature is June, the coldest monthly average temperature was in January. The most frequent temperature is 17°C (Figure 15). Daily relative humidity averages were highly variable, with tendentially lower humidity in the winter months (which were also the months with highest DNI sums) and high humidity during the monsoon season.

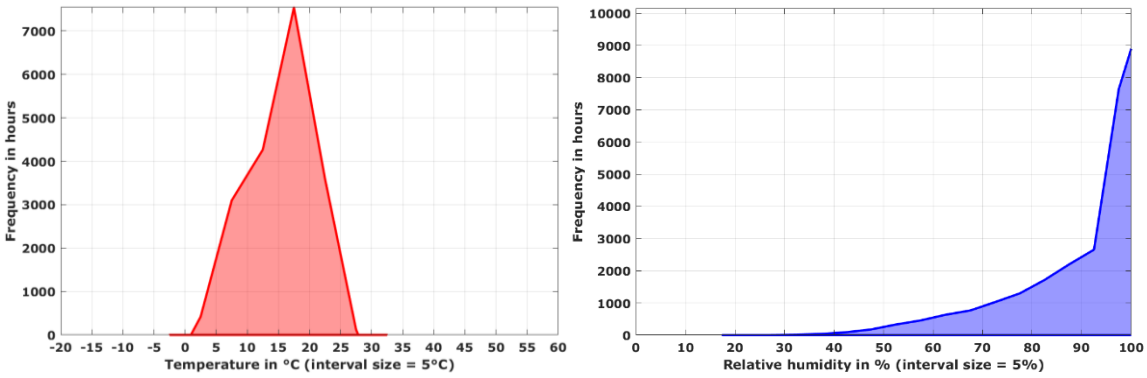

Figure 15: Frequency distribution of temperature and relative humidity (1-minute resolution)

4.3 Barometric pressure

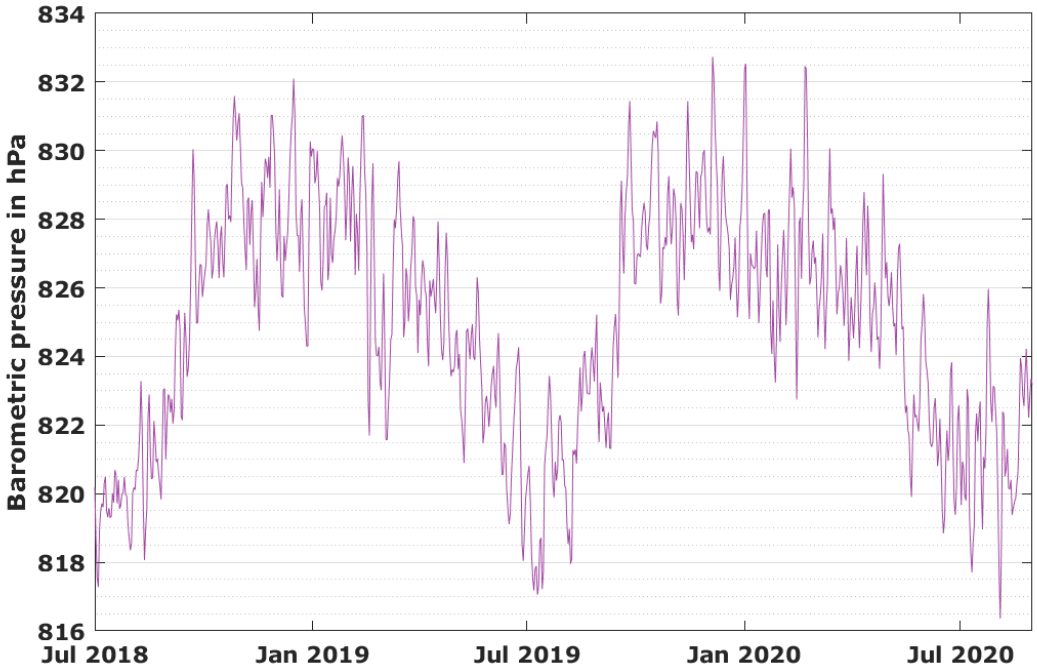

Figure 16: Daily averages of barometric pressure

Figure 16 shows daily averages of barometric pressure. Again, a clear seasonal dependence is visible: Higher pressure in the winter months and lower pressure in the summer months. Figure 17 shows the frequency distribution of recorded 1-minute resolution barometric pressure values.

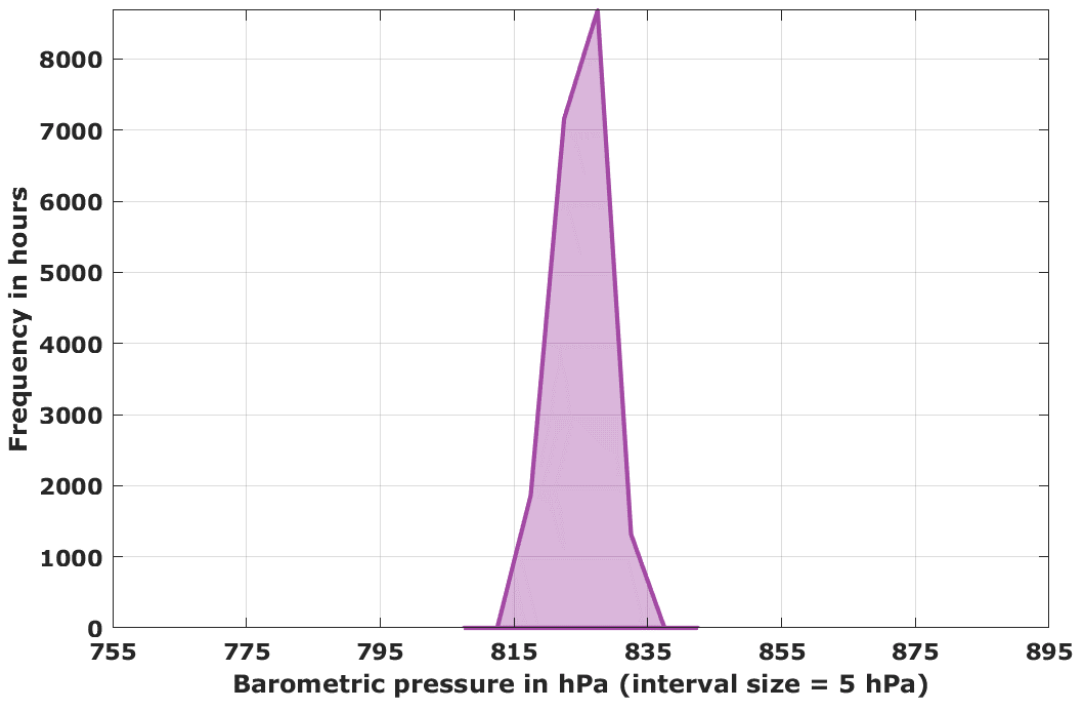

Figure 17: Frequency distribution of barometric pressure (1-minute resolution)

4.4 Precipitation

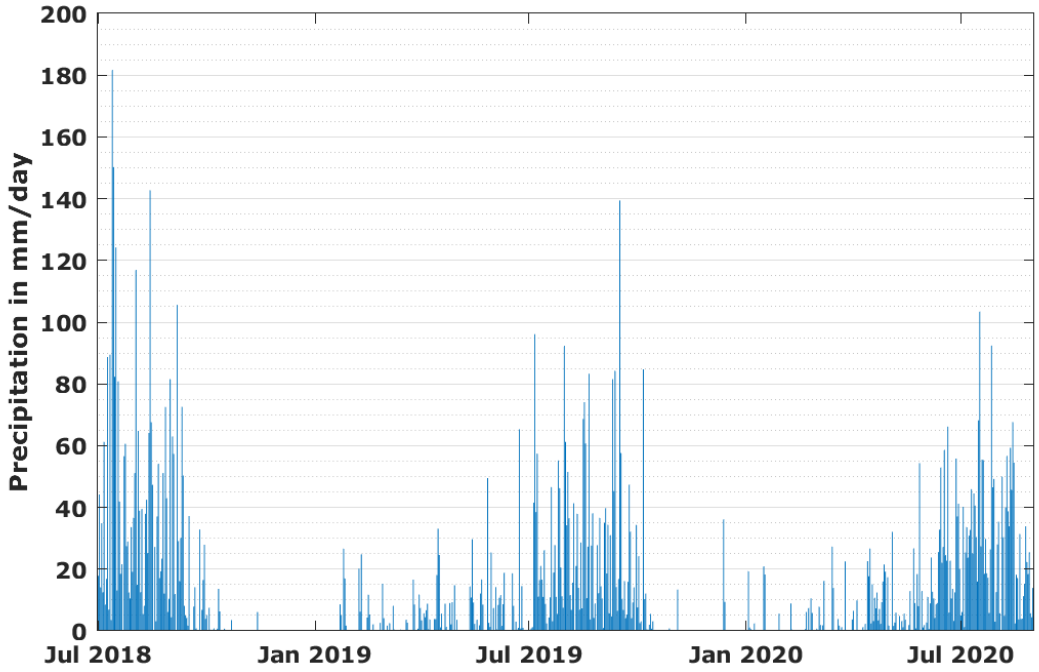

Figure 18: Daily sums of precipitation

Figure 18 shows the daily sums of precipitation. Again, a clear seasonal variability was observed with a dry period with little precipitation from November to January and an expressed rainy season in the months of April to September/October.

4.5 Wind speed and direction

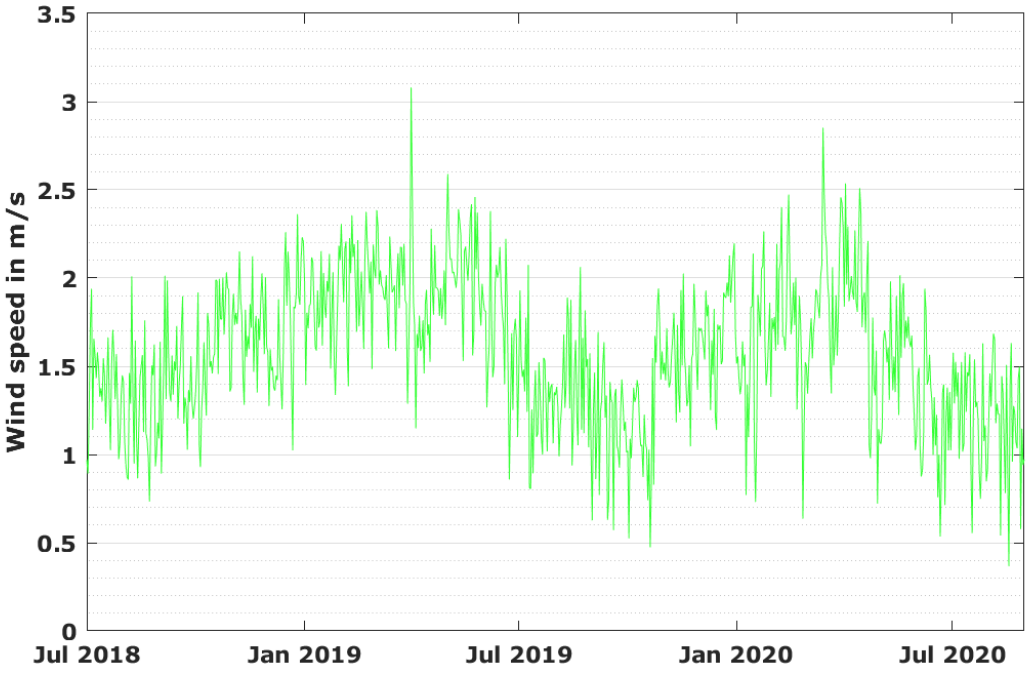

Figure 19: Daily averages of wind speed

Figure 19 shows the daily averages of wind speed. They are continuously low and almost no seasonal dependency was observed. The frequency distribution, shown in Figure 20, emphasizes that wind speeds of <4 m/s are common and wind gusts of up to only 8 m/s were observed with any meaningful quantity.

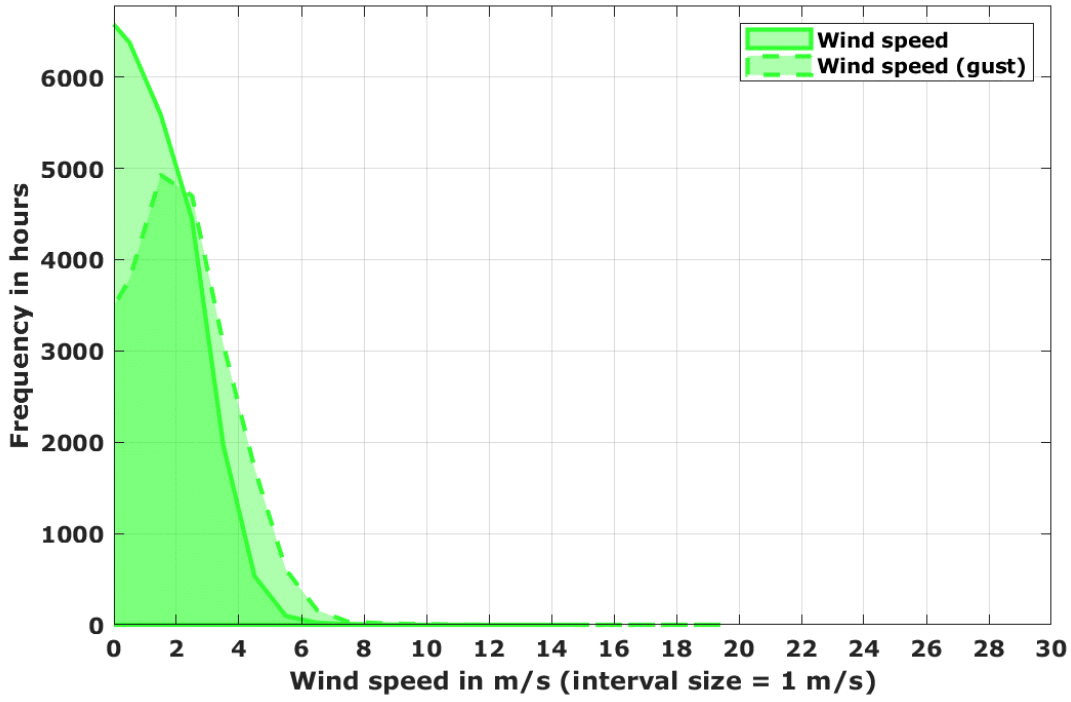

Figure 20: Frequency distribution of wind speeds (1-minute values)

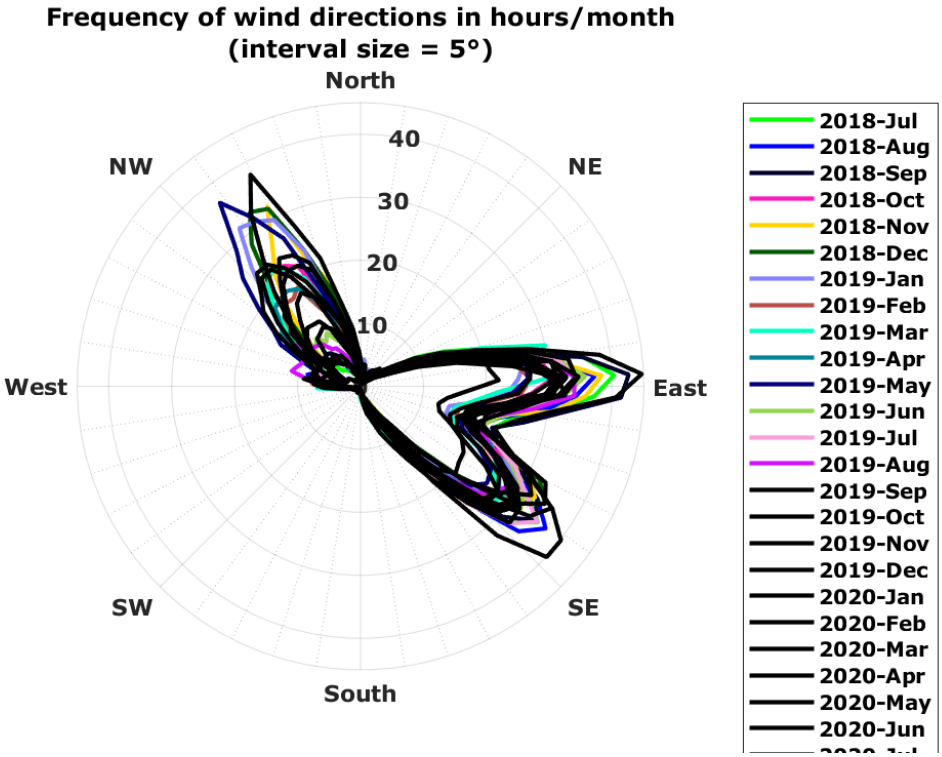

Figure 21: Wind direction distribution 2018-07 to 2020-08

Figure 21 shows the frequency distribution of wind direction in 1-minute time resolution. Two clear main wind directions are visible: From east-southeast during the summer months and from the northwest in the winter months. Figure 22 shows the direction distribution of the few high wind gusts >14 m/s that occurred.

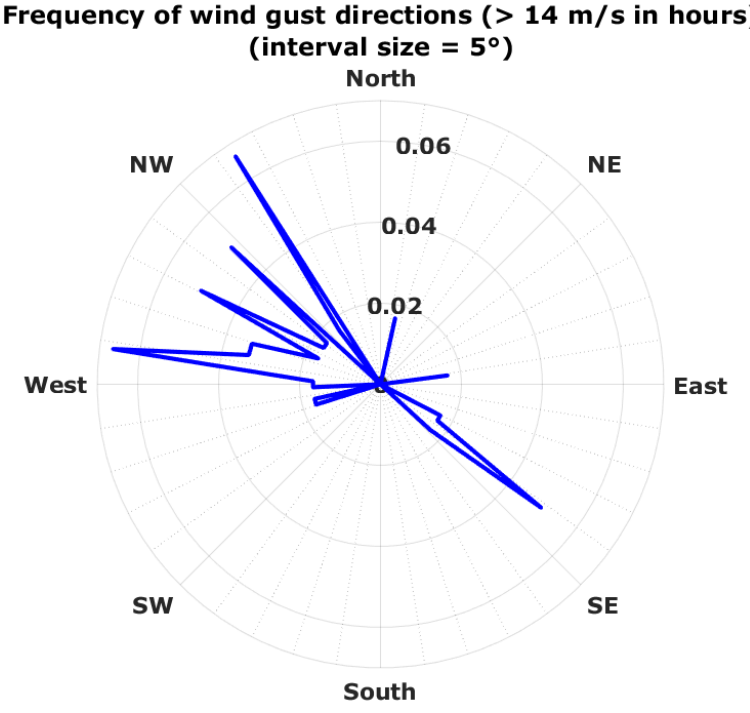

Figure 22: Wind gust direction distribution 2018-07 to 2020-08

5 On-site maintenance and irradiance sensor cleaning

The maintenance on site was done by local personnel. They were contracted and specially trained for this task upon installation of the station. The maintenance on site consisted mainly of visual inspection of the equipment, verifying the sensor alignment and cleaning the irradiance sensors and PV modules. The cleaning was scheduled to be performed on a work-daily basis, which was almost always adhered to throughout the whole measurement campaign. Overall, 72% of all days had a cleaning event.

The exact cleaning dates and times are recorded in the monthly measurement reports and in the measurement data.

Table 6 gives an overview of the maintenance frequency per month.

Table 6: Number of maintenance visits by local staff per month

Month	Maintenance visits
Jul 2018	25
Aug 2018	27
Sep 2018	24
Oct 2018	26
Nov 2018	22
Dec 2018	25
Jan 2019	22
Feb 2019	23
Mar 2019	20
Apr 2019	19
May 2019	14
Jun 2019	20
Jul 2019	16
Aug 2019	24
Sep 2019	16
Oct 2019	18
Nov 2019	18
Dec 2019	16
Jan 2020	22
Feb 2020	15
Mar 2020	16
Apr 2020	19
May 2020	20
Jun 2020	22
Jul 2020	21
Aug 2020	16

6 Irradiance sensor soiling rates and soiling behavior

6.1 Soiling rates of DNI sensor (pyrheliometer)

All data from the pyrheliometer was corrected for sensor soiling by applying a linearly interpolated cleanliness factor[1] to the measurement data where applicable and necessary, i.e. only where cleanliness factor at cleaning was not 1. It has to be noted that cleanliness factors can only be determined under certain conditions:

- The cleaning is performed correctly and swiftly (no influencing of sensors except during a few seconds in the cleaning process)
- The irradiation conditions are stable enough to distinguish signal increase resulting from dust removal from natural fluctuations
- The signal increase resulting from dust removal is sufficiently large to be detectable

If no analysis is possible, soiling correction is not applied.

Table 7 on the next page shows

- Simplified average sensor cleanliness factors of the pyrheliometer DNI sensor detected at the above described cleaning events
- Simplified average daily soiling rate of the pyrheliometer. This rate expresses how much the irradiance sensor signal is reduced each day without cleaning. Simplified in this context means that the rate is a simple average of the change of cleanliness factors over all days of the month
- The minimum cleanliness factors (i.e., maximum sensor soiling) observed just before the sensor cleaning. Especially on/after strong wind occasions such as e.g. dust storms, high singular soiling rates can be observed. The daily cleaning ensures that these single events with high soiling do not influence long periods of data (usually only up to one day) and were mostly well corrigible

[1] Sensor cleanliness factor is defined as the dimensionless factor by which the recorded measurement value has to be divided in order to obtain the soiling-corrected value. E.g., if at cleaning a signal increase of 3% has been detected, the factor before the cleaning is 1/(1+0.03) = 0.97, after the cleaning (clean sensors) = 1.

Table 7: Average sensor cleanliness factors (pyrheliometer)

Month	Average sensor cleanliness	Minimum cleanliness factor	Average daily soiling rate
Jul 2018	1.00	1.00	0.0%
Aug 2018	1.00	1.00	0.0%
Sep 2018	1.00	1.00	0.0%
Oct 2018	1.00	0.99	0.0%
Nov 2018	1.00	1.00	0.0%
Dec 2018	1.00	1.00	0.0%
Jan 2019	1.00	0.99	0.0%
Feb 2019	0.99	0.99	0.3%
Mar 2019	0.99	0.97	0.5%
Apr 2019	0.99	0.97	0.3%
May 2019	0.99	0.96	0.3%
Jun 2019	1.00	1.00	0.0%
Jul 2019	1.00	0.96	0.0%
Aug 2019	1.00	1.00	0.0%
Year 1	**1.00**	**0.96**	**0.1%**
Sep 2019	1.00	0.97	0.1%
Oct 2019	0.99	0.96	0.2%
Nov 2019	0.99	0.99	0.2%
Dec 2019	1.00	0.99	0.1%
Jan 2020	1.00	0.99	0.1%
Feb 2020	1.00	0.99	0.0%
Mar 2020	0.99	0.99	0.1%
Apr 2020	0.99	0.98	0.1%
May 2020	1.00	1.00	0.0%
Jun 2020	1.00	1.00	0.0%
Jul 2020	1.00	1.00	0.0%
Aug 2020	1.00	1.00	0.0%
Year 2	**1.00**	**0.96**	**0.1%**

The soiling influence on the measurement data (after correction) was small, and only few singular events of notable pyrheliometer soiling were detected. Summarizing, it can be said that pyrheliometer soiling is not an issue to data quality, because the sensor cleaning schedule was well adhered to during the entire measurement campaign and soiling correction was applied to the data. Also, the measurement site is not situated in a dusty environment.

6.2 Soiling rates of GHI and DHI sensors (pyranometers)

Due to the work-daily cleaning and the ventilation units that largely keep dust from settling on the pyranometer glass domes, soiling of the pyranometers was not an issue.

Further, due to the geometry of the sensor window (hemispheric glass dome), dust deposition is usually not uniformly distributed over the sensor field of view. For example, with wind coming from a certain direction, the glass dome may be dust-covered on the windward side only, lacking any dust cover on the leeward side. Thickness of the soiling layer may also vary over the height of the glass dome. Figure 23 shows an extreme example of this characteristic (from a site in a different country).

Such asymmetric distribution of soiling, when present, leads to different cleanliness factors of the sensor during the course of the day depending of the elevation angle of the sun (azimuth angle is constant on tracked systems). This asymmetric distribution is unknown and signal increase can only be observed at the time of cleaning.

Meaningful cleanliness factors can therefore not be obtained and sensor soiling correction is generally not applied to thermopile pyranometer measurements by CSP Services.

Figure 23: Asymmetric pyranometer glass dome soiling (exemplary picture)

7 Measurement accuracy and uncertainty

The overall data availability is 100% and the local maintenance (irradiance sensor cleaning and visual check) was done mostly on schedule and according to the defined procedures. Cleaning was usually done work-daily. All ground measurement data was subject to a multi-step data quality control process:

- Transmission of measurement data to CSP Services' server in near-real time
- Daily application of automatic data screening routines (e.g. gap test, step test, physical limits, consistency of solar irradiance components)
- Daily visual inspection of measurement data curves by experienced operators
- Soiling correction of irradiance values measured with pyrheliometer, similar to the method developed by [2]
- Continuous comparison of redundant measurements
- Verification of pyranometer calibration with traveling standard

The documentation of the ground measurement data includes:

- Report for weather station installation (including the calibration certificates of solar sensors)
- Maintenance visit report for the regular inspection visit
- Documentation of each sensor cleaning with time and date through a maintenance button on the automatic weather stations, pressed by the operator after sensor cleaning (included in the measurement data)

7.1 Coincidence of DNI measurements

The DNI measured by the pyrheliometer can be compared to DNI values calculated from the measured GHI and DHI values and the solar zenith angle (DNI_{calc}). DNI_{calc} and the coincidence between the two DNI values can be determined along the following formulas[2]:

$$DNI_{calc} = \frac{GHI - DHI}{\cos(SZA)}, \qquad \text{with } SZA\text{: Solar Zenith Angle} \qquad (1)$$

$$DNI_{coincidence} = DNI - DNI_{calc} \qquad (2)$$

This DNI coincidence is an indicator for the accuracy of the irradiance measurement, the deviation between the measured and calculated DNI should stay within reasonable limits. The usual limits are ±20 W/m² or 2-3% of the measured DNI for instantaneous values for higher sun elevations and high DNI values; high deviations of DNI_{calc} for low sun elevations are normal due to the cosine effect (close to sun elevation of zero, cos(SZA) converges to zero, thus dividing by cos(SZA) results in very high DNI_{calc} values). The comparison of DNI_{calc} and the measured DNI is used continuously for the daily irradiance measurement data quality control.

[2] F. Wolfertstetter, K. Pottler, N. Geuder, R. Affolter, A.A. Merrouni, A. Mezrhab, R. Pitz-Paal: Monitoring of mirror and sensor soiling with TraCS for improved quality of ground-based irradiance measurements. Energy Procedia 49 (2014), 2422-2432. doi:10.1016/j.egypro.2014.03.257.

Figure 24 shows the correlation of DNI and DNI_{calc} in a scatterplot of 1min and 10min resolution measurement values. The following effects can be seen:

- For low DNI values, spread is partly due to the cosine effect as explained above.
- The majority of values are distributed in a narrow range around the bisecting line and almost symmetrical with a small bias toward higher DNI_{calc} values.
- In the 1min-resolution graph (left), a few values that seem to form in a cone widening around the bisecting line can be observed. Further, there is a large amount of outliers. Both can be explained by the period of tracker misalignment, sensor shading by external obstacles and the effect of the cleaning of the sensors by the operators
- In 10min time resolution, the spread is much less due to averaging effects

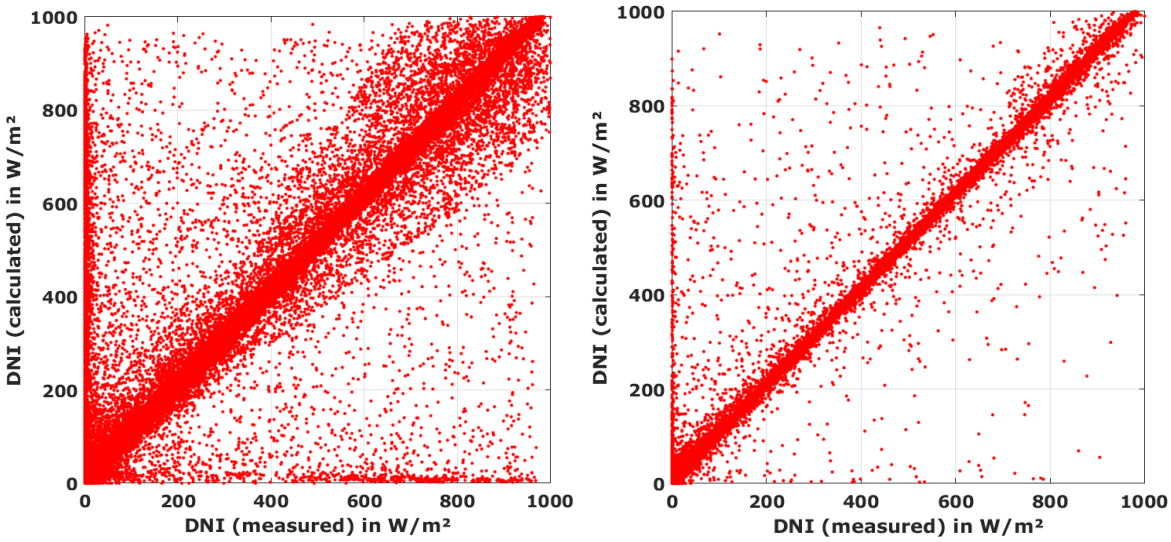

Figure 24: Correlation of DNI_{calc} and DNI (Left: 1min resolution. Right: 10min resolution)

In general, the coincidence can still be considered as good. The amount of outliers due to shading of sensors is a consequence of the site location. One major source of shading, the mast with a large PV module, was neither existing nor announced to be added when the location was selected. Other than external influences that could not be avoided, the data quality benefits of the stringent maintenance procedures, good sun tracker with active sun tracking, high sensor quality and accurate calibration.

For the further use of the measurement data, data points with DNI coincidence values outside ±20 W/m² or 2-3% of the measured DNI as well as clear outliers are recommended to be filtered and discharged.

7.2 Coincidence of GHI measurements

Using the same formula (1) and replacing DNI_{calc} with the measured DNI, the coincidence of GHI can be calculated from the DNI and DHI measurement. Analogue to DNI, GHI coincidence is defined as measured GHI minus calculated GHI.

Figure 25 shows the correlation of calculated and measured GHI. Again, the large amount of outliers can be seen in the one-minute resolution data. In the 10-minute averages, the correlation looks much better.

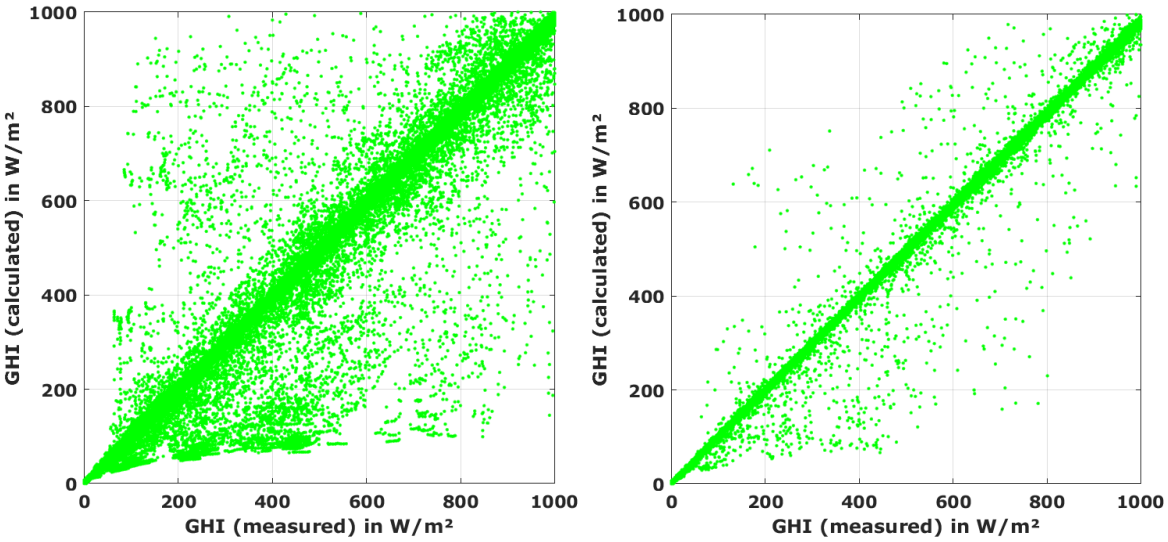

Figure 25: Correlation of GHI_{calc} and GHI (Left: 1min resolution. Right: 10min resolution)

7.3 Measurement uncertainty

The measurement uncertainty was assessed along the guideline in the NREL Best Practices Handbook for the Collection and Use of Solar Resource Data for Solar Energy Applications [1].

Best practices guidelines for selection of equipment, calibration, installation as well as operation and maintenance were followed and maintenance performance was assessed to include potential additional uncertainty contributions that could have occurred.

Two stages with related uncertainty contributions can be identified according to [1]:

- Instrument calibration (laboratory calibration by manufacturer): Uncertainty of calibration is specified in individual calibration certificates.
- Sources of uncertainty in field measurement are
    - Instrument-related (e.g. datalogger precision, pyrheliometer temperature response)
    - Installation-related (e.g. tracker alignment accuracy)
    - Operation-related (mainly frequency and thoroughness of cleaning)

DNI measurements

In the NREL Best Practices Handbook [1], typical calibration uncertainties for pyrheliometers are estimated with ±1.8% (at 95% level of confidence). The calibration certificate for the installed CHP1 pyrheliometer states a lower value of ±1.1%. Since this is well justified and the calibration verification did not give any reason of doubt, this lower value is assumed to be applicable.

In the field, much focus was given on using high-class measurement equipment (high-accuracy sensors, sun tracker and datalogger), excellent installation and alignment and regular maintenance and cleaning. The handbook estimates high-quality final measurement campaign DNI uncertainty with ±2.0% to ±2.5% for pyrheliometers for sub-hourly values (at 95% confidence interval).

For this measurement campaign, a measurement uncertainty of ±2.0% (at 95% confidence interval) for DNI values is estimated (after filtering and excluding values with bad coincidence as described above).

GHI and DHI measurements

In the literature, pyranometer calibration uncertainty is estimated with ±3.2% for solar zenith angles (SZA) between 30° and 60°. This is composed of an uncertainty of ±1.2% at a fixed, narrow incidence angle and a higher contribution of ±2.0% at a broader range of incidence angles [1]. Field measurements in well-maintained measurement campaigns can be estimated with uncertainties of ±3.0% for SZA between 30° and 60° and up to ±7.0% to ±10.0%for SZA>60° for GHI. For DHI, the uncertainty contribution resulting from SZA is irrelevant, since the direct irradiance is blocked by the shading ball assembly.

The calibration certificates for the installed CMP21 pyranometers state a value of ±1.35%. Calibration in the laboratory is done at a fixed incidence angle, thus this value replaces the literature estimate of ±1.2%. Since this is well justified and calibration verification did not give any reason of doubt, the value of ±1.35% is accepted.

The CMP21 pyranometers have an additional individual characterization for incidence angle and temperature sensitivity, and an incidence angle and temperature correction was applied to the GHI measurement values. Thus, the uncertainty resulting from broader incidence angles is much reduced. For the DHI, the temperature correction was applied. Therefore, the lower boundary of the literature values is assumed.

For this measurement campaign, a measurement uncertainty (at 95% confidence interval) of

- ±3.0% for all GHI values at SZA between 30° and 60°
- ±7.0% for all GHI values at SZA below 30° or above 60°
- ±2.0% for all DHI values

is estimated (after filtering and excluding values with bad coincidence as described above).

8 Conclusion

26 months of meteorological measurement data were collected at the site on DHM agro-meteorological station in Lumle with a Tier1 automatic weather station between July 2018 and August 2020. The data was measured with a tracked pyrheliometer, ventilated pyranometers and additional meteorological sensors.

- Except for minor measurement problems and a four-months period in the early phase with tracker misalignment resulting in no DHI/DNI measurement being recorded, there were no further significant operational difficulties
- Local maintenance and irradiance sensor cleaning were carried out on a work-daily schedule with acceptably little exceptions, each visit was recorded and documented
- Three regular (preventive) maintenance visits to the station were performed, and one additional (fruitless) visit to rectify tracker alignment
- The measurement data was monitored on a daily basis by CSP Services operators, applying automatic quality assessment routines according to international best practices guidelines and visual inspection of the data by experienced operators
- The deviation between the installed irradiance sensors (redundant thermopile measurements) was within the expected limits
- The calibration of the used thermopile irradiance sensors was successfully validated upon two field calibration verification campaigns in October 2019 and October 2020. For the field calibration verification, traveling standard sensors calibrated at the WRC in Davos, Switzerland, were used as calibration reference
- Measurement uncertainty is found to be within the expectable range given in best-practices literature

The 2-year measurement campaign at the site was successfully carried out, yielding a time series of on-site solar and meteorological measurement data in high quality. All measurement data was submitted to the World Bank in regular intervals by uploading to the energydata.info website. Additionally, the installation and maintenance reports as well as all calibration certificates and detailed descriptions of the measurement equipment were submitted to the World Bank.

9 References

[1] M. Sengupta, A. Habte, C. Gueymard, S. Wilbert and D. Renné, *Best Practices Handbook for the Collection and Use of Solar Resource Data for Solar Energy Applications: Second Edition,* Golden, Colorado: National Renewable Energy Laboratory, 2017.

[2] F. Wolfertstetter, , K. Pottler, A. Alami, A. Mezrhab and R. Pitz-Paal, "A novel method for automatic real-time monitoring of mirror soiling rates," in *SolarPACES 2012*, Marrakesh, Morocco, 2012.

CSP Services GmbH, Köln, Germany

CSPS Technical Documentation

Client: The World Bank

Selection #: 1230234

- Solar Resource Measurement Campaign Nepal –

24-Month Site Measurement Report Nepalgunj, Nepal

Birk Kraas
Anne Forstinger

CSP Services GmbH
Friedrich-Ebert-Ufer 30
51143 Köln/Cologne, Germany
Email: b.kraas@cspservices.de

Version 04 December 2020

CSP Services
CONCENTRATING SOLAR POWER SERVICES

CSP Services GmbH, Köln, Germany

24-Month Station Operation Report

Table 1: Site and installation information

Site and Installation Information	
Site:	Nepal Agricultural Research Council (NARC) Regional Agricultural Research Station (RARS), Nepalgunj
Coordinates, Elevation:	28.11302°N, 81.58899°E (WGS84), 130 m
Station Type:	ESMAP Tier1 automatic weather station
Date of installation:	2018-06-26
Date of maintenance visits:	2018-10-28, 2019-10-18 & -19

CSP Services GmbH
Friedrich-Ebert-Ufer 30
51143 Köln · Germany
T: +49 2203 959 0030
F: +49 2203 180 2528
www.cspservices.de

Geschäftsführer
(Managing Directors):
Dr. Klaus Pottler
Dr.-Ing. Steffen Ulmer

Sitz der Gesellschaft
(Registered Office): Köln
Amtsgericht Köln
HRB 61644
USt-ID-No: DE814904840

Bank Account:
IBAN: DE18 5001 0060 0049 6816 08
BIC (Swift-Code): PBNKDEFF
Postbank · Frankfurt-Main · Germany

1 Contents

2 Executive summary

24 months of meteorological measurement data was collected at the measurement site in Nepalgunj between July 2018 and June 2020. This report summarizes the station operation during the reported measurement period.

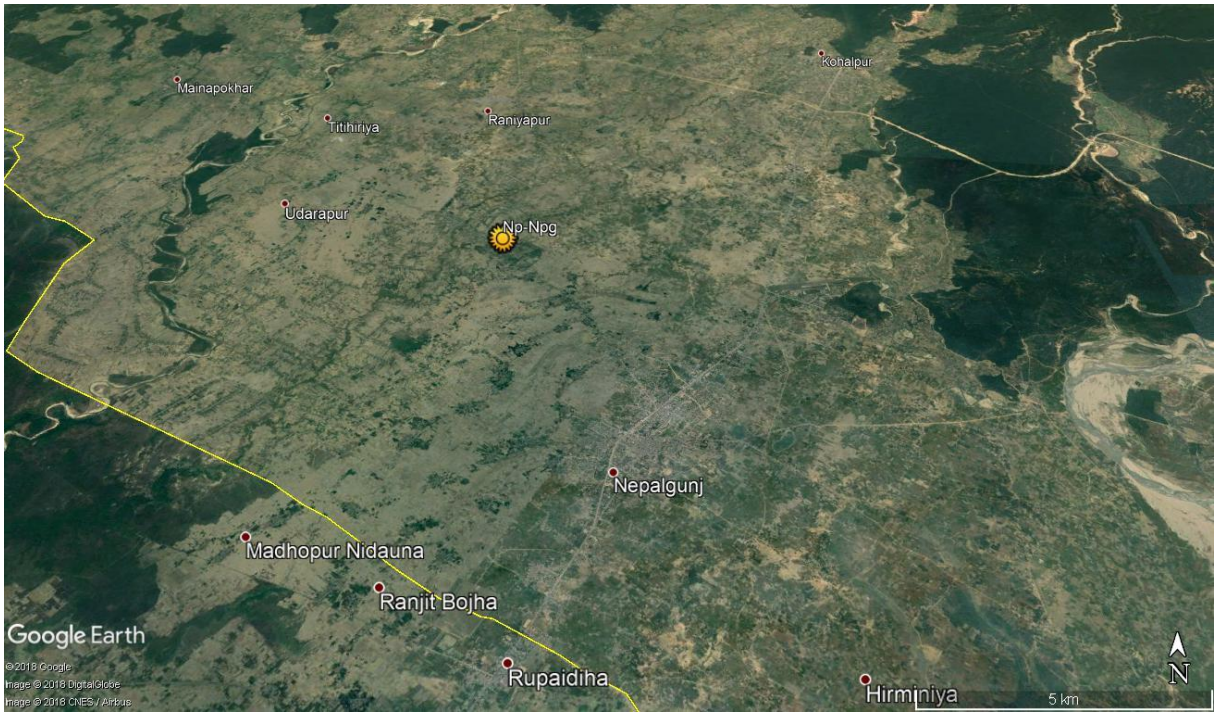

Figure 1: Site location near Nepalgunj (Image: Google Earth)

The Tier1 meteorological measurement station was installed at the site at RARS Nepalgunj on 26 June 2018 and visited for regular maintenance visit on 28 October 2018 and 19 October 2019.

Further scheduled maintenance visits and the planned solar irradiance sensor calibration in 2020 could not be conducted due to the lockdown and travel restrictions imposed or risk of travel resulting from the COVID-19 pandemic.

The station was operating correctly, the data availability was 100% (no data gaps) and the local maintenance (work-daily sensor cleaning and visual check) was done mostly on schedule and according to the defined procedures.

The measurement data collected after the reporting period is not subject of this report.

3 Equipment description and functionality, sensor calibration

3.1 Measurement equipment

The Tier1 automatic weather station is equipped with a datalogger and a GSM modem, a sun tracker equipped with an ISO9060 First Class pyrheliometer for DNI measurement and ISO9060 Secondary Standard pyranometers for measurement of GHI and DHI. As additional meteorological sensors, an anemometer and a wind vane for wind speed and direction measurement on 10 m height, a barometric pressure sensor, a tipping bucket rain gauge and a temperature and humidity sensor are installed. The exact types of sensor/equipment and serial numbers are listed in the tables below.

Table 2: Equipment and serial numbers

Equipment and serial numbers		
Automatic Weather Station	CSP Services MHP Automatic Weather Station	CSPS.MT.18.205
Main Control Box	CSP Services	CSPS.CA.18.202.0004
Datalogger	Campbell CR1000	E12054
Datalogger peripherals	CFM100 CF Module	14205
Sun Tracker	K&Z Solys2	180410
Sun Sensor	K&Z Sun Sensor Kit	170323
GSM Modem	Sierra Wireless Xtend	
GPS Module	Garmin 16x HVS	1A4250269
Power Supply	4x100 W PV modules, 4x150 Ah solar battery	Connected as 200 W, 300 Ah @24VDC

Table 3: Measured Parameters and Sensors

Measured parameter	Unit	Sensor type	Serial number
GHI	W/m²	K&Z CMP21, w. CVF4 ventilation unit	170866
DHI	W/m²	K&Z CMP21, w. CVF4 ventilation unit	170867
DNI	W/m²	K&Z CHP1	180583
Temperature	°C	Campbell CS215	E20180
Humidity	%	Campbell CS215	E20180
Pressure	hPa	Setra 278	7225864
Precipitation	mm	Young 52203	TB 14419
Wind Speed	m/s	NRG #40C anemometer	1795-00303670
Wind direction	°N	NRG #200P wind vane	1799-00019698

3.2 Equipment functionality

The functionality of the equipment was good, the station was operating without significant problems.

On many occasions, dew or droplets on the pyrheliometer was noticed. This presumably happened at morning fog events. Impact on the data was negligible since the dew evaporated quickly, and in severe cases data was corrected by replacing measured DNI (affected by dew) with the DNI calculated from GHI and DHI, which were usually not affected by dew due to sensor ventilation.

Notable events at the station are listed in Table 4.

Table 4: Notable events during operation

Date	Event
2018-07-18,	Dew on pyrheliometer front window
2018-08-25, -27	Dew on pyrheliometer front window
2018-10-14, -16	Dew on pyrheliometer front window
2018-10-28	Station maintenance (regular maintenance visit)
2018-11-05, -06, -07, -16, -17, -20, -21, -23, -24, -25, -29	Dew on pyrheliometer front window
2018-12-01, -02, -03, -04, -06, -07, -08, -09, -10, -14, -15, -16, -19, -21, -22, -23, -24, -25, -26, -27, -28, -29, -30, -31	Dew on pyrheliometer front window
2019-01-03, -04, -08, -09, -10, -12, -17, -18, -19, -20, -24, -28	Dew on pyrheliometer front window
2019-02-02, -11, -12	Dew on pyrheliometer front window
2019-03-05, -07	Dew on pyrheliometer front window
2019-10-18, -19	Station maintenance (regular maintenance visit)
2019-11-13, -21, -25	Dew on pyrheliometer front window
2019-12-01, -04, -05, -09, -14, -31	Dew on pyrheliometer front window
2020-01-04, -25, -26, -28, -30, -31	Dew on pyrheliometer front window
2020-02-10	Dew on pyrheliometer front window
2020-03-08	Dew on pyrheliometer front window
2020-05-02	Dew on pyrheliometer front window

3.3 Sensor calibrations

Factory calibrations

All sensors were calibrated before deployment in the field. The thermopile pyranometers and pyrheliometers were calibrated in the factory by the manufacturer according to applicable ISO standards. Other meteorological sensors (wind speed sensor, barometric pressure sensors) were also calibrated by the respective manufacturer. Calibration certificates were handed over with the installation report.

Pyrheliometer and pyranometer field calibration verification

Upon the second regular maintenance visit in October 2019, an irradiance sensor comparison against traveling standard sensors was performed. The travelling standard sensors were calibrated against the World Radiometric Reference (WRR) at Davos (Switzerland) prior to their delivery to Nepal. This calibration comparison and its result were reported in the 12-month site measurement report.

In the second year of operation, the on-site sensor comparison could not be repeated due to the COVID-19 pandemic which made visit of the site unfeasible.

4 Measurement results

Table 5 shows the monthly summary values of all measurement variables at this weather station. Each parameter is discussed in more detail in the following sections.

Table 5: Monthly irradiation sums and average meteorological data

Month	Irradiance sums [kWh/m²]			Avg. Temp. [°C]	Avg. RH [%]	Avg. WS [m/s]	Avg. Press [hPa]	Sum Rain [mm]	Usable data
	GHI	DNI	DHI						
Jul 2018	144	66	93	29.5	85	1.5	980	323	100 %
Aug 2018	120	47	83	28.2	91	1.1	983	343	100 %
Sep 2018	144	87	84	28.5	86	1.0	988	62	100 %
Oct 2018	154	154	56	24.5	73	1.3	994	0	100 %
Nov 2018	111	110	51	19.7	77	1.2	996	0	100 %
Dec 2018	105	124	43	14.8	77	1.1	999	0	100 %
Jan 2019	98	90	50	14.3	80	1.4	999	37	100 %
Feb 2019	98	72	55	16.6	84	1.5	997	46	100 %
Mar 2019	170	156	62	21.9	64	1.9	993	4	100 %
Apr 2019	180	138	76	28.8	52	2.2	989	3	100 %
May 2019	204	159	80	32.0	41	2.5	985	35	100 %
Jun 2019	189	125	88	31.8	64	2.2	982	218	100 %
Year 1	**1717**	**1328**	**821**	**24.2**	**73**	**1.6**	**990**	**1071**	**100 %**
Jul 2019	147	67	90	29.4	86	1.3	981	321	100 %
Aug 2019	165	95	89	29.8	86	1.2	983	159	100 %
Sep 2019	129	71	78	28.0	89	1.3	988	285	100 %
Oct 2019	132	92	71	25.3	83	1.0	994	0	100 %
Nov 2019	103	84	56	21.5	82	1.0	996	1	100 %
Dec 2019	80	78	42	13.9	88	0.9	1000	107	100 %
Jan 2020	74	49	49	13.5	91	0.9	999	18	100 %
Feb 2020	118	103	56	16.6	80	1.2	998	51	100 %
Mar 2020	168	159	58	21.6	74	2.0	994	51	100 %
Apr 2020	186	158	69	27.2	56	2.0	991	18	100 %
May 2020	194	156	75	29.1	65	1.9	987	50	100 %
Jun 2020	145	76	87	29.3	81	1.6	983	103	100 %
Year 2	**1641**	**1188**	**820**	**23.8**	**80**	**1.4**	**991**	**1164**	**100%**

4.1 Solar irradiance

Figure 2 shows the measured monthly irradiance sums in a bar chart. A seasonal dependency of the irradiance sums is visible. Monthly global irradiance sums are generally higher in the summer season whereas the monthly direct irradiance sums are generally higher in winter, with diffuse irradiance behaving the opposite way to direct irradiance. This can be explained with the monsoon season that reduced DNI during the monsoon months with strong cloud cover. GHI is still high in these months because of the longer daylight duration per day and high sun elevation. In winter (dry season), the sky is more often showing clear-sky conditions leading to higher DNI values.

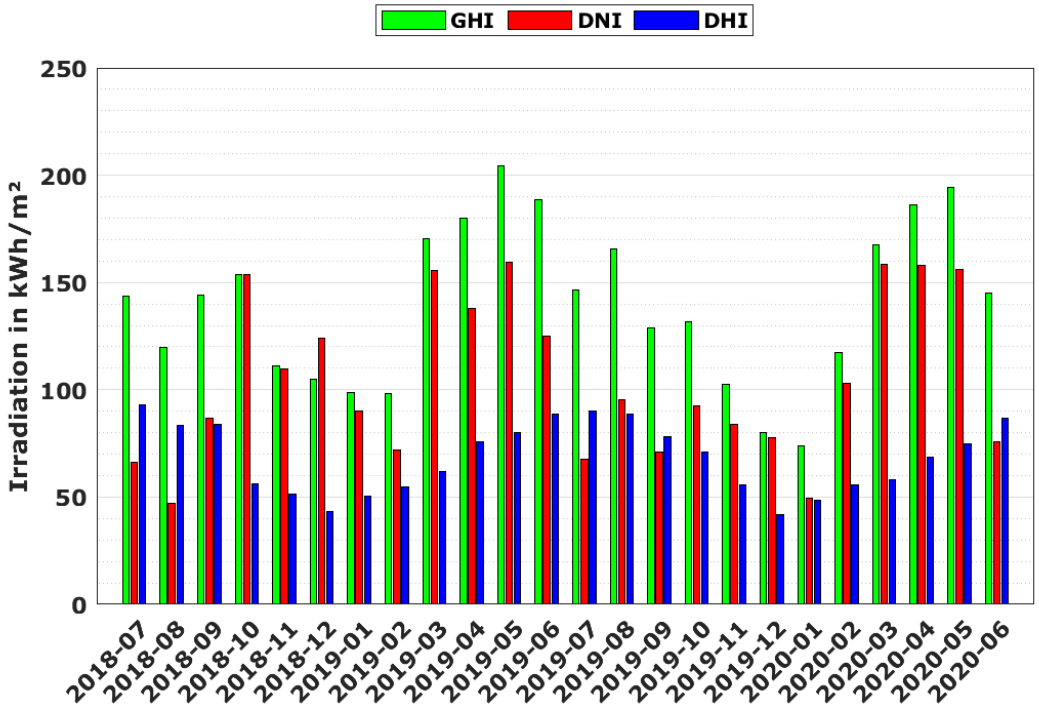

Figure 2: Monthly irradiation sums 2018-07 to 2020-06

The frequency distribution of hourly irradiance values (Figure 3) shows clear occurrence peaks for DNI (scale on the left axis) and DHI (scale on the right axis). The frequency distribution of GHI values (scale on left axis) is broader with a less expressed occurrence peak. The peak for DNI values is at around 600 W/m² and generally, DNI values above 400 W/m² are frequent. The diffuse hourly irradiance frequency peaks just below 200 W/m². The frequency distributions indicate a overcast-sky dominated climate with high diffuse irradiance values at this site.

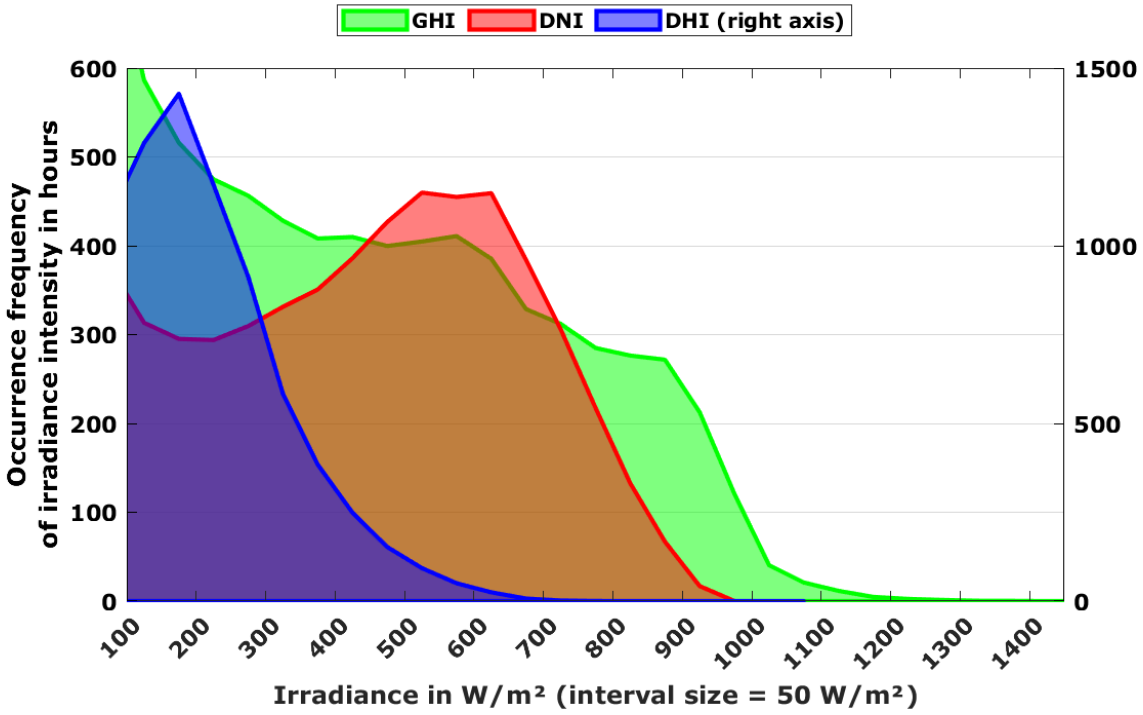

Figure 3: Frequency distribution of hourly irradiance averages 2018-07 to 2020-06

Figure 4 and Figure 5 show the irradiance intensity for GHI and DNI over the 24 months measurement period. The irradiation intensity and the length of the days vary with the seasons.

GHI is strongest during the summer period (Figure 4), corresponding to the high solar elevation periods. Cloudy periods with low GHI values occur mostly in the monsoon period.

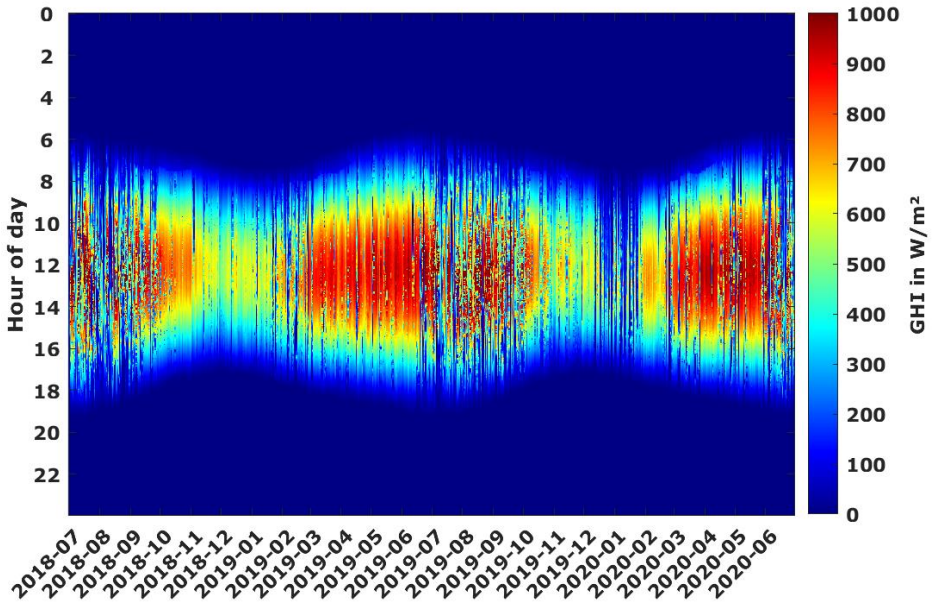

Figure 4: GHI irradiance intensity 2018-07 to 2020-06

The DNI values (Figure 5) show high irradiance intensities of above 700 W/m² and more during brief periods in the winter months and after the end of the monsoon period. Periods with low or no DNI (cloud cover or aerosol load) occur mainly in monsoon season. Due to the higher sensitivity of DNI to reductions by cloud cover or aerosols, low DNI periods occur more often than for GHI, hence the more fragmented appearance of the DNI plot.

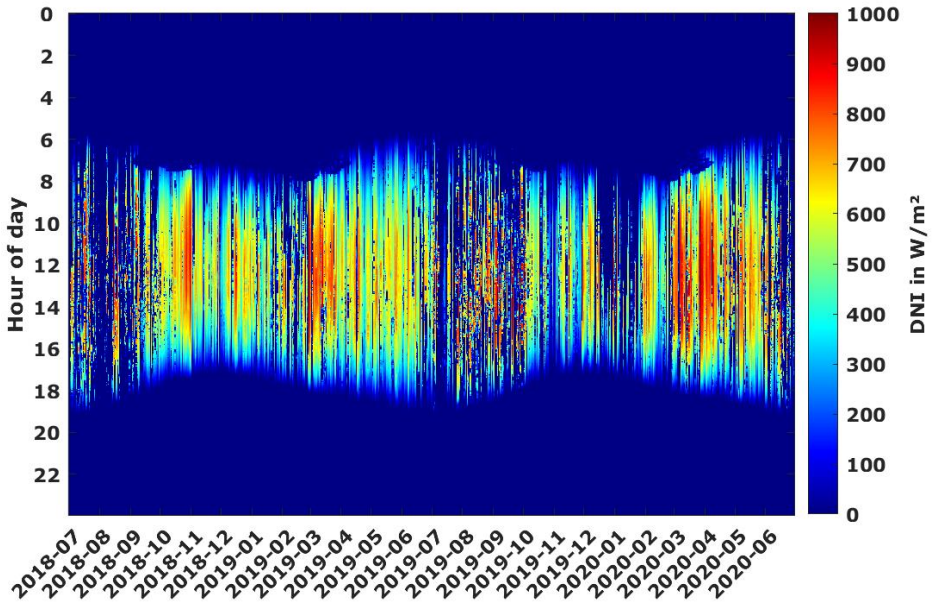

Figure 5: DNI irradiance intensity 2018-07 to 2020-06

4.2 Temperature and humidity

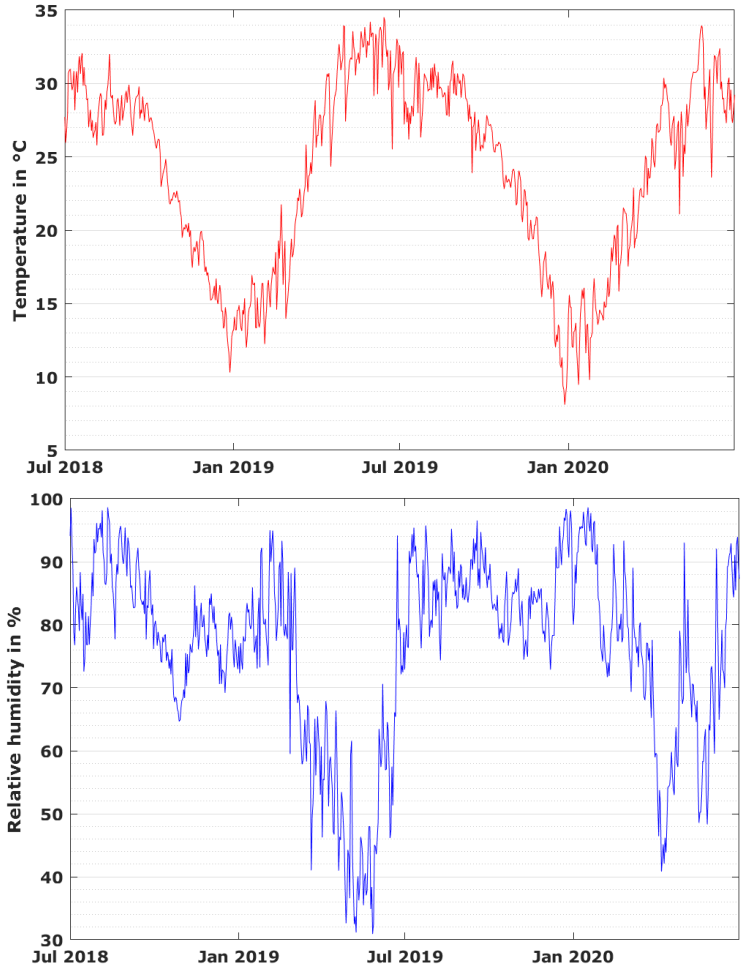

Figure 6: Daily temperature and relative humidity averages (1-minute resolution)

Figure 6 shows daily averages of temperate and relative humidity. A seasonal dependency is visible. Temperature is lowest in the northern hemisphere winter months (November to February) and high in the summer months. The month with the highest average temperature is June, the coldest monthly average temperature was in January. The most frequent temperature is 27°C and relative humidity between 90% and 100% is frequent (Figure 7). Daily relative humidity averages were highly variable, with tendentially lower humidity in the spring months (which were also the months with highest DNI sums) and high humidity during the monsoon season.

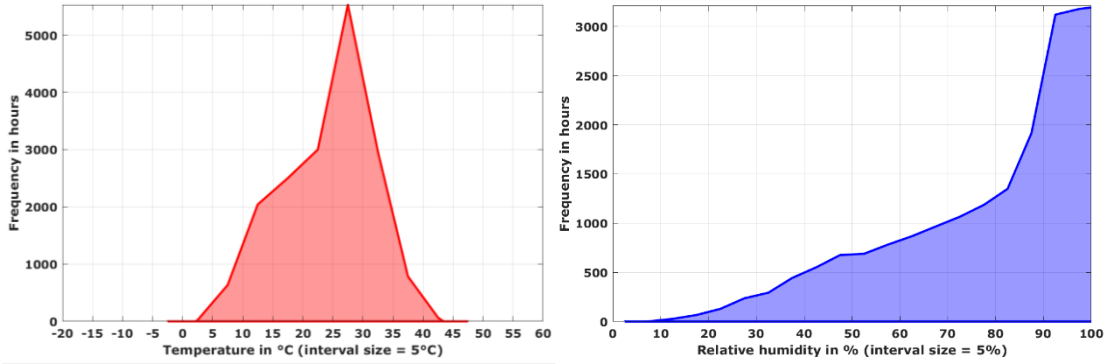

Figure 7: Frequency distribution of temperature and relative humidity (1-minute resolution)

4.3 Barometric pressure

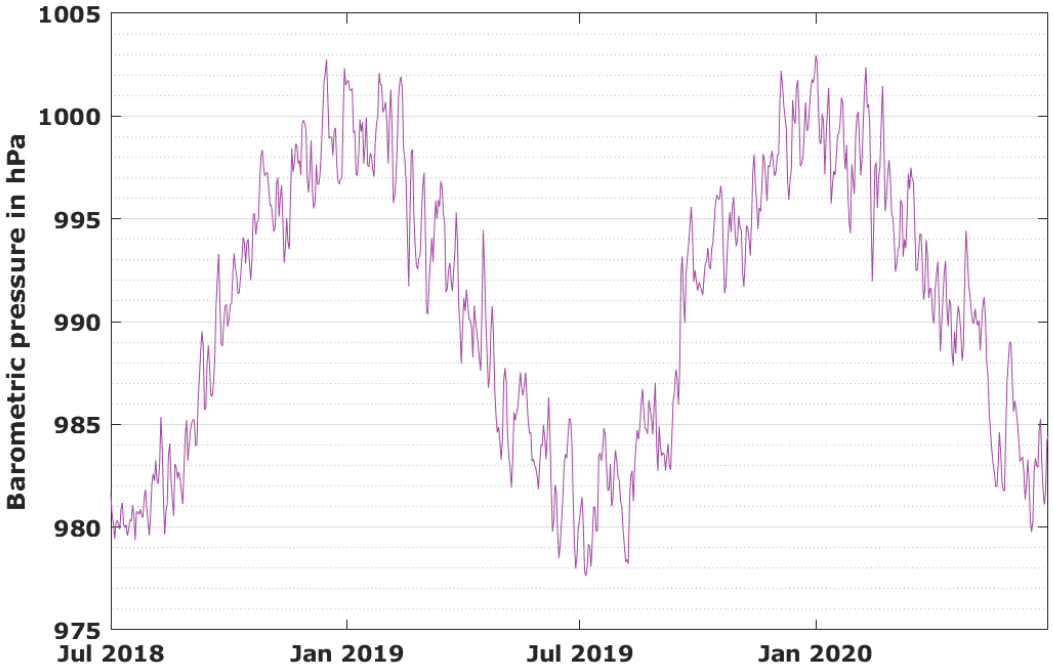

Figure 8: Daily averages of barometric pressure

Figure 8 shows daily averages of barometric pressure. Again, a clear seasonal dependence is visible: Higher pressure in the winter months and lower pressure in the summer months. Figure 9 shows the frequency distribution of recorded 1-minute resolution barometric pressure values.

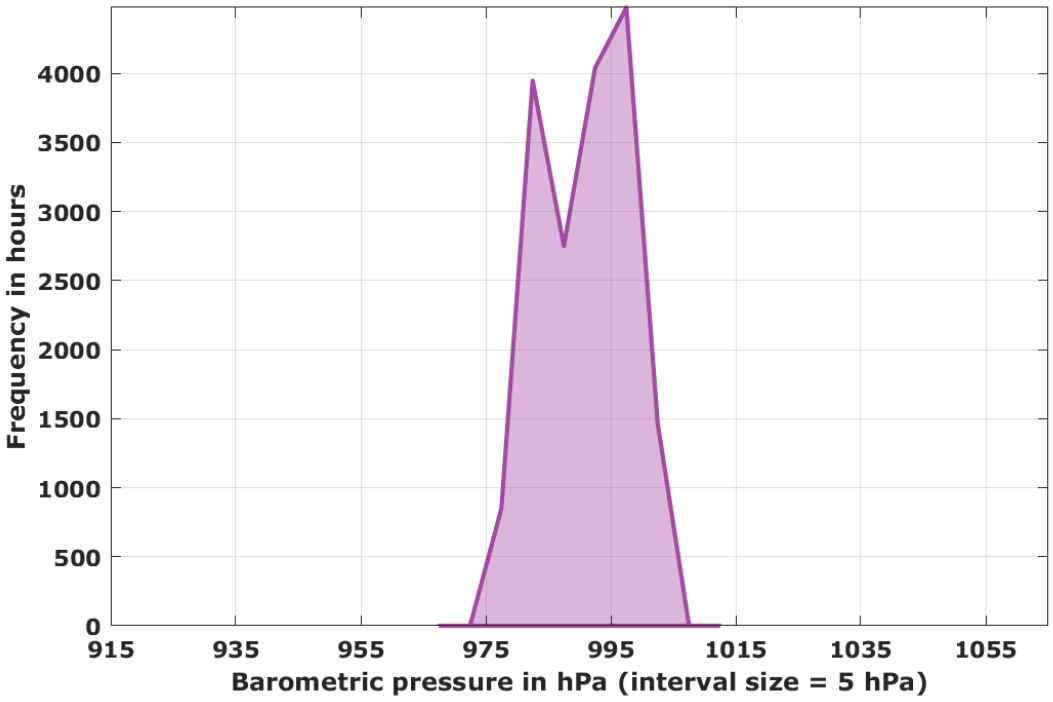

Figure 9: Frequency distribution of barometric pressure (1-minute resolution)

4.4 Precipitation

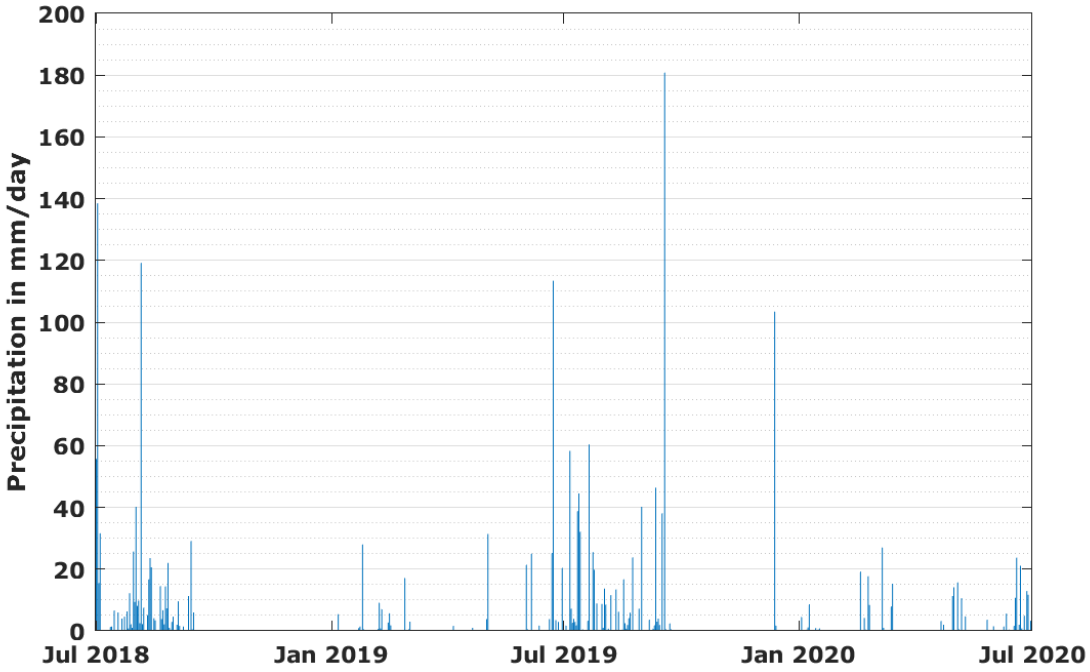

Figure 10: Daily sums of precipitation

Figure 10 shows the daily sums of precipitation. Again, a clear seasonal variability was observed with a dry period with almost no precipitation from November to January and an expressed rainy season in the months of June to September. The same periods were observed in both years of the measurement campaign.

4.5 Wind speed and direction

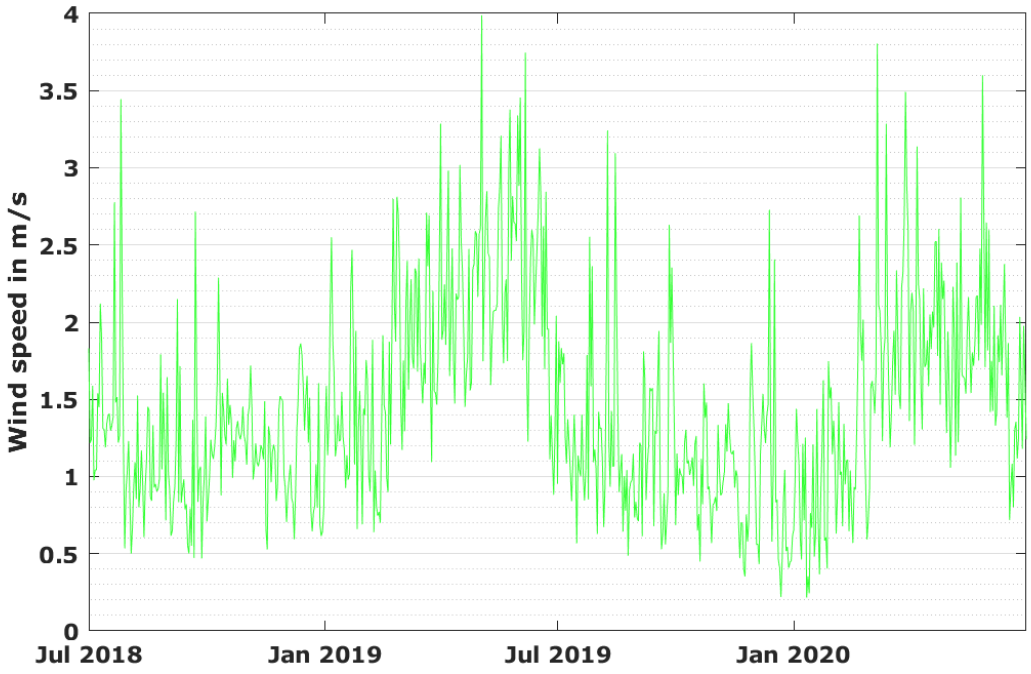

Figure 11: Daily averages of wind speed

Figure 11 shows the daily averages of wind speed. They show a strong seasonal dependence with lower wind speed in the winter months. The frequency distribution, shown Figure 12, emphasizes that wind speeds of <4 m/s are common and wind gusts of up to only 8 m/s were observed with any meaningful quantity.

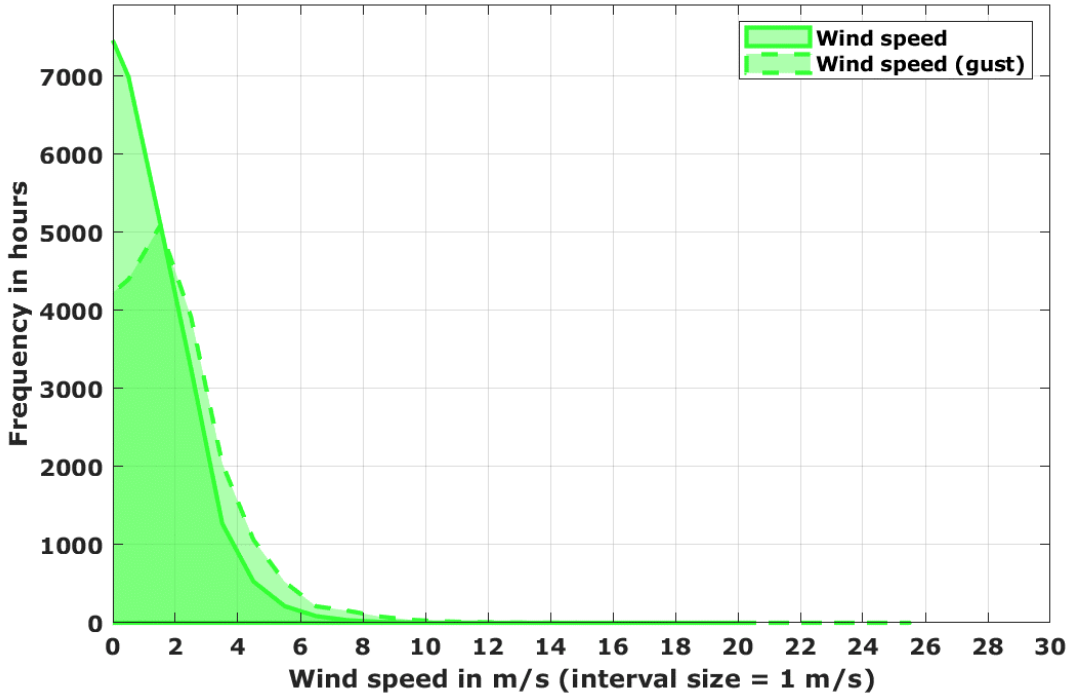

Figure 12: Frequency distribution of wind speeds (1-minute values)

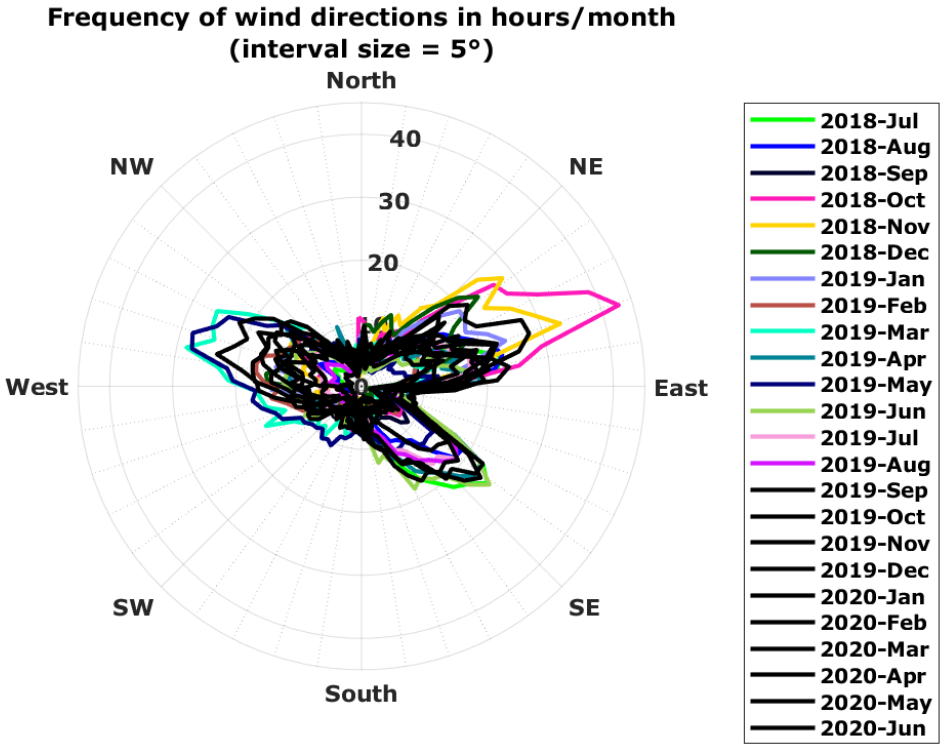

Figure 13: Wind direction distribution 2018-07 to 2020-06

Figure 13 shows the frequency distribution of wind direction in 1-minute time resolution. The prevailing wind directions are west-northwest in the spring and northeast-east in the autumn and southeast in the summer. Figure 14 shows that strong wind gusts commonly are from north-northwest directions.

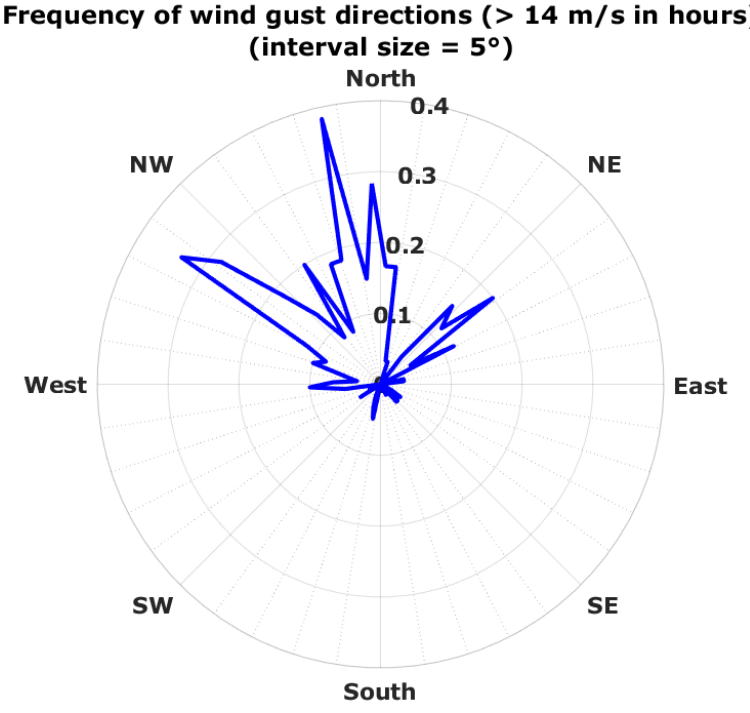

Figure 14: Wind gust direction distribution 2018-07 to 2020-06

5 On-site maintenance and irradiance sensor cleaning

The maintenance on site was done by local personnel. They were contracted and specially trained for this task upon installation of the station. The maintenance on site consisted mainly of visual inspection of the equipment, verifying the sensor alignment and cleaning the irradiance sensors and PV modules. The cleaning was scheduled to be performed on a work-daily basis, which was almost always adhered to throughout the whole measurement campaign with a ramp-up phase in the beginning of the campaign. Overall, 72% of all days had a cleaning event.

The exact cleaning dates and times are recorded in the monthly measurement reports and in the measurement data.

Table 6 gives an overview of the maintenance frequency per month.

Table 6: Number of maintenance visits by local staff per month

Month	Maintenance visits
Jul 2018	21
Aug 2018	25
Sep 2018	17
Oct 2018	22
Nov 2018	21
Dec 2018	20
Jan 2019	18
Feb 2019	14
Mar 2019	19
Apr 2019	19
May 2019	20
Jun 2019	13
Jul 2019	17
Aug 2019	18
Sep 2019	15
Oct 2019	24
Nov 2019	29
Dec 2019	31
Jan 2020	31
Feb 2020	28
Mar 2020	29
Apr 2020	29
May 2020	23
Jun 2020	20

6 Irradiance sensor soiling rates and soiling behavior

6.1 Soiling rates of DNI sensor (pyrheliometer)

All data from the pyrheliometer was corrected for sensor soiling by applying a linearly interpolated cleanliness factor[1] to the measurement data where applicable and necessary, i.e. only where cleanliness factor at cleaning was not 1. It has to be noted that cleanliness factors can only be determined under certain conditions:

- The cleaning is performed correctly and swiftly (no influencing of sensors except during a few seconds in the cleaning process)
- The irradiation conditions are stable enough to distinguish signal increase resulting from dust removal from natural fluctuations
- The signal increase resulting from dust removal is sufficiently large to be detectable

If no analysis is possible, soiling correction is not applied.

Table 7 on the next page shows

- Simplified average sensor cleanliness factors of the pyrheliometer DNI sensor detected at the above described cleaning events
- Simplified average daily soiling rate of the pyrheliometer. This rate expresses how much the irradiance sensor signal is reduced each day without cleaning. Simplified in this context means that the rate is a simple average of the change of cleanliness factors over all days of the month
- The minimum cleanliness factors (i.e., maximum sensor soiling) observed just before the sensor cleaning. Especially on/after strong wind occasions such as e.g. dust storms, high singular soiling rates can be observed. The daily cleaning ensures that these single events with high soiling do not influence long periods of data (usually only up to one day) and were mostly well corrigible

[1] Sensor cleanliness factor is defined as the dimensionless factor by which the recorded measurement value has to be divided in order to obtain the soiling-corrected value. E.g., if at cleaning a signal increase of 3% has been detected, the factor before the cleaning is 1/(1+0.03) = 0.97, after the cleaning (clean sensors) = 1.

Table 7: Average sensor cleanliness factors (pyrheliometer)

Month	Average sensor cleanliness	Minimum cleanliness factor	Average daily soiling rate
Jul 2018	1.00	1.00	0.0 %
Aug 2018	1.00	1.00	0.0 %
Sep 2018	1.00	0.99	0.0 %
Oct 2018	1.00	0.99	0.1 %
Nov 2018	1.00	1.00	0.0 %
Dec 2018	1.00	1.00	0.0 %
Jan 2019	1.00	1.00	0.0 %
Feb 2019	1.00	0.99	0.0 %
Mar 2019	1.00	0.99	0.3 %
Apr 2019	0.99	0.95	1.1 %
May 2019	0.99	0.97	1.3 %
Jun 2019	0.99	0.96	1.0 %
Year 1	**1.00**	**0.95**	**0.3 %**
Jul 2019	1.00	1.00	0.0 %
Aug 2019	1.00	1.00	0.0 %
Sep 2019	1.00	1.00	0.0 %
Oct 2019	1.00	0.99	0.0 %
Nov 2019	1.00	0.99	0.1 %
Dec 2019	1.00	0.99	0.0 %
Jan 2020	1.00	1.00	0.0 %
Feb 2020	1.00	0.99	0.1 %
Mar 2020	1.00	0.99	0.1 %
Apr 2020	1.00	0.98	0.7 %
May 2020	0.99	0.99	0.7 %
Jun 2020	1.00	1.00	0.0 %
Year 2	**1.00**	**0.98**	**0.1 %**

In several months, there have been notable sensor soiling rates at the site. However, the soiling influence on the measurement data (after correction) was small, and only few singular events of notable pyrheliometer soiling were detected. Summarizing, it can be said that pyrheliometer soiling is not an issue to data quality, because the sensor cleaning schedule was well adhered to during the entire measurement campaign and soiling correction was applied to the data.

6.2 Soiling rates of GHI and DHI sensors (pyranometers)

Due to the work-daily cleaning and the ventilation units that largely keep dust from settling on the pyranometer glass domes, soiling of the pyranometers was not an issue.

Further, due to the geometry of the sensor window (hemispheric glass dome), dust deposition is usually not uniformly distributed over the sensor field of view. For example, with wind coming from a certain direction, the glass dome may be dust-covered on the windward side only, lacking any dust cover on the leeward side. Thickness of the soiling layer may also vary over the height of the glass dome. Figure 15 shows an extreme example of this characteristic (from a site in a different country).

Such asymmetric distribution of soiling, when present, leads to different cleanliness factors of the sensor during the course of the day depending of the elevation angle of the sun (azimuth angle is constant on tracked systems). This asymmetric distribution is unknown and signal increase can only be observed at the time of cleaning.

Meaningful cleanliness factors can therefore not be obtained and sensor soiling correction is generally not applied to thermopile pyranometer measurements by CSP Services.

Figure 15: Asymmetric pyranometer glass dome soiling (exemplary picture)

7 Measurement accuracy and uncertainty

The overall data availability is 100% and the local maintenance (irradiance sensor cleaning and visual check) was done mostly on schedule and according to the defined procedures. Cleaning was usually done work-daily. All ground measurement data was subject to a multi-step data quality control process:

- Transmission of measurement data to CSP Services' server in near-real time
- Daily application of automatic data screening routines (e.g. gap test, step test, physical limits, consistency of solar irradiance components)
- Daily visual inspection of measurement data curves by experienced operators
- Soiling correction of irradiance values measured with pyrheliometer, similar to the method developed by [1]
- Continuous comparison of redundant measurements
- Verification of pyranometer calibration with traveling standard

The documentation of the ground measurement data includes:

- Report for weather station installation (including the calibration certificates of solar sensors)
- Maintenance visit report for the regular inspection visit
- Documentation of each sensor cleaning with time and date through a maintenance button on the automatic weather stations, pressed by the operator after sensor cleaning (included in the measurement data)

7.1 Coincidence of DNI measurements

The DNI measured by the pyrheliometer can be compared to DNI values calculated from the measured GHI and DHI values and the solar zenith angle (DNI_{calc}). DNI_{calc} and the coincidence between the two DNI values can be determined along the following formulas[2]:

$$DNI_{calc} = \frac{GHI - DHI}{\cos(SZA)}, \qquad \text{with } SZA\text{: Solar Zenith Angle} \tag{1}$$

$$DNI_{coincidence} = DNI - DNI_{calc} \tag{2}$$

This DNI coincidence is an indicator for the accuracy of the irradiance measurement, the deviation between the measured and calculated DNI should stay within reasonable limits. The usual limits are ±20 W/m² or 2-3% of the measured DNI for instantaneous values for higher sun elevations and high DNI values; high deviations of DNI_{calc} for low sun elevations are normal due to the cosine effect (close to sun elevation of zero, cos(SZA) converges to zero, thus dividing by cos(SZA) results in very high DNI_{calc} values). The comparison of DNI_{calc} and the measured DNI is used continuously for the daily irradiance measurement data quality control.

[2] F. Wolfertstetter, K. Pottler, N. Geuder, R. Affolter, A.A. Merrouni, A. Mezrhab, R. Pitz-Paal: Monitoring of mirror and sensor soiling with TraCS for improved quality of ground-based irradiance measurements. Energy Procedia 49 (2014), 2422-2432. doi:10.1016/j.egypro.2014.03.257.

Figure 16 shows the correlation of DNI and DNI_{calc} in a scatterplot of 1min and 10min resolution measurement values. The following effects can be seen:

- For low DNI values, spread is partly due to the cosine effect as explained above.
- The majority of values are distributed in a narrow range around the bisecting line and almost symmetrical with a small bias toward higher DNI_{calc} values.
- Other outliers can be explained by sensor shading in the morning and evening and the effect of the cleaning of the sensors by the operators
- In 10min time resolution, the spread is much less due to averaging effects

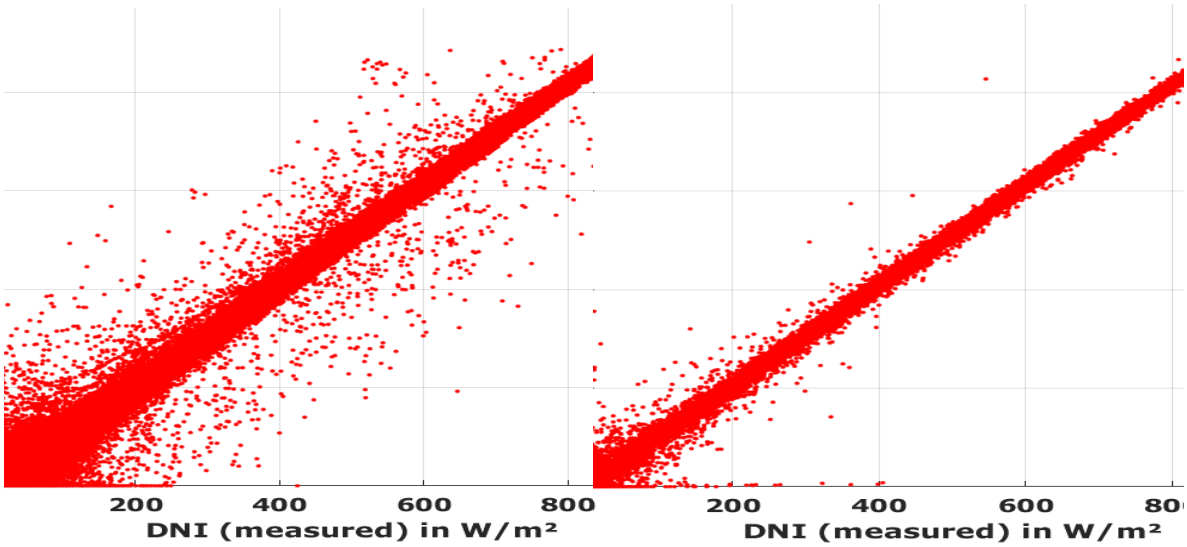

Figure 16: Correlation of DNI_{calc} and DNI (Left: 1min resolution. Right: 10min resolution)

In general, the coincidence can be considered as good, which is a consequence of the stringent maintenance procedures, high-quality sun tracker with active sun tracking, high sensor quality and accurate calibration. For the further use of the measurement data, data points with DNI coincidence values outside ±20 W/m² or 2-3% of the measured DNI are recommended to be filtered and discharged.

7.2 Coincidence of GHI measurements

Using the same formula (1) and replacing DNI_{calc} with the measured DNI, the coincidence of GHI can be calculated from the DNI and DHI measurement. Analogue to DNI, GHI coincidence is defined as measured GHI minus calculated GHI.

Figure 17 shows the correlation of calculated and measured GHI. Again, the correlation can be considered as good with only few outliers which (as for the DNI coincidence) are mostly due to maintenance influences, shading occurrences and short periods with non-ideal tracker alignment.

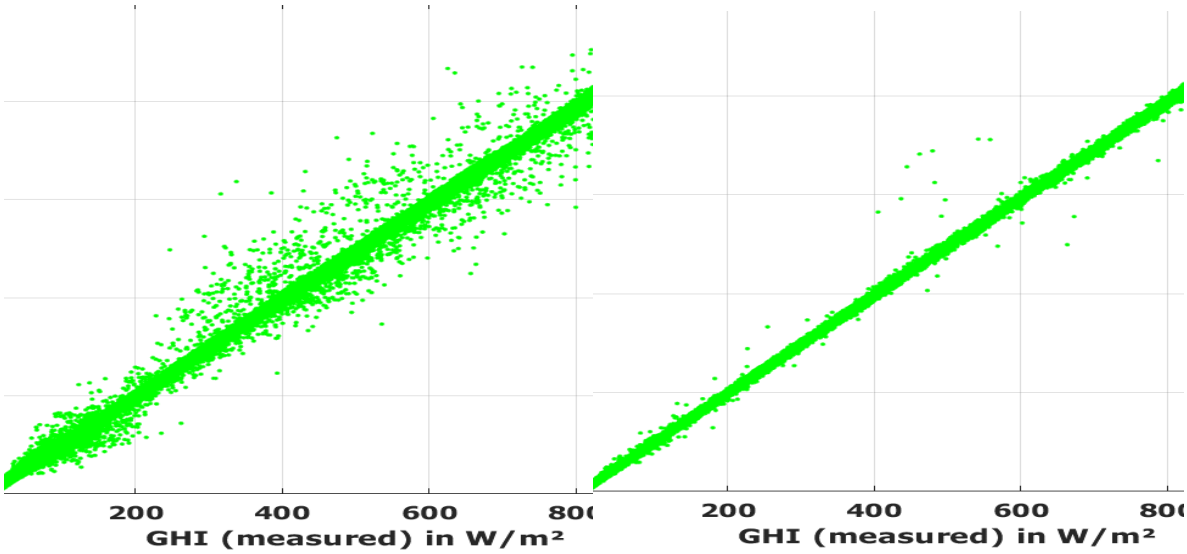

Figure 17: Correlation of GHI_{calc} and GHI (Left: 1min resolution. Right: 10min resolution)

7.3 Measurement uncertainty

The measurement uncertainty was assessed along the guideline in the NREL Best Practices Handbook for the Collection and Use of Solar Resource Data for Solar Energy Applications [2].

Best practices guidelines for selection of equipment, calibration, installation as well as operation and maintenance were followed and maintenance performance was assessed to include potential additional uncertainty contributions that could have occurred.

Two stages with related uncertainty contributions can be identified according to [2]:

- Instrument calibration (laboratory calibration by manufacturer): Uncertainty of calibration is specified in individual calibration certificates.
- Sources of uncertainty in field measurement are
    - Instrument-related (e.g. datalogger precision, pyrheliometer temperature response)
    - Installation-related (e.g. tracker alignment accuracy)
    - Operation-related (mainly frequency and thoroughness of cleaning)

DNI measurements

In the NREL Best Practices Handbook [2], typical calibration uncertainties for pyrheliometers are estimated with ±1.8% (at 95% level of confidence). The calibration certificate for the installed CHP1 pyrheliometer states a lower value of ±1.1%. Since this is well justified and the calibration verification did not give any reason of doubt, this lower value is assumed to be applicable.

In the field, much focus was given on using high-class measurement equipment (high-accuracy sensors, sun tracker and datalogger), excellent installation and alignment and regular maintenance and cleaning. The handbook estimates high-quality final measurement campaign DNI uncertainty with ±2.0% to ±2.5% for pyrheliometers for sub-hourly values (at 95% confidence interval).

For this measurement campaign, a measurement uncertainty of ±2.0% (at 95% confidence interval) for DNI values is estimated (after filtering and excluding values with bad coincidence as described above).

GHI and DHI measurements

In the literature, pyranometer calibration uncertainty is estimated with ±3.2% for solar zenith angles (SZA) between 30° and 60°. This is composed of an uncertainty of ±1.2% at a fixed, narrow incidence angle and a higher contribution of ±2.0% at a broader range of incidence angles [2]. Field measurements in well-maintained measurement campaigns can be estimated with uncertainties of ±3.0% for SZA between 30° and 60° and up to ±7.0% to ±10.0%for SZA>60° for GHI. For DHI, the uncertainty contribution resulting from SZA is irrelevant, since the direct irradiance is blocked by the shading ball assembly.

The calibration certificates for the installed CMP21 pyranometers state a value of ±1.35%. Calibration in the laboratory is done at a fixed incidence angle, thus this value replaces the literature estimate of ±1.2%. Since this is well justified and calibration verification did not give any reason of doubt, the value of ±1.35% is accepted.

The CMP21 pyranometers have an additional individual characterization for incidence angle and temperature sensitivity, and an incidence angle and temperature correction was applied to the GHI measurement values. Thus, the uncertainty resulting from broader incidence angles is much reduced. For the DHI, the temperature correction was applied. Therefore, the lower boundary of the literature values is assumed.

For this measurement campaign, a measurement uncertainty (at 95% confidence interval) of

- ±3.0% for all GHI values at SZA between 30° and 60°
- ±7.0% for all GHI values at SZA below 30° or above 60°
- ±2.0% for all DHI values

is estimated (after filtering and excluding values with bad coincidence as described above).

8 Conclusion

24 months of meteorological measurement data were collected at the site on Regional Agricultural Research Station (RARS) Nepalgunj with a Tier1 automatic weather station between July 2018 and June 2020. The data was measured with a tracked pyrheliometer, ventilated pyranometers and additional meteorological sensors.

- There were no significant operational difficulties
- Local maintenance and irradiance sensor cleaning were carried out on a work-daily schedule with good schedule adherence, each visit was recorded and documented
- Two regular (preventive) maintenance visits to the station were performed
- The measurement data was monitored on a daily basis by CSP Services operators, applying automatic quality assessment routines according to international best practices guidelines and visual inspection of the data by experienced operators
- The deviation between the installed irradiance sensors (redundant thermopile measurements) was within the expected limits
- The calibration of the used thermopile irradiance sensors was successfully validated upon a field calibration verification campaign after 17 months of measurement. For the field calibration verification, traveling standard sensors calibrated at the WRC in Davos, Switzerland, were used as calibration reference
- Measurement uncertainty is found to be within the expectable range given in best-practices literature

The 2-year measurement campaign at the site was successfully carried out, yielding a time series of on-site solar and meteorological measurement data in high quality. All measurement data was submitted to the World Bank in regular intervals by uploading to the energydata.info website. Additionally, the installation and maintenance reports as well as all calibration certificates and detailed descriptions of the measurement equipment were submitted to the World Bank.

9 References

[1] F. Wolfertstetter, , K. Pottler, A. Alami, A. Mezrhab and R. Pitz-Paal, "A novel method for automatic real-time monitoring of mirror soiling rates," in *SolarPACES 2012*, Marrakesh, Morocco, 2012.

[2] M. Sengupta, A. Habte, C. Gueymard, S. Wilbert and D. Renné, *Best Practices Handbook for the Collection and Use of Solar Resource Data for Solar Energy Applications: Second Edition,* Golden, Colorado: National Renewable Energy Laboratory, 2017.